Purification and Biophysical Characterisation of HIV-1 Vpu and Identification of Novel Drug Molecules

---

Zikhona Njengele

A Thesis submitted to the Faculty of Science, University of the Witwatersrand, Johannesburg in fulfilment of the requirements for the degree of Doctor of Philosophy

Johannesburg, 2019

Declaration

I, Zikhona Njengele (Student number: 302782), am a student registered for the degree of Doctor of Philosophy (PhD) in the academic year 2019.

I hereby declare the following:

- I am aware that plagiarism (the use of someone else's work without their permission and/or without acknowledging the original source) is wrong.
- I confirm that all the work submitted for examination is my own unaided work except where I have explicitly indicated otherwise.
- I have followed the required conventions in referencing the thoughts and ideas of others.
- I understand that the University of the Witwatersrand may take disciplinary action against me if there is a belief that this is not my own unaided work or that I have failed to acknowledge the source of the ideas or words in my writing.

Signature: Z. Njengele 29/05/2019. Date: 29th May 2019

Abstract

HIV-1 has developed various strategies to evade host immune responses, and these are mainly carried out by viral accessory proteins. HIV-1 Vpu, which is encoded by HIV-1 and some SIV isolates, plays many crucial roles in the pathogenesis of HIV-1. These include cell surface reduction of CD4; enhancement of virion release from infected cells by antagonising the host restriction factor, BST-2, as well as cell surface down-modulation of the major histocompatibility complex class I (MHC I) and NKT-and-B antigen (NTB-A) ligands recognised by cytotoxic T lymphocytes (CTL) and Natural Killer (NK) cells, respectively. By interfering with the expression of these molecules, HIV-1 Vpu helps HIV-1 infected cells evade recognition by these immune cells. The roles played by HIV-1 Vpu in ensuring that HIV-1 evades immunity make this protein an attractive target for new therapeutic interventions against the HIV-1 infection.

In this study, a library of 24 novel small molecular compounds was screened against the interaction of HIV-1 Vpu with BST-2. From the screening assays, two compounds, Compound 1 (ethyl 2-[(5-phenyl)-1*H*-imidazol-1-yl]acetate) and Compound 8 (5-(3-methoxyphenyl)-1*H*-imidazol-1-yl]acetohydrazide), were identified as potential hits with inhibition percentages of ~80% and 69%, and IC_{50} values of 11.6 ± 1.1 µM and 17.6 ± 0.9 µM, respectively. The compounds were further characterised through a range of direct and cell-based assays *in vitro* to determine their cytotoxicity, antiviral activity and potential ability to directly bind HIV-1 Vpu. The identified compounds were tested alongside 6-aza-2-thiouridine and Lapachol, two compounds that previously showed activity in restoring cell surface expression levels of BST-2 in the presence of HIV-1 Vpu. Compound 1 and Lapachol were able to inhibit the replication of HIV-1 (EC_{50} = 6.3 ± 0.7 and 17.3 ± 0.6 µM, respectively) at non-toxic concentrations (CC_{50} = 184.5 ± 0.8 and 152.8 ± 0.6 µM) *in vitro*. While Compound 8 did not show any traits of toxicity towards the mammalian cells used in our experiments (CC_{50} = 159.5 ± 0.9 µM), this compound did not exhibit any appreciable activity in hindering the replication of HIV-1 in the *in vitro* phenotypic assay. Conversely, 6-aza-2-thiouridine was toxic towards MT-4 cells (CC_{50} = 14.6 ± 0.5 µM), and as a result, the antiviral activity of this compound could not be correctly confirmed. The binding energetics of the compounds to HIV-1 Vpu were determined using ITC. 6-aza-2-thiouridine exhibited highest affinity for HIV-1 Vpu (K_D of 4.5 µM), followed by Compound 1 (18.5 µM) and

lastly, Compound 8 (20.8 µM). The binding of these compounds to HIV-1 Vpu proved to be enthalpically driven, with ΔH values of -3.98, -0.99 and -23.36 kJ/mol for Compound 1, Compound 8 and 6-aza-2-thiouridine, respectively. The results proved that these compounds do interact directly with HIV-1 Vpu, albeit with low binding affinity. The binding energetics for Lapachol, however, could not be evaluated, as this compound frequently precipitated out of solution at the molar ratios required for ITC experiments.

Overall, Compound 1 showed greater activity in inhibiting the HIV-1 Vpu/BST-2 interaction, was more potent in hindering the replication of HIV-1 *in vitro* and also showed better affinity for HIV-1 Vpu compared to Compound 8; and as a result, this compound was identified as a better lead compound. To the best of our knowledge, this is the first study to provide a detailed assessment of the binding energetics that occur between HIV-1 Vpu and potential inhibitors. The chemical structure of the active compound identified in this study can provide basis for development of novel HIV-1 inhibitors that target the binding HIV-1 Vpu to BST-2. Through structural modifications, the biological activity of this compound can be improved.

Dedication

In loving memory of my *Big Sis*:

Nolonwabo 'Loloza' Njengele

1981 – 2013

"*Education is the great engine of personal development. It is through education that the daughter of a peasant can become a doctor, that the son of a mine worker can become the head of the mine, that a child of farmworkers can become the president of a great nation. It is what we have, not what we are given, that separates one person from another*."

– Nelson Rolihlahla Mandela

Acknowledgements

First and foremost, I would like to thank the Almighty God for giving me the strength and ability to undertake this project. All glory and honour belong to Him!

To my supervisors, Dr. Salerwe Mosebi and Prof. Yasien Sayed, I can never thank you enough for the unwavering support, guidance and motivation you have shown me throughout the course of this study. What a great honour it has been to work with and learn from you! *If I have seen further than others, it is by standing on the shoulders of giants* – Sir Isaac Newton.

Dr. Jason Thompho Rashamuse for designing and synthesising the compounds tested in this study.

Monare Thulo (soon-to-be Doctor) for assistance with the ITC experiments.

I would like to thank the University of the Witwatersrand and the South African National Research Foundation for the financial support.

Thank you to the Centre for Metal-based Drug Discovery, Advanced Materials Division, MINTEK for providing the resources to conduct this research.

To my family, Busi, Lihlumelo and Hlalubonga, you are the wind beneath my wings. To my parents, Nomonde and Vulindlela Njengele (*uNozulu, Mpafane, Thukela kunye noJola, Mphankomo, Qengeba*) – thank you for instilling the importance of education in me from a very early age and for all the tremendous sacrifices you have made to ensure that I achieve my goals. *Ndiswele imilomo eliwaka*!

To my husband, Dr. Phumlani Tetyana, you were always there during the highs and lows of this journey, encouraging and comforting me. Thank you for being a constant source of support in all that I do.

Research Outputs

Conference Contributions

1. **Njengele Z**., Mosebi S. and Sayed Y. Analysis of the interaction of BST-2 with HIV-1 Vpu as a potential novel target for anti-HIV drug intervention. *Poster Presentation*. South African Society of Biochemistry and Molecular Biology 25th Congress, East London International Convention Centre, South Africa, 10 – 14th July 2016.

2. **Njengele Z**., Mosebi S. and Sayed Y. Exploring the interaction of HIV-1 Vpu with BST-2 as a potential target for HIV therapy. *Oral Presentation*. 8TH SA AIDS Conference, Durban International Convention Centre, South Africa, 13 – 16th June 2017.

Publications

1. **Njengele Z.**, Kleynhans R., Sayed Y., and Mosebi S. 2016. Expression, Purification and Characterization of a full-length Recombinant HIV-1 Vpu from inclusion bodies. *Protein Expression and Purification* **128**, 109 – 114.

Table of Contents

Declaration ..... ***i***

Abstract ..... ***ii***

Dedication ..... ***iv***

Acknowledgements ..... ***v***

Research Outputs ..... ***vi***

Table of Contents ..... ***vii***

List of Figures ..... ***xii***

List of Tables ..... ***xv***

List of Abbreviations ..... ***xvii***

Chapter 1: Introduction ***1***

1.1 HIV-1 Overview 1

1.2 The HIV-1 Genome and Encoded Proteins 2

1.3 The HIV-1 Replication Cycle 5

1.4 Current Treatment Strategies for HIV-1 7

1.5 Immune Responses against Viral Infections 10

1.5.1 Introduction to the Human Immune System 10

1.5.2 HIV-1 Specific Responses 11

1.6 Human Restriction Factors targeting HIV-1 Replication 12

1.7 The Intrinsic Restriction Factor: BST-2 13

1.7.1 The Structural Elements of BST-2 13

1.7.2 Additional Functions of BST-2 16

1.8 HIV-1 Accessory Proteins Counteract Immunity 17

1.9 Contribution of HIV-1 Vpu to Pathogenesis 18

1.9.1 General Properties of HIV-1 Vpu 18

1.9.2 The Role of HIV-1 Vpu in CD4 Surface Down-Modulation 21

1.9.3 HIV-1 Vpu Downregulates NTB-A, PVR and CD1d 21
1.9.4 HIV-1 Vpu Inhibits the NK cell-mediated ADCC and the NF-κB Pathway 22
1.9.5 Surface Down-Modulation of MHC molecules 23
1.9.6 The Ion Channel Activity of HIV-1 Vpu 24
1.9.7 Enhancement of Virion Release 25
1.10 The HIV-1 Vpu/BST-2 Interaction as a Potential Target for HIV-1 Therapy 30
1.11 Project Rationale and Motivation 32
1.12 Research Aim and Objectives 33
1.13 References 34

***Chapter 2: Materials and Methods* 54**
2.1 Materials 54
2.1.1 HIV-1 Vpu Expression plasmid 54
2.2 Methodology 55
2.2.1 Verification of the plasmid DNA sample 55
2.2.2 Heterologous Overexpression, Solubilisation and Purification of HIV-1 Vpu 55
2.2.3 Determination of protein concentration 57
2.2.4 Biochemical analysis of the purified recombinant HIV-1 Vpu 58
2.2.5 Structural Characterisation of HIV-1 Vpu 60
2.2.6 Analysis of the protein-protein interaction between HIV-1 Vpu and BST-2 62
2.2.7 Biochemical screening of inhibitors for the HIV-1 Vpu/BST-2 interaction 66
2.2.8 Determination of the pharmacochemical properties of the inhibitors 69
2.2.9 Determination of the antiviral activity of the compounds 71
2.2.10 Analysis of the binding of the compounds to HIV-1 Vpu 73
2.3 References 76

Chapter 3: The Overexpression, Purification and Characterisation of HIV-1 Vpu 79

3.1 Introduction 79

3.2 Verification of the HIV-1 Vpu plasmid DNA 80

3.3 Overexpression and Solubilisation of HIV-1 Vpu 80

3.4 Purification of HIV-1 Vpu 81

3.5 Biochemical Analysis of the Purified Recombinant HIV-1 Vpu 83

3.5.1 SDS-PAGE and Western blot Analysis 83

3.5.2 Qualitative ELISA test 85

3.6 Structural Characterisation of HIV-1 Vpu 86

3.6.1 Secondary Structural Characterisation 86

3.6.2 Tertiary Structural Characterisation 86

Quaternary Structural Characterisation of HIV-1 Vpu 88

3.7 Discussion 90

3.8 References 92

Chapter 4: Screening of Inhibitors against the interaction of HIV-1 Vpu with BST-2 93

4.1 Introduction 93

4.2 Confirmation of the binding of HIV-1 Vpu with BST-2 94

4.2.1 HIV-1 Vpu/BST-2 interaction using ELISA 94

4.2.2 Evaluation of the binding of HIV-1 Vpu with BST-2 using AlphaScreen 95

4.3 Screening of Inhibitors against the HIV-1 Vpu/BST-2 interaction 97

4.4 AlphaScreen as a Secondary Screening Assay 98

4.5 Dose-Response analysis of the Compounds 99

4.6 Evaluation of the Biological and Biophysical properties of the identified compounds 101

4.6.1 In silico prediction of the drug-like properties of the compounds 101

4.6.2 Assessment of the Aqueous Solubility of the Compounds 103

4.6.3 Determination of the Cytotoxicity effects of the compounds 105

4.6.4 Determination of the anti-HIV-1 activity of the compounds 106

4.6.5 Determination of the Therapeutic Index values of the test compounds 108

4.7 Discussion 109

4.8 References 114

Chapter 5: Analysis of the binding of the Ligands to HIV-1 Vpu ***117***

5.1 Introduction 117

5.2 Effects of ligand binding on the thermal stability of HIV-1 Vpu 118

5.3 Ligand binding analysis using intrinsic Fluorescence 120

5.4 Thermodynamic analysis of the binding of the identified inhibitors to HIV-1 Vpu 122

5.5 Discussion 128

5.6 References 132

Chapter 6: Summary of Findings and General Conclusions ***134***

6.1 Successful Expression and Purification of HIV-1 Vpu 134

6.2 Evaluation of the identified hit compounds 135

6.2.1 Analysis of the drug-likeness of the compounds 138

6.2.2 Effects of the compounds on the HIV-1 Vpu/BST-2 interaction 138

6.2.3 Effects of the compounds on host cells and viral replication 138

6.2.4 Affinity of the compounds for HIV-1 Vpu 139

6.3 Concluding Remarks 140

6.4 Recommendations for Future Work 141

6.5 References 142

Appendix A: ***143***

A.1.1 Plasmid map of pcDNA-Vphu 143

Appendix B: ***144***

B.1.1 BLAST results obtained for the pcDNA-Vphu sequence: 144

Appendix C: ***145***

C.1.1 Expression and Purification Trials of BST-2 145

Appendix D: ***148***

D.1.1 Fluorescence Spectra of the Titration of the Test Compounds into reaction Buffer 148

D.1.2 Fluorescence Spectra of the Titration of the Test Compounds into HIV-1 Vpu 150

List of Figures

Chapter 1

Figure 1.1: Genome organisation and structure of the HIV-1 virion. 3

Figure 1.2: Schematic illustration of the HIV-1 life cycle.. 6

Figure 1.3: Schematic representations of the different hypothetical models of BST-2 orientation. 15

Figure 1.4: Schematic representation of HIV-1 Vpu.. 20

Figure 1.5: Schematic representation of the different modes of HIV-1 Vpu-mediated BST-2 counteraction during HIV-1 infection.. 27

Figure 1.6: Schematic representation of the binding of HIV-1 Vpu to BST-2. 28

Figure 1.7: Chemical structures of BIT225, Lapachol and 6-aza-2-thiouridine, the three compounds that have been shown to inhibit the activity of HIV-1 Vpu. 31

Chapter 2

Figure 2.1: Schematic representation of the HIV-1 Vpu/BST-2 interaction in the AlphaScreen assay. 64

Figure 2.2: Representation of the HIV-1 Vpu in complex with BST-2 through their respective α-helical transmembrane domains.. 67

Chapter 3

Figure 3.1: SDS–PAGE analysis of the recombinant HIV-1 Vpu protein expressed using *E. coli cells*.. 81

Figure 3.2: The elution profile of HIV-1 Vpu from the Q-Sepharose anion exchange column.. 82

Figure 3.3: Overview of the purification process of HIV-1 Vpu using ion exchange chromatography.. 84

Figure 3.4: Qualitative ELISA analysis of the purified recombinant HIV-1 Vpu.. 85

Figure 3.5: Far-UV circular dichroism spectrum of the purified recombinant HIV-1 Vpu. 87

Figure 3.6: Fluorescence emission spectra of HIV-1 Vpu. 87

Figure 3.7: Quaternary structural characterisation of HIV-1 Vpu. 89

Chapter 4

Figure 4.1: HIV-1 Vpu-BST-2 ELISA to confirm the binding of HIV-1 Vpu to BST-2.. 94

Figure 4.2: Streptavidin ELISA to test the biotinylation of HIV-1 Vpu. 95

Figure 4.3: Measuring the binding affinity of HIV-1 Vpu for BST-2 using the AlphaScreen assay... 96

Figure 4.4: Recurring nitrogen heterocyclic scaffolds identified from the virtual screening of novel small molecule compounds against the interaction of HIV-1 Vpu with BST-2 using the pepMMsMIMIC program. 97

Figure 4.5: Inhibition percentage results obtained for the 24 in-house synthesised compounds against the HIV-1 Vpu/BST-2 interaction using ELISA.. 98

Figure 4.6: Inhibition results obtained for the eight hit compounds that were identified as potential inhibitors for the interaction of HIV-1 Vpu with BST-2 using AlphaScreen. 99

Figure 4.7: Dose response curves used to generate the IC50 values of Compound 1 and 8 using the AlphaScreen assay..... 100

Figure 4.8: Representative aqueous solubility graphs..... 104

Figure 4.9: Representation of the stages involved in the drug discovery and development process. . 111

Chapter 5

Figure 5.1: Thermal shift assay for the binding of the ligands to HIV-1 Vpu.. 119

Figure 5.2: Intrinsic Tryptophan fluorescence spectra of HIV-1 Vpu with the test compounds. 121

Figure 5.3: A representative calorimetric profile of the titration of HIV-1 Vpu with Compound 1... 123

Figure 5.4: A representative calorimetric profile of the titration of HIV-1 Vpu with Compound 8... 124

Figure 5.5: A representative calorimetric profile of the titration of HIV-1 Vpu with 6-aza-2-thiouridine.. 125

Figure 5.6: A representative calorimetric profile of the titration of HIV-1 Vpu with Lapachol..... 126

Appendix A

Figure A.1: Map of the *pcDNA-Vphu* plasmid vector that was used for the overexpression of HIV-1 Vpu. 143

Appendix B

Figure B.1: Sequence alignment results of the pcDNA-Vphu sequence obtained from Inqaba Biotech using protein BLAST. 144

Appendix C

Figure C.1: SDS-PAGE and Western blot analysis of the recombinant BST-2. 147

Appendix D

Figure D.1: Intrinsic tryptophan fluorescence spectra of the titrations of the test compounds into reaction buffer. 149

Figure D.2: Intrinsic tryptophan fluorescence spectra of the titrations of the test compounds into 5 µM HIV-1 Vpu. 151

List of Tables

Chapter 1

Table 1.1: The size and functions of HIV-1 proteins 4

Table 1.2: List of FDA Approved HIV-1 Inhibitors 9

Table 1.3: Summary of the functions of HIV-1 Vpu and their relevance in HIV-1 pathogenesis 29

Chapter 2

Table 2.1: Reagents from the NIH AIDS Reagent Program used within this study 54

Chapter 4

Table 4.1: IC_{50} (µM) values of the two hit compounds that showed high activity in inhibiting the HIV-1 Vpu/BST-2 interaction 101

Table 4.2: Analysis of the drug-likeness of the test compounds using Lipinski's rule-of-five. 102

Table 4.3: Summary of the aqueous solubility data obtained for the two hit compounds in comparison 6-aza-2-thiouridine, Lapachol and Chloramphenicol 105

Table 4.4: CC_{50} values (µM) indicating the effect of the test compounds on the viability of MT-4 cells.. 107

Table 4.5: EC_{50} values (µM) indicating the potency of the test compounds in inhibiting the replication of the HIV-1 LAV strain in MT-4 cells. 107

Table 4.6: Therapeutic Index values indicating the safety profiles of the two newly identified HIV-1 Vpu/BST-2 inhibitors alongside the two control compounds. 108

Chapter 5

Table 5.1: Melting temperature of HIV-1 Vpu in the presence and absence of the identified hit compounds. 119

Table 5.2: Thermodynamic parameters obtained for the interaction of HIV-1 Vpu with Compound 1, Compound 8 and 6-aza-2-thiouridine using ITC at 20 ºC. 127

Chapter 6

Table 6.1: Summary of the Lipinski Score, IC_{50}, CC_{50}, EC_{50}, Therapeutic Indexes, ΔT_m, K_D and ΔG values obtained from the characterisation studies conducted on the test compounds 136

List of Abbreviations

ADCC	Antibody dependent cell-mediated cytotoxicity
ADMET	Absorption, Distribution, Metabolism, Excretion and Toxicity
AIDS	Acquired immunodeficiency syndrome
APOBEC3G	apolipoprotein B mRNA-editing enzyme, catalytic polypeptide-like 3G
BLAST	Basic Local Alignment Tool
BSA	Bovine serum albumin
BST-2	Bone marrow stromal antigen 2
β-TrCp	Beta-transducine repeat containing protein
cART	Combination antiretroviral therapy
CC_{50}	50% Cytotoxic Concentration
CCR5	C-C chemokine receptor type 5
CD	Circular Dichroism
CXCR4	C-X-C chemokine receptor type 4
DNA/cDNA	Deoxyribonucleic acid/ complementary deoxyribonucleic acid
EC_{50}	50% Effective Concentration
ELISA	Enzyme-linked immunosorbent assay
Env	Envelope glycoprotein
ER	Endoplasmic reticulum
ESCRT	Endosomal sorting complex required for transport
FDA	Food and Drug Administration
gp	Glycoprotein
GPI	Glycosylphosphatidylinositol

HIV-1	Human immunodeficiency virus type 1
IC_{50}	50% Inhibitory Concentration
IN	Integrase
ITC	Isothermal titration calorimetry
K_D	Dissociation constant
LAV	Lymphadenopathy-associated virus
LEDGF	Lens epithelium derived growth factor
LTR	Long terminal repeats
MHCI	Major histocompatibility complex class I
MHCII	Major histocompatibility complex class II
MOI	Multiplicity of infection
MTS	3-(4,5-dimethylthiazol-2-yl)-5-(3-carboxymethoxyphenyl)-2-(4-sulfophenyl)-2H- tetrazolium
Nef	Negative factor
NF-κB	Nuclear factor κB
NK	Natural killer
NKT	Natural killer T
NMR	Nuclear magnetic resonance
NRTI	Nucleoside reverse transcriptase inhibitor
NNRTI	Non-nucleoside reverse transcriptase inhibitor
NTB-A	NK-T and B cell antigen
PBMC	Peripheral blood mononuclear cells
PR	Protease
RPMI	Roswell Park Memorial Institute
SIV	Simian immunodeficiency virus
ssRNA	Single-stranded RNA
Tat	Transcriptional activator

TI	Therapeutic Index
Tm	Melting Temperature
TRAF	TNF receptor associated factor
TRIM5α	Alpha isoform of tripartite motif protein 5
Vif	Viral infectivity factor
Vpr	Viral protein R
Vpu	Viral protein U
vRNA	viral RNA

List of Symbols

α	Alpha
Å	Angstrom
β	Beta
CO_2	Carbon dioxide
ºC	Degrees Celsius
g	Grams
κ	Kappa
kDa	Kilodaltons
kJ	Kilojoules
L	Litre
µg	Micrograms
µL	Microlitres
µM	Micromolar
mg	Milligrams
mL	Millilitres
mM	Millimolar
M	Molar
mol	Moles
nM	Nanomolar
%	Percentage
v/v	Volume to volume ratio
w/v	Weight to volume ratio
x g	Relative centrifugal gravitational force

The IUPAC-IUBMB one- and three-letter abbreviations for the 20 standard amino acids were used where applicable

Chapter 1: Introduction

1.1 HIV-1 Overview

The Acquired Immunodeficiency Syndrome (AIDS), which is caused by the human immunodeficiency virus type I (HIV-1), presents one of the major pandemics in history, having claimed nearly 40 million lives since its discovery in 1981. According to the World Health Organisation's (WHO) Global AIDS update of 2017 (UNAIDS, 2017), approximately 37 million people across the globe were living with an HIV-1 infection at the end of 2016; with the Eastern and Southern African region accounting for approximately 53% of the total number, and 42% of all AIDS related mortalities. In the same study, South Africa was reported to have the highest global estimates of people living with a HIV infection. An estimated 7.1 million people were reported to be living with HIV-1 in South Africa at the end of 2016, with over 110 000 AIDS related mortalities reported in 2016 alone (UNAIDS, 2017). This means that nearly 13% of the South African population are living with HIV-1 (7.1 million out of a total population of 56.52 million people). This alarming statistic reflects that South Africa is the epicentre of the HIV/AIDS pandemic.

Although the number of new infections and the mortality rate show a significant decline from previous years (UNAIDS, 2017), the total number of people living with HIV-1 globally continues to increase, and as a result, HIV-1 still remains pandemic. Over the past three and a half decades, extensive investigation from different research institutes across the world went into understanding the virus at a molecular level. As a result, over 30 effective antiretroviral agents have been developed and approved by the United States Food and Drug administration (FDA) for the fight against HIV-1. While many successful antiretrovirals have been developed, HIV-1 monotherapy has failed due to development of resistant strains against the drugs. In an attempt to address this problem, the combination anti-retroviral therapy (cART), which includes a combination of two or more antiretroviral agents with different modes of action, was introduced (Carpenter *et al.*, 1997; Maenza & Flexner, 1998). While the introduction of cART led to decreased AIDS related deaths, turning the infection into a manageable chronic condition (Palella *et al*., 1998), drug resistance remains a concern even with the use of this multi-drug treatment. The frequent occurrence of drug resistant viral mutants can be attributed to the HIV-1 reverse transcriptase enzyme's lack of proofreading

ability and the high replication rate of HIV-1 (O'Neil *et al*., 2002; Weiss *et al*., 2002). Furthermore, the risk of HIV-1 drug resistance increases with poor patient compliance to prescribed drugs, or when structured treatments are interrupted (Nachega *et al*., 2011). This makes the identification of new therapeutic drug targets and the continued search for new drugs with novel modes of action a high priority in the HIV-1 research field.

1.2 The HIV-1 Genome and Encoded Proteins

HIV-1 is an enveloped single stranded ribonucleic acid (ssRNA) virus that belongs to the *Retroviridae* family and is a member of the *lentivirus* genus. The HIV-1 genome is made up of two identical positive sense ssRNA copies, with each copy containing nine genes that encode up to 15 viral proteins. Flanking the ends of each RNA are 5' and 3'long terminal repeat (LTR) sequences that function as regulatory elements for the expression of the viral proteins (Cullen *et al*., 1991; Jones & Peterlin, 1994).

The genomes of primate *lentiviruses* are considerably more complex than those of other retroviruses. The HIV-1 genome consists of three main genes common to all retroviruses; namely, group-specific antigen *(gag)*, polymerase (*pol)* and envelope (*env*) genes as illustrated in Figure 1.1 A. The *gag* gene encodes the matrix (p17, MA), capsid (p24, CA) and the nucleocapsid (p7, NC), which are the major structural components of the virion core (Göttlinger *et al*., 1991; Freed *et al*., 1998) (Figure 1.1 B). The *env* gene encodes surface proteins called glycoprotein 120 (gp120) and gp41, which are crucial for the virus to bind and enter host cells (Turner & Summer, 1999; Arrildt *et al*., 2012); while the *pol* gene encodes the viral enzymatic proteins, which include reverse transcriptase (p66/p51, RT), integrase (p31, IN) and protease (p11, PR) (Gelderblom, 1991). In addition to these genes, HIV-1 consists of six extra genes; two regulatory genes (*tat* and *rev*), and four accessory genes (*vif*, *vpr*, *vpu* and *nef)*. The regulatory genes *tat* and *rev* encode the trans–activator of transcription (Tat) and the regulator of expression of viral proteins (Rev), respectively, essential for the HIV-1 gene expression (Ruben *et al.,* 1989). The accessory genes *vif*, *vpr*, *vpu* and *nef* encode the viral infectivity factor (Vif), viral protein R (Vpr), viral protein U (Vpu) and the negative regulatory factor (Nef), respectively (reviewed in Table 1.1). Even though they are not essential for viral replication *in vitro*, the accessory proteins function in a variety of ways to manipulate the cellular environment for the virus's advantage *in vivo*, thereby promoting viral persistence and maintaining effective immune evasion (Malim & Emerman, 2008).

A.

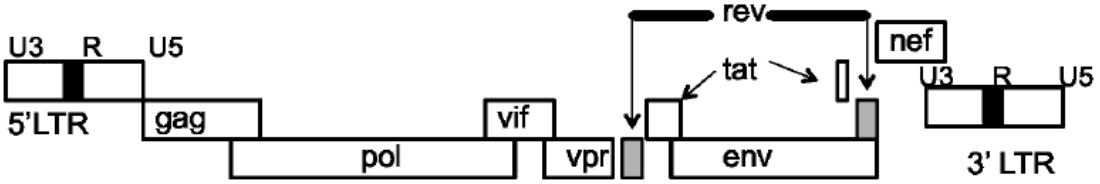

B.

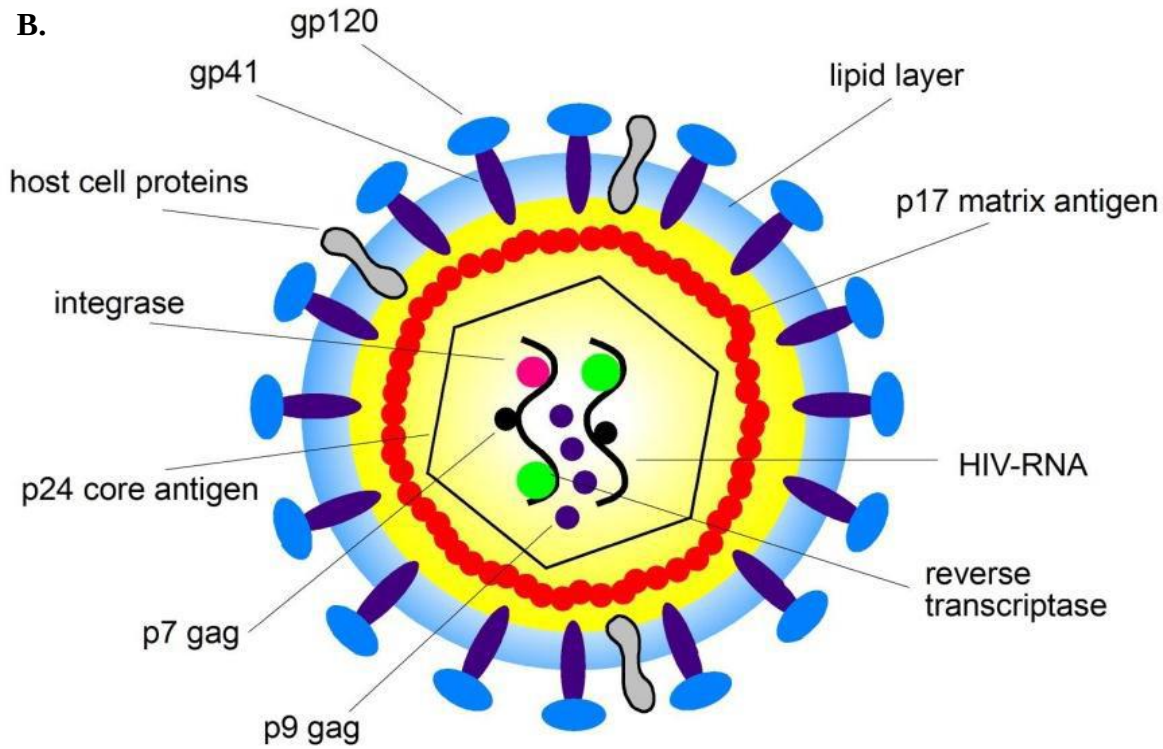

Figure 1.1: Genome organisation and structure of the HIV-1 virion A. Schematic representation of the genetic organisation of the HIV-1 genome. Figure adapted from Stonos *et al.*, 2014. **B.** Structure of an HIV-1 virion. Envelope glycoproteins, gp120 and gp41, protrude from the lipid bilayer derived from the host cell plasma membrane. The viral core consists of two copies of positive sense single stranded RNA enclosed by the viral capsid protein, p24, together with the reverse transcriptase and integrase enzymes required for the formation of new HIV particles (taken from Rubbert *et al*., 2011).

Table 1.1: The size and functions of HIV-1 proteins

Proteins	Size (kDa)	Function
Regulatory Proteins		
Tat	14	Regulates viral gene expression[1]
Rev	13	Nuclear transport of viral RNA[1]
Accessory Proteins		
Nef	27	Downregulates cell surface expression of CD4. Stimulates viral infectivity[2]
Vpr	14	Nuclear localisation of the pre-integration complex. Blocks cell division[3]
Vif	23	Promotes virus infectivity[4]
Vpu	9	Triggers degradation of CD4 receptors. Enhances budding[5]
Structural Proteins		
Gag		
Matrix	17	Interacts with env during viral assembly and budding[6]
Capsid	24	Core capsid which contains the vRNA copies[6]
Nucleocapsid	9	Nucleocapsid, binds vRNA[6]
Pol		
Protease	10	Cleavage and maturation of polyprotein precursors[6]
Reverse transcriptase	117	Conversion of vRNA into double stranded DNA[6]
Integrase	31	Mediates the insertion of the HIV-1 proviral cDNA into the host DNA[6]
Env		
gp160	160	Gp120 and gp41 precursor[7]
gp120	120	CD4 binding[7]
gp41	41	Membrane fusion[7]

1. Seelamgari *et al.,* 2004. 2. Glushakova *et al.,* 2001; 3. Zhang *et al.,* 2001; Sherman *et al.,* 2002; 4. Sheehy *et al.,* 2003; 5.Montal, 2003; 6. Kuiken *et al.,* 2008; 7. Capon and Ward, 1991.

1.3 The HIV-1 Replication Cycle

The life cycle of HIV-1 is comprised of the following major steps: attachment, fusion, reverse transcription, integration, transcription and translation, assembly, budding and maturation (Figure 1.2). During attachment, the HIV-1 gp120 attaches to the CD4 receptor and a respective chemokine co-receptor (C-C chemokine receptor type 5 (CCR5) and/or the C-X-C chemokine receptor type 4 (CXCR4)) on the surface of host cells (Chen *et al.*, 2009; Kwong *et al*., 1998). This leads to fusion of the viral and cell membranes, and the viral core, encapsulated by the capsid protein, gets released into the cytoplasm of the target cell. Once in the cytoplasm, the viral core is disassembled in a poorly characterised process called uncoating, and reverse transcription occurs (Chen *et al*., 2013; Xu *et al*., 2013). Reverse transcription is a process catalysed by RT, whereby the viral RNA genome is converted into a double-stranded DNA molecule (Harrich & Hooker, 2002). The viral DNA is then actively transported into the nucleus in the form of a pre-integration complex which contains the viral DNA, IN, Vpr and several cellular factors (Farnet & Haseltine, 1991). The viral DNA is irreversibly integrated into the host genome by IN in association with a host protein, lens epithelium derived growth factor (LEDGF/p75) (Miller *et al*., 1997; Shun *et al*., 2007). At this point, the virus hijacks host mechanisms, and the integrated viral genome undergoes transcription into messenger RNA (mRNA) in a process catalysed by cellular RNA polymerase II. The generated mRNA consists of mixed splicing sites and encodes the 15 viral proteins (Purcell & Martin, 1993). Transcribed mRNA molecules are exported out of the nucleus into the cytoplasm where translation into polypeptide chains takes place. The viral proteins and genomic viral RNA transcripts accumulate on the plasma membrane of the infected cell where they assemble to make up new viral particles (Adamson & Freed, 2007). The newly formed virions bud out of the cell membrane as nascent immature viral particles. Once the virus is released from the plasma membrane, viral PR cleaves the Gag and Gag-Pol polyprotein chains into mature individual proteins, yielding infectious HIV-1 particles capable of initiating a new cycle of infection (Adamson & Freed, 2007).

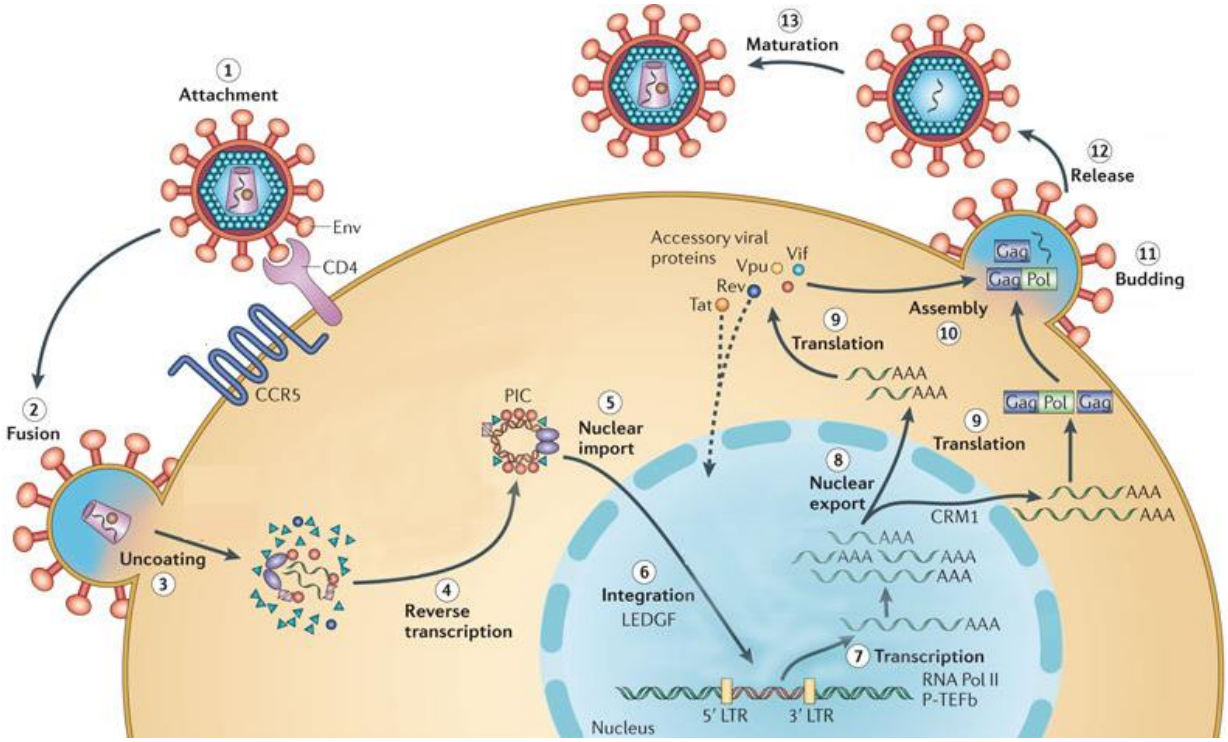

Figure 1.2: Schematic illustration of the HIV-1 life cycle. Upon receptor/co-receptor binding, the viral membrane fuses with the cellular membrane through multiple conformational changes in the Env protein, releasing the viral core into the cytoplasm. Reverse transcription of the viral genome occurs, followed by nuclear import and integration into the host chromosome where it gets transcribed. RNA transcripts are then exported from the nucleus, giving rise to all the components for viral assembly and budding. Adapted from Engelman & Cherepanov (2012).

1.4 Current Treatment Strategies for HIV-1

Each stage of the HIV-1 viral life cycle represents a potential target for drug intervention. To date, 35 different small molecule antiretroviral drugs have been approved by the FDA for the fight against HIV-1, and these are divided into 5 different classes based on the phase of the HIV-1 replication cycle they target: viral entry inhibitors, fusion inhibitors, RT inhibitors, IN inhibitors and PR inhibitors (as summarised in Table 1.2). Treatment with these can reduce HIV-1 associated morbidity and prolong survival but cannot undo the HIV-1 infection (Palella *et al*., 1998; Vittinghoff *et al*., 1999). Consistent with the increase in the number of antiretroviral drugs, however, an increase in drug resistance mutations has been reported, and the emergence of such strains compromises the long-term efficacy of the antiretroviral agents (Witmer & Danovich, 2009). Mutations in the viral genome, mostly caused by the error–prone RT as well as drug pressure, contribute to viral resistance against antiretroviral agents. To circumvent the problem of drug resistant mutants, combinatorial therapy, cART, was introduced. Although treatment with cART does not eradicate the virus, low plasma viremia (<50 RNA copies/mL) has been reported with the use of this cocktail therapy (Weller & Williams, 2001).

Currently, two drugs, enfuvirtide and maraviroc have been approved for the inhibition of fusion and viral entry, respectively. Enfuvirtide blocks viral attachment by binding and locking gp41 (Wild *et al*., 1993; Chen *et al*., 2002; Kilby *et al*., 2003) while maraviroc acts as a CCR5 antagonist, thereby blocking viral fusion with the host cell (Dragic *et al*., 2000; Briz *et al*., 2006). Three subclasses of antiretrovirals with different mechanisms of action target the functioning of the HIV-1 RT enzyme, and these are nucleoside RT inhibitors (NRTIs), nucleotide RT inhibitors (NtRTIs) and non-nucleoside RT inhibitors (NNRTIs). The NRTIs (Abacavir, Didanosine, Emtricitrabine, Lamivudine, Stavudine and Zidovudine) and NtRTIs (Tenofovir) are nucleoside/nucleotide analogues, whose incorporation during DNA strand synthesis causes premature termination (Balzarini, 1994; De Clercq & Neyts, 2009), while the NNRTIs (Nevirapine, Delavirdine, Efavirenz, Rilpivirine and Etravirine) function through non-competitive binding to an allosteric site located about 10 Å away from RT's active site, negatively impacting on the catalytic activity of the enzyme (De Clerq *et al*., 2004; Pauwels, 2004). The latest class of antiretrovirals to obtain approval by the FDA inhibit integration of the viral DNA into the host cell genome by targeting IN. There are currently three clinically available IN inhibitors, and these include Raltegravir, Dolutegravir and Elvitegravir (Serrao

et al., 2009; Hazuda *et al*., 2009; Klibanov, 2009). Inhibitors such as Saquinavir, Ritonavir, Indinavir, Nelfinavir, Amprenavir, Lopinavir, Atazanavir, Tipranavir and Darunavir inhibit the functioning of HIV-1 PR (Weinsing *et al*., 2010). PR inhibitors act as competitive inhibitors of the enzyme as they bind to the active site of PR, blocking the activity of the enzyme, and subsequently preventing the cleavage of viral proteins (Bannworth *et al*., 2007). The uncleaved viral proteins are considered defective and, as a result, the virion cannot mature into an infectious particle.

In the recent years, extensive effort has been put towards studying and the identification of host cell factors that are involved in HIV-1 replication. Since the HIV-1 genome only encodes 15 proteins, successful completion of the viral life cycle requires complex interactions with various host cell factors at each stage of the replication cycle. In addition to the host factors that are used by the virus (known as cofactors), the intrinsic immune system expresses a number of proteins that inhibit different steps of the viral replication cycle, and these are collectively known as restriction factors.

Table 1.2: List of FDA Approved HIV-1 Inhibitors

Brand Name	Generic Name	Approval Date
NRTIs		
Combivir	Lamivudine and Zidovudine	27-Sep-97
Emtriva	Emtricitabine, FTC	02-Jul-03
Epivir	Lamivudine, 3TC	17-Nov-95
Epzicom	Abacavir and Lamivudine	02-Aug-04
Hivid	Zalcitabine, Dideoxycytidine, ddC (no longer in the market)	19-Jun-92
Retrovir	Zidovudine, Azidothymidine, AZT, ZDV	19-Mar-87
Trizivir	Abacavir, Zidovudine, and Lamivudine	14-Nov-00
Truvada	Tenofovir disoproxil fumarate and Emtricitabine	02-Aug-04
Videx EC	Enteric coated didanosine, ddI EC	31-Oct-00
Videx	Didanosine, Dideoxyinosine, ddI	9-Oct-91
Zerit	Stavudine, d4T	24-Jun-94
NtRTIs		
Viread	Tenofovir disoproxil fumarate, TDF	26-Oct-01
NNRTIs		
Edurant	Rilpivirine	20-May-11
Intelence	Etravirine	18-Jan-08
Rescriptor	Delavirdine, DLV	4-Apr-97
Sustiva	Efavirenz, EFV	17-Sep-98
Viramune (Immediate Release)	Nevirapine, NVP	21-Jun-96
Viramune XR (Extended Release)	Nevirapine, NVP	25-Mar-11
Ziagen	Abacavir sulfate, ABC	17-Dec-98
Protease Inhibitors		
Agenerase	Amprenavir, APV (no longer in the market)	15-Apr-99
Aptivus	Tipranavir, TPV	22-Jun-05
Crixivan	Indinavir, IDV,	13-Mar-96
Fortovase	Saquinavir (no longer in the market)	7-Nov-97
Invirase	Saquinavir mesylate, SQV	6-Dec-95
Kaletra	Lopinavir and Ritonavir, LPV/RTV	15-Sep-00
Lexiva	Fosamprenavir Calcium, FOS-APV	20-Oct-03
Norvir	Ritonavir, RTV	1-Mar-96
Prezista	Darunavir	23-Jun-06
Reyataz	Atazanavir sulfate, ATV	20-Jun-03
Viracept	Nelfinavir mesylate, NFV	14-Mar-97
Fusion Inhibitors		
Fuzeon	Enfuvirtide, T-20	13-Mar-03
Entry Inhibitors		
Selzentry	Maraviroc	06-August-07
Integrase Inhibitors		
Isentress	Raltegravir	12--Oct-07
Tivicay	Dolutegravir	13-August-13
Vitekta	Elvitegravir	24-Sep-14

1.5 Immune Responses against Viral Infections

1.5.1 Introduction to the Human Immune System

The human immune system possesses two different lines of defense that intervene at different stages during an infection and are complementary to each other. The first line of defense against infection is mediated by the innate immune system. Innate immunity involves immediate intervention of immune cells and cellular pathways acting against a broad range of infectious agents such as parasites, bacteria and viruses (Medzhitov & Janeway, 1997; Cooper & Alder, 2006). The innate immune system acts in a non-pathogen-specific manner, recognising general pathogen-associated molecular patterns (PAMPs), which are non-specific markers of infection such as bacterial lipopolysaccharides, viral DNA or RNA within an infected cell (Janeway, 1989). These PAMPs are recognised by pattern recognition receptors (PRRs) on the surface of phagocytic cells, and the binding of PRRs with their associated PAMPs results in the release of cytokines, such as type I interferons (IFNs) (Medzhitov & Janeway, 1997; Akira & Takenda, 2004). This creates an antiviral state within an infected cell, leading to the activation and recruitment of the innate immune cells (Akira *et al*., 2006; Paolini *et al*., 2015). The innate immune system, however, lacks immunologic memory and remains unchanged even after multiple encounters with the same antigen.

Following the initial non-specific immune response, a more specific response based on antigen recognition, called the adaptive immune response, is established. This type of immunity presents the advantage of memory acquisition, making it more capable of mounting faster and more specific responses to the same antigen in the future (Janeway *et al*., 2005). The adaptive immune response comprises of two interrelated strategies, namely, the humoral and the cellular immune responses. The humoral immune response is directed by B lymphocytes, while the cellular response is mediated by T lymphocytes (Janeway *et al*., 2005). The cell-mediated immunity is activated when naïve T cells encounter a specific antigen on the surface of an antigen presenting cell. The T cells become activated and produce interleukin (IL); leading to their proliferation and differentiation into effector T cells (Janeway *et al*., 2005). Antigens carried by major histocompatibility complex (MHC) class I molecules are presented to $CD8^+$ T cells, and these differentiate into cytotoxic T lymphocytes (CTLs) that kill virally infected cells by releasing soluble antiviral factors such as perforin, granulysin and granzyme (Janeway & Medzhitov, 2002; Santana & Esquivel-Guadarrama, 2006). Antigens carried by MHC class II (MHCII) molecules on the other hand are presented

to $CD4^+$ T cells which differentiate into Type I T helper (T_h1) or Type II T helper (T_h2) cells (Janeway *et al*., 2005). T_h1 cells produce cytokines that activate macrophages and lead to cell-mediated immunity, while T_h2 cells release cytokines that activate B lymphocytes to produce neutralising antibodies, thereby stimulating humoral immunity (Janeway, 2005; Santana & Esquivel-Guadarrama, 2006). Neutralising antibodies can either bind to pathogens and prevent their entry into cells or coat the surface of pathogens to attract phagocytes and enhance phagocytosis in a process called opsonisation. The fragment crystallisable (Fc) domain of these neutralising antibodies is recognised by Fc receptors on natural killer (NK) cells (Janeway *et al*., 2005).

1.5.2 HIV-1 Specific Responses

As is the case with most viral infections, infection by HIV-1 results in a strong activation of the innate immune system that is followed by the development of adaptive immune responses. The ssRNA genome of HIV-1 is recognised by PRRs and the stimulation of these receptors induces the production of several cytokines and activation of immune cells, with NK cells being the key effectors of innate immunity against HIV-1. Following induction of antibodies through the humoral immune response, NK cells target and kill HIV-1 infected cells through the antibody-dependent cell-mediated cytotoxicity (ADCC) and antibody dependent cell mediated virus inhibition (ADCVI) mechanisms (Chung *et al*., 2008; Chung *et al*., 2009). ADCC is a pathway whereby NK cells bind to the Fc portion of an antibody that is bound to a virally infected cell and induce lysis of the infected cell through release of cytotoxic granules; while ADCVI refers to viral inhibition as a result of the death of the infected cell. In addition to this, NK cells also secrete pro-inflammatory cytokines that initiate the induction of the antigen-specific immune responses to the HIV-1 infection (Cocchi *et al*., 1995).

Immediately after infection, a large increase in the number of $CD8^+$ T cells is reported (Roos *et al.*, 1994). CTLs peak at approximately 12 months post infection and have been shown to inhibit viral replication as reported above. Furthermore, CTLs produce large amounts of chemokines called Regulated upon Activation, Normal T-cell Expressed (RANTES), which are ligands of the CCR5 co-receptor (Cocchi *et al*., 1995). Through competitive inhibition, RANTES are able to block the entry of the CCR5-tropic HIV-1 into target cells.

The antibody mediated immunity has been the main area of interest since the discovery of HIV-1. Neutralising antibodies that target HIV-1 bind to the gp120 fraction of the Env glycoprotein and interfere with the binding of the virus to host cell receptors, CD4 and CCR5/CXCR4, thereby blocking viral fusion with the host cell membrane (Kwong *et al*., 1998; Klasse & Sattentau, 2012). HIV-1, however, has developed a strategy to minimise recognition by these antibodies. Env is heavily glycosylated, consisting of 24 potential N-glycosylation sites covering most of the protein's surface and 50% of its mass is comprised of glycans (Doores, 2015). It has been proposed that one of the major roles played by these carbohydrates is to form a shield that covers Env and thereby help the virus evade recognition by the neutralising antibodies (Moore *et al*., 2012). However, only a small subset of the antibodies produced by B cells upon HIV-1 infection exhibit neutralising properties. Non-neutralising antibodies function by binding HIV-1 Env through their Fab regions while they use their Fc domains to interact with receptors on different effector cells such NK cells. The non-neutralising antibodies have been implicated in ADCC through the recruitment of NK cells as well as antibody-dependent cellular phagocytosis with the help of phagocytes (Forthal *et al.,* 2013).

In the recent years, a new component of innate immunity towards HIV-1 was discovered. This component, called intrinsic immunity, forms part of the innate immune system and comprises of several genes that encode host restriction factors. Host restriction factors have the ability to inhibit viral replication and manipulate susceptibility of the host cell to HIV-1 infection (An *et al*. 2004; O'Brien & Nelson 2004; An & Winkler 2010). These human restriction factors are further discussed below.

1.6 Human Restriction Factors targeting HIV-1 Replication

In response to viral infections, host cells have developed a set of proteins that restrict HIV-1 replication and spread. These proteins, called host restriction factors, counteract different steps in the viral lifecycle using different mechanisms of action (Lu *et al*., 2013). Although constitutively expressed in some cell types, the expression of these proteins can be upregulated by IFN-α during induction of the innate immune response to viral infection. So far, restriction factors such as the apolipoprotein B mRNA-editing enzyme-catalytic, polypeptide-like 3 (APOBEC3), the tripartite motif-containing protein 5α (TRIM5α), the sterile alpha motif and HD-domain containing protein 1 (SAMHD1) and the bone marrow stromal antigen 2 (BST-2, also known as Tetherin CD317 or HM1.24) are known to be

involved in the control of HIV-1 (Harris *et al*., 2012; Pujol *et al*., 2016; Richardson *et al*., 2014). APOBEC3, TRIM5α and SAMHD1 all counter the reverse transcription step of HIV-1 replication (Coren *et al*., 2015; Wang *et al*., 2012; Laguette *et al*., 2011), while BST-2 acts on the budding of mature virions from infected cells (Casartelli *et al*., 2010; Pujol *et al*., 2016). APOBEC3 functions by deaminating cytosine residues in the newly synthesised proviral DNA, converting them to uracil residues (Harrison *et al*., 2012; Wang *et al*., 2012). This process, known as hypermutation, leads to genome instability and subsequent inability to produce virions with effective replicative fitness. Despite numerous studies conducted to understand how TRIM5α inhibits retroviral infection, the exact mechanism of this restriction factor remains unknown. Previous studies suggested that TRIM5α interacts with the incoming viral core after membrane fusion, leading to capsid disruption and proteosomal degradation, which ultimately inhibits reverse transcription (Coren *et al*., 2015; Richardson *et al*., 2014). SAMHD1 on the other hand acts by hydrolyzing deoxynucleoside triphosphates (dNTPs) to deoxynucleoside and inorganic triphosphate, reducing intracellular dNTP concentrations and thereby inhibiting reverse transcription (Lahouassa *et al*., 2012). BST-2 functions by trapping nascent virions at the cell surface, preventing them from budding off and initiating subsequent infections; this restriction factor is discussed in detail in section 1.7 below.

1.7 The Intrinsic Restriction Factor: BST-2

BST-2 has been identified as an effective cellular factor in blocking the release of HIV-1 virions (along with virions of other enveloped mammalian viruses) by directly cross-linking them to membranes of infected cells (Jouvenet *et al*., 2009). The retained virions subsequently get endocytosed and have been visualised in the early and late endosomes (Neil *et al*., 2008). By preventing the release of these virions, BST-2 ensures that infection is restricted to the originally infected cell, limiting subsequent infections.

1.7.1 The Structural Elements of BST-2

In terms of structure, BST-2 is a 19.7 kDa type II single pass transmembrane (TM) protein, made up of 180 amino acids (Ishikawa *et al*., 1995). The protein is comprised of four main domains, namely, a short 21 amino acid cytoplasmic N-terminal domain, an α-helical TM domain, a coiled-coil extracellular domain, and a C-terminal glycosylphosphatidylinositol (GPI) anchor (Figure 1.3 A) (Kupzing *et al*., 2003). BST-2 is not only localised at the plasma

membrane, where HIV-1 assembly and budding occurs, but also within several endosomal membrane compartments, such as the trans-Golgi network (TGN) as well as early and recycling endosomes. Using domain replacement experiments, the double anchor topology of BST-2, rather than its primary amino acid sequence, was shown to be crucial for this protein's antiviral activity (Perez-Caballero *et al*., 2009). The budding virions were proposed to incorporate one of the membrane anchor domains (either the TM domain or GPI anchor) while the other end remains connected to the plasma membrane of the infected cells, tethering the nascent virions onto the cells (Perez-Caballero *et al*., 2009). In support of this model, immunoelectron microscopy studies demonstrated that BST-2 is associated with virions and located between the viral and cell membranes (Perez-Caballero *et al*., 2009; Fitzapatrick *et al*., 2010; Hammonds *et al*., 2010). In this said model, the extracellular domains of BST-2 form a bridge that spans the gap between the cell and the virion membranes. However, it is not yet clear whether it is the TM domain or the GPI anchor that is inserted into the viral envelope, as both the TM helix and the GPI anchor can be incorporated into HIV-1 virions (Fitzapatrick *et al*., 2010). Another structural element of BST-2 that has been reported to be essential for its antiviral activity is the formation of homodimers (Andrew *et al*., 2009). The extracellular domain of BST-2 contains three cysteine residues that are highly conserved across mammalian orthologs of the protein, and these are C53, C63 and C91 (Figure 1.3 A) (Andrew *et al*., 2009; Perez-Caballero *et al*., 2009). These residues are responsible for the intermolecular disulphide bonds that result in homodimerisation (Andrew *et al*., 2009). Mutational analysis showed that mutation at all three positions resulted in total loss of antiviral activity, while partial bond formation in at least one of the positions showed moderate antiviral activity (Andrew *et al*., 2009; Perez-Caballero *et al*., 2009). These observations suggested that the dimerisation of BST-2 is indeed essential for its antiviral activity. Initially, it was thought that BST-2 could form either parallel or anti-parallel dimers (Figure 1.3 B, C and D). However, subsequent findings showed that removal of either the TM domain or the GPI anchor demolishes the antiviral activity of BST-2 (Arias *et al*., 2011; Perez-Caballero *et al*., 2009), and this supports the parallel homodimer model. These findings also suggest that anti-parallel dimers are very unlikely and cannot effectively tether virions.

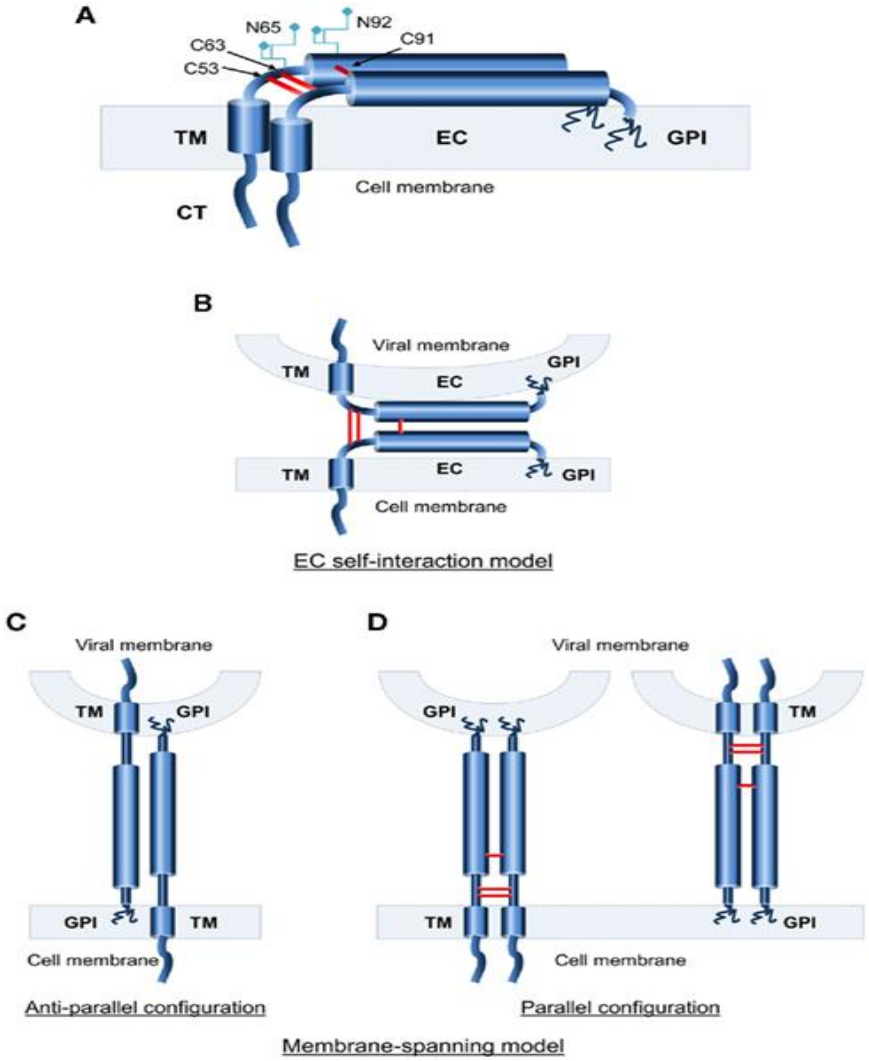

Figure 1.3: Schematic representations of the different hypothetical models of BST-2 orientation. A. Schematic representation of the BST-2 domain structure. BST-2 features a short cytoplasmic N-terminus followed by an α-helical single-pass TM domain, a coiled-coil extracellular domain and a C-terminal GPI anchor. Disulphide linkages are depicted in red, and two N-linked glycosylation sites (N65 and N92) shown in blue. **B.** Individual BST-2 monomers incorporated into the same membrane at both ends. **C.** BST-2 monomers incorporated into different membranes in an anti-parallel orientation. **D.** Parallel BST-2 monomers incorporated into different membranes. Figure adapted from Arias *et al.* (2011).

1.7.2 Additional Functions of BST-2

The aggregation of HIV-1 viral particles on the surface of infected cells caused by BST-2 causes the infected cells to be more susceptible to the NK cell-mediated ADCC mentioned above. Reports show that the non-neutralising antibodies bind to the Env protein on the tethered virions and subsequently recruit effector NK cells (Alvarez *et al*., 2014; Arias *et al*., 2014). This leads to degranulation of NK cells, resulting in the release of perforins and granzymes, and the subsequent lysis and death of the HIV-1 infected cells. The NK cell-mediated ADCC is increasingly recognised as one of the most efficient immune responses against HIV-1 infection.

Furthermore, by tethering enveloped viruses to the surface of infected cells, BST-2 also stimulates innate immune responses (Galao *et al*., 2012). Before its identification as a restriction factor, BST-2 was reportedly identified as an activator of the nuclear factor kappa-light-chain-enhancer of activated B cells (NF-κB) transcription factor (Matsuda *et al*., 2003). NF-κB plays a crucial role in the innate immune and antiviral responses as it regulates the expression of numerous genes involved in cell survival, inflammation, and immunity. In the absence of a stimulus, NF-κB is sequestered within the cell cytosol in an inactive form bound by the inhibitor of κB (IκB) protein, which is in turn regulated by an upstream kinase known as IκB kinase complex (IKK) (Gilmore *et al*., 2006). The BST-2-mediated NF-κB activation was reported to map to a di-tyrosine motif (Y_6xY_8) in the cytoplasmic tail of BST-2, which was previously identified as an endocytosis signal (Rollason *et al*., 2007; Galao *et al*., 2012; Tokarev *et al*., 2013). Mutagenesis studies by Galao *et al*. (2012) further discovered that the three amino acids downstream of the Y_6xY_8 motif were also essential for the NF-κB activation, thereby extending the NF-κB signalling motif to Y_6xY_8CRV. It was reported that it is the accumulation of trapped virions on the surface of infected cells that leads to the phosphorylation of the two conserved tyrosine residues within the Y_6xY_8CRV motif of BST-2.

The tyrosine phosphorylation leads to the recruitment of the spleen tyrosine kinase (Syk), and the subsequent formation of the TNF receptor-associated factor (TRAF) 2, TRAF 6, and E2 ubiquitin conjugating enzyme 13 (Ubc13)-mediated stimulation of the TGF-β-activated kinase 1 (TAK1) complex (Skuang *et al*., 2009; Galao *et al*., 2012). This, in-turn, induces the phosphorylation and proteasomal degradation of IκB by IKK, which results in the activation

of NF-κB. The activated NF-κB is then translocated to the nucleus where it activates expression of inflammatory genes.

1.8 HIV-1 Accessory Proteins Counteract Immunity

To establish a successful infection, intracellular pathogens, including HIV-1, must evade host immunity. One way that HIV-1 achieves this goal is through the activity of the viral accessory proteins. The HIV-1 accessory proteins antagonise the antiviral activity of the host cell restriction factors, thereby allowing the virus to replicate and spread more efficiently (Malim & Emerman, 2008; Malim, 2014). These viral proteins act by binding to the restriction factors, inducing their degradation and/or mis-localisation to a subcellular location where they can no longer execute their antiviral activity. For example, Vif simultaneously binds APOBEC3 and the E3 ubiquitin ligase complex, inducing the proteasomal degradation of APOBEC3 (Sheehy *et al*., 2003; Marin *et al*., 2003). By driving the ubiquitin-dependent degradation of APOBEC3, Vif enables HIV-1 to escape the APOBEC3-mediated antiviral restriction (Stopak *et al*., 2003; Mangeat *et al*., 2003; Zhang *et al*., 2003). A similar mechanism is employed by HIV-1 Vpu to eliminate BST-2 from cells. HIV-1 Vpu acts as an adaptor that promotes an interaction between the ubiquitin ligase substrate adaptor, Beta transducing repeat-containing protein (β-TrCP), and BST-2. This promotes ubiquitination of the BST-2 by the Skp1-Cullin1-F Box (SCF) E3 ubiquitin ligase complex.

In non-dividing mammalian cells, free diffusion of cellular contents into the nucleus is limited to components that are less than 40 kDa (Feldherr & Feldherr, 1960; Kogan & Rappaport, 2011). HIV-1, however, is unique among retroviruses in that it is able to infect non-dividing cells (Lewis & Emerman, 1994). Vpr has been shown to play an important role in the localisation of the HIV-1 PIC into the nucleus, playing a critical role in the infection of non-dividing cells by HIV-1 (Heinzinger *et al*., 1994; Kogan & Rappaport, 2011). Another unique activity performed by HIV-1 Vpr is the blockade of the cell cycle in the G2/M phase, a process commonly known as the G2 arrest (Jowett *et al*., 1995; Rogel *et al*., 1995). The G2 is a phase where the viral LTR promoter is more active; so, arresting the cell cycle in this phase increases the rate of HIV-1 transcription and viral replication (Goh *et al*., 1998). Nef plays a role in the stimulation of virion infectivity and the downregulation of CD4 and the MHC I molecules (Goldsmith *et al*., 1995; Mangasarian & Trono, 1997). Nef interacts with CD4 and recruits the clathrin adaptor protein AP-2, leading to the formation of clathrin-coated pits. Clathrin-coated vesicles containing CD4 are then endocytosed to the lysosomes

where they get degraded (Aiken *et al*., 1994). The Nef-mediated CD4 downregulation protects infected cells from undergoing a second round of infection, known as super-infection, which may otherwise lead to death of the infected cells and lower production of new virions (Benson *et al*., 1993). Using a similar mechanism, Nef also downregulates the cell-surface expression of MHC I molecules, and this results in HIV-1 infected cells evading detection and eradication by CTLs (Schwartz *et al*., 1996).

1.9 Contribution of HIV-1 Vpu to Pathogenesis

1.9.1 General Properties of HIV-1 Vpu

HIV-1 Vpu is one of the smallest HIV-1 proteins comprising of 81 amino acids and a molecular weight of 9 kDa (Cohen *et al.*, 1988; Strebel *et al.*, 1988). HIV-1 Vpu is a type I transmembrane (TM) protein that is expressed in HIV-1 and a few simian immunodeficiency virus (SIV) isolates such as SIVcpz (chimpanzee) and SIVgsn (greater spot-nosed monkey), but not in HIV-2 (Dube *et al*., 2010a). HIV-1 Vpu is expressed in the later stages of viral infection from a bicistronic mRNA that also encodes HIV-1 Env, ensuring synchronous expression of the two proteins (Dube *et al*., 2010a; Strebel *et al*., 1996). HIV-1 Vpu is inserted into membranes of infected cells, but not incorporated into mature virions. The localisation of this protein varies among different HIV-1 subtypes. In subtype B strains, HIV-1 Vpu accumulates mainly within intracellular membranes such as the TGN and the endoplasmic reticulum (ER), while in subtype C strains, HIV-1 Vpu is found both at the plasma membrane and the TGN (Dube *et al*., 2009; Pacyniak *et al*., 2005). The localisation of HIV-1 Vpu is determined by specific trafficking signals within the primary amino acid sequence of the protein. Arginine (R) 30 and Lysine (K) 31 have been shown to be responsible for the accumulation of the protein in the TGN (Dube *et al*., 2009; Fritz *et al*., 2012), while ExxxLV and Tryptophan (W) 76 are responsible for association with the plasma membrane (Petit *et al*., 2011; Vigan & Neil, 2010).

HIV-1 Vpu is comprised of a short luminal N-terminal domain (residues 1 – 3), an α-helical TM domain (residues 4 – 27) which functions as an anchor, and a hydrophilic C-terminal domain (residues 28 – 81) that protrudes into the cytoplasm (Figure 1.4 A and B; Strebel *et al.*, 1988). The TM domain and the cytoplasmic domain are connected by a short, flexible hinge region. Using two-dimensional nuclear magnetic resonance (NMR) spectroscopy, Wray *et al.*, 1995 and Federau *et al.*, 1996 determined that the cytoplasmic domain of HIV-1

Vpu contains two α-helices (residues 32 – 49 and 57 – 71, respectively) that are separated by an unstructured linker region (residues 50 – 56). The linker region contains two highly conserved serine (S) residues at position 52 and 56 (D**S**GNE**S**; Figure 1.4 A and B), and these are subject to phosphorylation by casein kinase II (CK-II) (Cohen *et al*., 1988; Strebel *et al*., 1988; Schubert *et al*., 1994). Phosphorylation of these serine residues facilitates recruitment of β-TrCP, a subunit of the $SCF^{\beta\text{-}TrCP}$ E3 ubiquitin ligase complex, allowing HIV-1 Vpu to perform some of its basic functions as discussed below. HIV-1 Vpu has been attributed to two major functions in the HIV-1 replication cycle. Firstly, HIV-1 Vpu targets newly synthesised CD4 receptor molecules for proteasomal degradation, and it also enhances the release of viral particles from infected cells through counteracting the antiviral activity of BST-2.

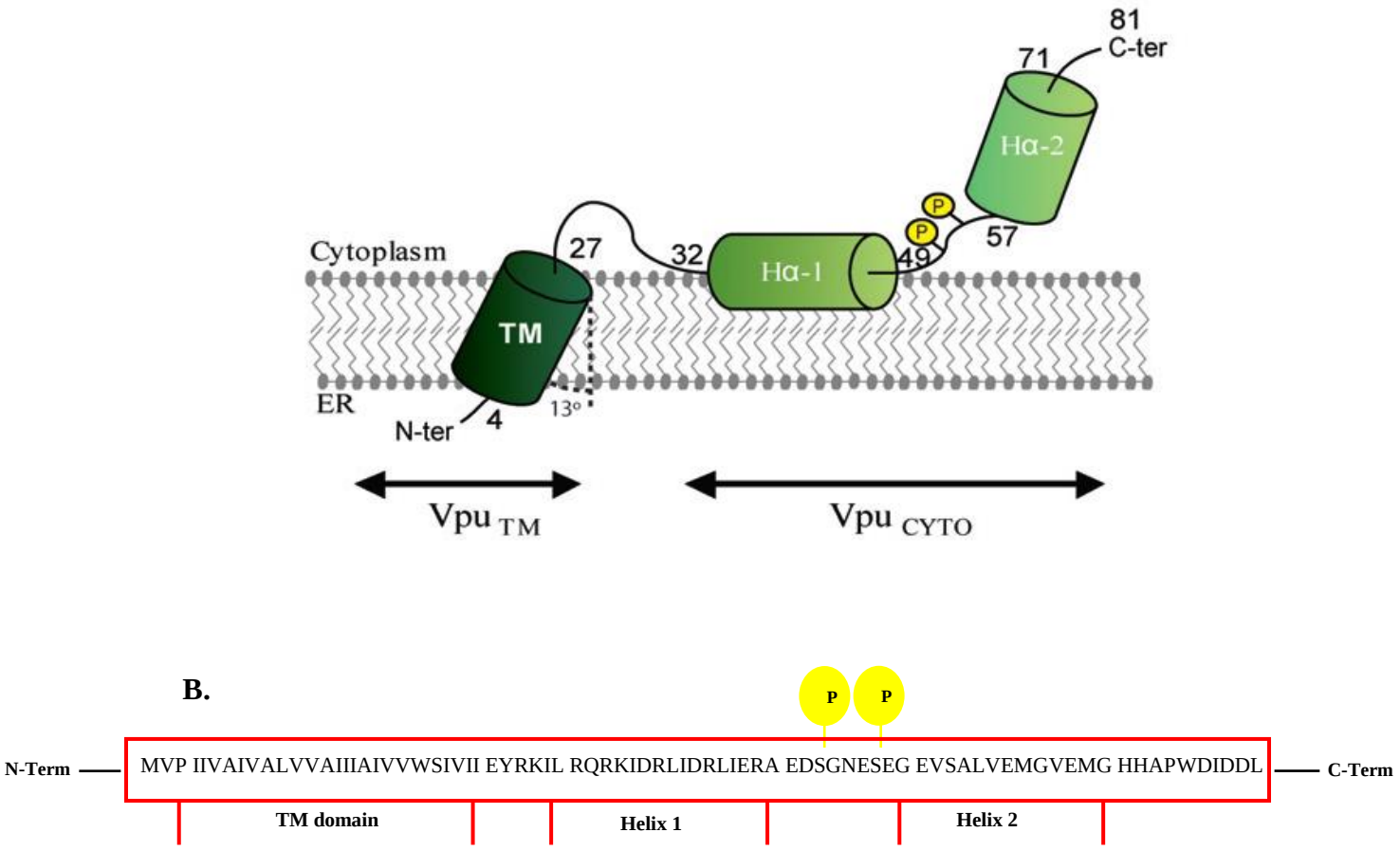

Figure 1.4: Schematic representation of HIV-1 Vpu. A. The predicted secondary and tertiary structure of HIV-1 Vpu showing the relatively short N-terminal domain, the transmembrane domain (TM) and the two α-helices in the cytoplasmic domain and the as determined by NMR elucidation. The two conserved serine residues, which are sites of phosphorylation, are shown in yellow. **B.** Sequence presentation of HIV-1 Vpu, with the amino acids that constitute the different domains shown. Figure 1.4A: adapted from Dube *et al.*, 2010b.

1.9.2 The Role of HIV-1 Vpu in CD4 Surface Down-Modulation

One of the major roles played by HIV-1 Vpu during HIV-1 infection is the downregulation of CD4 levels in the ER. In addition to super-infection, the presence of CD4 in the ER results in the formation of complexes between HIV-1 Vpu and the Env precursor protein, gp160. This binding leads to gp160 getting trapped in the ER, and its trafficking to the plasma membrane being inhibited (Lama *et al*., 1999). HIV-1 Vpu has also been shown to bind to the cytoplasmic tail of newly synthesised CD4 molecules through its cytoplasmic α-helices in the ER, causing CD4 to be retained in the ER (Cortes *et al*., 2002; Levesque *et al*., 2003; Tanaka *et al*., 2003). Furthermore, the binding of the $SCF^{\beta\text{-}TrCP}$ E3 ubiquitin ligase complex to serine 52 and 56 of HIV-1 Vpu results in the polyubiquitination of CD4 (Margottin *et al.,* 1998; Meusser & Sommer *et al*., 2004; Binette *et al*., 2007). The ubiquitination of CD4 induces the degradation of the protein through an ER-associated protein degradation (ERAD)-like process, which leads to proteosomal degradation of the protein (Schubert *et al*., 1998; Magadan *et al*., 2010). HIV-1 Vpu acts as an adaptor between CD4 and the E3 ubiquitin ligase complex but does not get ubiquitinated or degraded in the process. This HIV-1 Vpu-mediated degradation of CD4 destabilises CD4–gp160 complexes in the ER, allowing Env to mature and to be incorporated into progeny virions while also minimizing super-infection of infected cells (Wildum *et al*., 2006).

1.9.3 HIV-1 Vpu Downregulates NTB-A, PVR and CD1d

In the recent years, a novel activity of HIV-1 Vpu was reported, and that is the downregulation of the NK cells co-activating receptor, NK-T-and-B cell antigen (NTB-A) on the surface of HIV-1 infected cells (Richard & Cohen, 2010; Shah *et al*., 2010). NTB-A is a member of the signalling lymphocytic activation molecule (SLAM) family of receptors, that function as co-activators to initiate the degranulation of NK cells in which lytic granules are released in order to facilitate lysis of the target cell (Bottino *et al*., 2001; Ward *et al*., 2007). HIV-1 Vpu interferes with NK-cell degranulation by downregulating NTB-A levels on the surface of HIV-1 infected cells, thereby protecting infected cells from lysis by NK cells (Ward *et al*., 2007; Fogli *et al*., 2008). In studies where a HIV-1 Vpu mutant was used, 50% more NK cell degranulation was observed compared to wild-type HIV-1 infections, resulting in a higher capacity to lyse HIV-1-infected cells (Shah *et al*., 2010). HIV-1 Vpu binds NTB-A through its TM domain, possibly resulting in the mis-trafficking of the co-receptor and as such, sequestration of NTB-A in an intracellular compartment (Shah *et al*., 2010).

Using a similar mechanism as reported for the NTB-A downregulation, HIV-1 Vpu has been implicated in modulating yet another NK cell ligand called the poliovirus receptor (PVR or CD155) (Matusali *et al*., 2012). PVR is recognised by the activating receptor, DNAX accessory molecule-1 (DNAM-1, also known as CD226), expressed by NK cells (Shibuya *et al*., 1996; Tahara-Hanaoka *et al*., 2004). Upon engagement by PVR, DNAM-1 enhances cytokine production and the release of lytic granules by NK cells. By downregulating the expression of PVR on the surface of HIV-1-infected cells, HIV-1 Vpu further contributes to the evasion of recognition and lysis of infected cells by NK cells (Tomasec *et al*., 2005; Magri *et al*. 2011). Although Nef plays a major role in the downregulation of PVR, this modulation was shown to be much more enhanced in the presence of HIV-1 Vpu, while the opposite was also observed in instances where the HIV-1 Vpu-deficient virus was used (Matusali *et al*., 2012). Using mutational analysis, it was shown that although the TM domain of HIV-1 Vpu is crucial for targeting PVR, as was reported for BST-2 downregulation, the S_{52} and S_{56} residues are largely dispensable (Matusali *et al*., 2012).

HIV-1 Vpu has also been found to downregulate the expression of CD1d on the surface of HIV-1 infected DCs (Moll *et al*., 2010). This protein is expressed on the surface of antigen presenting cells (APCs), such as monocytes, macrophages as well as DCs, and is responsible for the presentation of lipid antigens to NKT cells. This presentation leads to the simultaneous activation of NKT cells and the subsequent induction of the host immune responses. Therefore, by interfering with the CD1d antigen presentation pathway, HIV-1 Vpu prevents infected DCs from activating NKT cells, and therefore evades innate immune responses (Moll *et al*., 2010). HIV-1 Vpu achieves this by binding to recycled CD1d in the early endosomes, resulting in the sequestration of CD1d in an intracellular compartment, preventing it from recycling back to the plasma membrane.

1.9.4 HIV-1 Vpu Inhibits the NK cell-mediated ADCC and the NF-κB Pathway

By antagonising the antiviral activity of BST-2, HIV-1 Vpu does not only enhance the release of virions, but also helps HIV-1 protect infected cells from the NK cell-mediated ADCC (Alvarez *et al*., 2014; Arias *et al*., 2014). The downregulation of BST-2 by HIV-1 Vpu limits the number of trapped virions and thus the quantity of the Env glycoprotein on the surface of HIV-1 infected cells; this reduces the recognition of infected cells by cytotoxic-inducing antibodies and their susceptibility to NK-mediated ADCC (Viellette *et al*., 2013; Viellette *et al*., 2014). HIV-1 Vpu is also able to counteract the BST-2-mediated activation of the NF-κB

signalling, and this inhibitory effect requires the ability of HIV-1 Vpu to bind to the cellular β-TrCP-E3-ubiquitin ligase complex, which was previously shown to mediate the ubiquitination and proteosomal degradation of IκB and the subsequent activation of the NF-κB signalling (Cocka & Bates, 2012; Galao *et al*., 2012; Tokarev *et al*., 2013). Phosphorylated HIV-1 Vpu however, has high affinity for and competitively binds to β-TrCP, forming HIV-1 Vpu/β-TrCP complexes (Bour *et al*., 2001; Besnard-Guerin *et al*., 2004). This interferes with the cellular functions in which β-TrCP is normally involved, including the degradation of IκB (Tokarev *et al*., 2012). This leads to reduced NF-κB activation, meaning that the transcription of genes involved in cell proliferation and cytokine production cannot be triggered.

1.9.5 Surface Down-Modulation of MHC molecules

One of the less-defined roles of HIV-1 Vpu is the downregulation of MHC I molecules on the surface of HIV-1 infected cells (Kerkau *et al*., 1997). MHC I molecules present pathogen-derived peptides to specific CTLs, thereby inducing killing of pathogen-invaded cells by CTLs (Yewdell & Bennink, 1992). These molecules thus play a critical role in the eradication of virus infected cells, and as a result, viruses have developed strategies to interfere with the MHC I-mediated immune responses (Yewdell & Hill, 2002). One of the strategies employed by viruses to evade recognition by CTLs is to decrease the surface expression levels of MHC I molecules. Three of HIV-1's proteins are implicated in the down-modulation of these molecules from infected cells, namely, Nef, Tat and Vpu (Petersen *et al*., 2003). Although the mechanism by which HIV-1 Vpu downregulates MHC I has not been investigated since its effect on MHC I surface levels was observed, it was reported that HIV-1 Vpu interferes with the biosynthetic pathway of immature MHC I molecules, retaining them in the ER (Schwartz *et al*., 1996; Kerkau *et al*., 1997).

Further to this, HIV-1 Vpu has also been shown to downregulate the surface expression of mature MHC II molecules (Hussain *et al*., 2008). HIV-1 Vpu achieves this through an interaction with the MHC II invariant chain, CD74; a type II transmembrane protein that binds the α and β chains of MHC II molecules in the ER (Becker-Herman *et al.,* 2005). The interaction between HIV-1 Vpu and CD74 leads to reduced surface expression levels of mature MHC II molecules in HIV-1 infected cells followed by reduced antigen expression and decreased activation of T cells. The interaction of HIV-1 Vpu with CD74 maps to helix 1

in HIV-1 Vpu's cytoplasmic domain, and a 30-amino acid C-terminal domain of CD74 (Hussain *et al*., 2008).

1.9.6 The Ion Channel Activity of HIV-1 Vpu

Structural similarities between HIV-1 Vpu and the membrane channel-forming M2 protein encoded by the influenza A virus were noted shortly after the discovery of HIV-1 Vpu (Klimkait *et al.,* 1990). Because of these similarities, it was hypothesised that HIV-1 Vpu might be a functional analog of M2 in HIV-1 (Klimkait *et al.,* 1990; Schubert *et al.,* 1994; Friborg *et al.,* 1995). This led to investigations about the possible ion channel activity of this protein in lipid bilayers. Experimental studies confirmed that HIV-1 Vpu does indeed form ion channels (Ewart *et al.,* 1996; Schubert et al., 1996). The ion channel activity of HIV-1 Vpu was reported to be selective for monovalent cations such as sodium (Na^+) and potassium (K^+) as opposed to anions (Ewart *et al.,* 1996). The relevance of this activity of HIV-1 Vpu in viral pathogenesis, however, remains unclear. Schubert *et al.* (1996) reported a possible correlation between the ability of HIV-1 Vpu to form ion channels and its capacity to enhance virion release as both activities are mediated by the TM domain. Subsequent studies, however, argued against the involvement of the ion channel activity in down-regulating the BST-2 mediated restriction of virion release. Single point mutations that affected the ion channel activity of HIV-1 Vpu (i.e. S23A and S23L on HIV-1 Vpu's TM domain) did not impair the ability of this protein to enhance virion release. Conversely, mutations of A14 and A18 to asparagines affected the binding of HIV-1 Vpu to BST-2, thereby impairing the release of virions. These mutations, however, did not affect the ion channel activity of this protein (Bolduan *et al.,* 2011). In 2010, a novel antiretroviral drug, BIT225 (N-carbamimidoyl-5-(1-methyl-1H-pyrazol-4-yl)-2-naphthamide) was reported to inhibit the ion channel activity of HIV-1 Vpu (Khoury *et al*., 2010). Further studies involving BIT225 showed late stage inhibition of HIV-1 virion release from infected monocyte-derived macrophages (MDM) cells (Ewart *et al.,* 2004; Khoury *et al*., 2010), a phenotype similar to the BST-2 mediated restriction. Examination of the effect of BIT225 on the binding of HIV-1 Vpu to BST-2 showed that this compound does not hinder this interaction (Kuhl *et al.,* 2011). These findings suggest that both the ion channel activity and the binding of HIV-1 Vpu to BST-2 enhance the release of virions from infected cells.

1.9.7 Enhancement of Virion Release

HIV-1 Vpu counteracts the antiviral activity of BST-2, preventing it from trapping budding viral particles on the surface of HIV-1 infected cells, and promoting efficient viral release. HIV-1 Vpu overcomes the BST-2 restriction by removing the restriction factor from viral budding sites through intracellular trapping and sequestration, surface downregulation and/or trafficking alteration mechanisms discussed below.

1.9.7.1 BST-2 surface downregulation

HIV-1 Vpu is involved in enhancing the release of newly formed HIV-1 virions from the surface of infected cells by antagonising the antiviral activity of BST-2 (Strebel *et al*., 1988; Terwilliger *et al*., 1989). Although the exact mechanisms involved in the HIV-1 Vpu-mediated downregulation of BST-2 are not fully elucidated, current data suggests several possible mechanistic actions; i.e. degradation, cell-surface downregulation and trafficking alteration which results in intracellular sequestration of BST-2 within the endomembrane system (Figure 1.5; Dubé *et al*., 2010b). Although mechanistically distinct, these modes of antagonism all rely on the ability of HIV-1 Vpu to bind BST-2, since viral particle release was restored when mutations disrupting the binding of the two proteins were introduced (Douglas *et al*., 2009; Iwabu *et al*., 2009; Mangeat *et al*., 2009; Dubé *et al*., 2010b). Similar to the HIV-1 Vpu-mediated down-modulation of CD4, the β-TrCP protein from the SCF E3 ubiquitin ligase complex is required for the downregulation of BST-2 from the cell surface by HIV-1 Vpu (Mitchell *et al*., 2009; Mangeat *et al*., 2009). In support of this, mutation studies on the β-TrCP protein and the D**S**Gxx**S** β-TrCP binding motif on the HIV-1 Vpu impaired the HIV-1 Vpu-mediated BST-2 cell surface downregulation (Douglas *et al*., 2009; Dubé *et al*., 2010b). The interaction of HIV-1 Vpu with β-TrCP leads to the ubiquitination and lysosomal degradation of BST-2, ultimately resulting in a reduction in surface levels and an enhancement of viral release (Mitchell *et al*., 2009; Douglas *et al*., 2009).

1.9.7.2 Intracellular sequestration of BST-2

In addition to the degradation of BST-2 from the plasma membrane, HIV-1 Vpu alters the trafficking of BST-2 towards the cell surface, resulting in intracellular sequestration of BST-2 away from the plasma membrane, its site of action (Figure 1.5; Dubé *et al*., 2010b). HIV-1 Vpu interacts with BST-2 in the TGN, trapping BST-2 molecules in the TGN and blocking their trafficking along the secretory pathway, leading to reduced levels of BST-2 on the

plasma membrane. The trapped BST-2 is subsequently ubiquitinated through a β-TrCP E3 ligase complex-dependent mechanism (Mangeat *et al*., 2009; Mitchell *et al*., 2009; Douglas *et al*., 2009; Iwabu *et al*., 2009). The ubiquitinated BST-2 is then recognised and bound by the hepatocyte growth factor-regulated tyrosine kinase substrate (HRS), a key component of the endosomal sorting complex required for transport (ESCRT)-0 complex (Mitchell *et al*., 2009; Janvier *et al*., 2011). The ESCRT machinery is involved in the sorting of ubiquitinated membrane proteins to the multivesicular bodies (MVBs) for their subsequent degradation in the lysosomes. BST-2 thus undergoes ESCRT-0-dependent sorting for the lysosomal degradation pathway (Janvier *et al*., 2010).

1.9.7.3 Physical interactions between HIV-1 Vpu and BST-2

The ability of HIV-1 Vpu to interact with BST-2 has been shown to be crucial for both the downregulation of BST-2 from the cell surface, as well as the intracellular sequestration of BST-2. Co-immunoprecipitation studies confirmed that HIV-1 Vpu counteracts BST-2 *via* interactions through their α-helical TM domains (Arias *et al*., 2011; Skasko *et al*., 2012; Park *et al*., 2006; Zhou *et al*., 2012). Mutations at positions I34, L37 and L41 of BST-2 (Kobayashi *et al*., 2011), and positions A14, A18, and W22 of HIV-1 Vpu (Vigan & Neil, 2010) severely compromised the ability of HIV-1 Vpu to counteract BST-2, suggesting a high specificity of the interaction between these proteins. Solid state NMR studies revealed that the said residues lie on the same side of the helix in both proteins, suggesting that these residues possibly form the interaction interface between the HIV-1 Vpu and the BST-2 transmembrane helices (Figure 1.6).

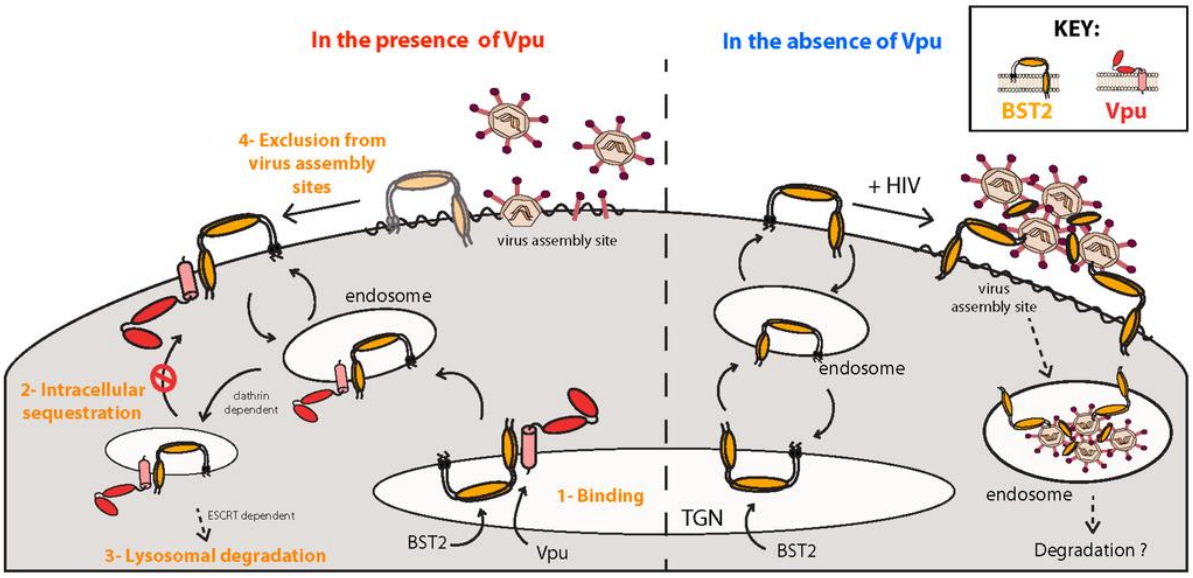

Figure 1.5: Schematic representation of the different modes of HIV-1 Vpu-mediated BST-2 counteraction during HIV-1 infection. In the absence of HIV-1 Vpu (right), accumulation of BST-2 on the cell surface results in the incorporation of BST-2 molecules into nascent virions, leading to inhibition of virus particle release. These BST-2-entrapped virions may be internalised and potentially degraded. **In the presence of HIV-1 Vpu** (left), HIV-1 Vpu binds BST-2 within the vesicular system, resulting in the sequestration of BST-2 in the endosomes. Sequestered BST-2 proceeds along the endosomal sorting complexes required for transport (ESCRT) pathway and subsequently gets degraded in the lysosomes. HIV-1 Vpu also binds BST-2 at the cell membrane and induces its removal using an AP-2 and clathrin-dependent system. This pool of BST-2 may subsequently recycle into endosomal compartments for sequestration and degradation. Figure adapted from Sugden *et al.* (2016).

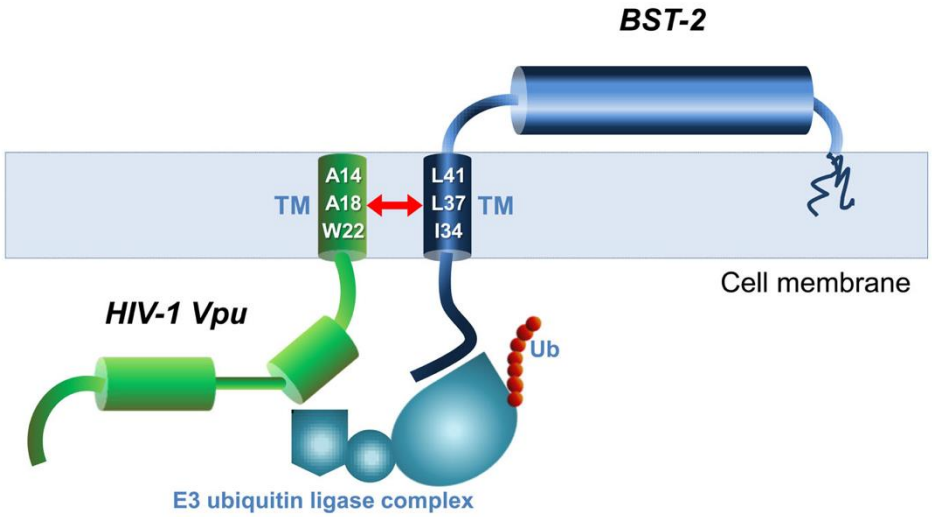

Figure 1.6: Schematic representation of the binding of HIV-1 Vpu to BST-2. HIV-1 Vpu binds BST-2 in the trans-Golgi network (TGN) and targets BST-2 for lysosomal degradation through the recruitment of the E3 ligase complex. This results in the free release of HIV-1 virions. Alanine 14, Alanine 18 and Tryptophan 22 on the HIV-1 Vpu with Isoleucine 34, Leucine 37 and Leucine 41 on the BST-2 have been identified as crucial residues for this interaction. Figure adapted from Arias *et al*. (2011).

Table 1.3: Summary of the functions of HIV-1 Vpu and their relevance in HIV-1 pathogenesis

Cellular Target	Co-factor	Mechanism	Biological effect	References
CD4	β-TrCP	Proteosomal degradation	Avoid super-infection	Wildum *et al*., 2006
BST-2	β-TrCP	Cell surface downregulation Lysosomal degradation	Enhance virion release Inhibit the BST-2-induced NF-κB pathway Inhibit the NK cell-mediated ADCC response	Dubé *et al*., 2010b Galao *et al*., 2012 Viellette *et al*., 2014
Unknown	Unknown	Ion channel activity	Enhance virion release	Kuhl *et al.*, 2011
NTB-A	Unknown	Cell surface downregulation	Avoid NK-cell-mediated killing	Fogli *et al*., 2008
CD1d	Unknown	Cell surface downregulation	Escape NKT recognition	Moll *et al*., 2010
PVR	Unknown	Cell surface downregulation	Avoid NK-cell-mediated killing	Magri *et al*. 2011
MHC molecules	Clathrin adaptor AP-1	Lysosomal degradation	Reduce antigen presentation Avoid killing by CTLs	Hussain *et al*., 2008 Petersen *et al*., 2003

1.10 The HIV-1 Vpu/BST-2 Interaction as a Potential Target for HIV-1 Therapy

HIV-1 has evolved various strategies to evade the host immune responses, and these are mainly carried out by the viral accessory proteins (including HIV-1 Vpu). As detailed above, HIV-1 Vpu plays many crucial roles in the pathogenesis of HIV-1; i.e. cell surface reduction of CD4, enhancement of virion release from infected cells, detraction of the expression of MHC I and II molecules, NTB-A, PVR and CD1d recognised by CTLs, NK cells and NKT cells, respectively. Overall, HIV-1 Vpu targets over six cell surface proteins involved in various aspects of the immune response, and this raises the possibility that HIV-1 Vpu may be one of the key factors used by HIV-1 to evade immunity. The crucial functions of HIV-1 Vpu make this protein an attractive target for therapeutic interventions for treating HIV-1 infection.

The HIV-1 Vpu-mediated downregulation of BST-2 is one of the major roles of HIV-1 Vpu and given the effective antiviral activity of BST-2 and its constitutive expression in several human immunocytes, it is rational to devise a strategy that can expose HIV-1 to this host restriction factor. Since the interaction between HIV-1 Vpu and BST-2 through their respective TM domains has previously been shown to be crucial for both the downregulation and the sequestration of BST-2 by HIV-1 Vpu, blocking the interaction between these two proteins should, in theory, expose HIV-1 infected cells to the antiviral activity of BST-2. This means that budding of virions from HIV-1 infected cells should be hindered, leading to an impairment in HIV-1 replication. Moreover, HIV-1 infected cells should be susceptible to the ADCC activity of NK cells, and the NF-κB pathway should also be activated.

In the recent years, several attempts have been made to discover small molecular compounds that can target HIV-1 Vpu. The identification of BIT225 as an HIV-1 inhibitor targeting HIV-1 Vpu proved HIV-1 Vpu to be a druggable target and opened the feasibility of developing a new class of anti-HIV-1 drugs that act against HIV-1 Vpu. Following the discovery of BIT225, two compounds, Lapachol (2-hydroxy-3-(3-methyl-2-butenyl-)-1,4-naphthoquinone) and 6-aza-2-thiouridine were discovered to restore cell surface levels of BST-2 in the presence of HIV-1 Vpu (Figure 1.7; Mi *et al*., 2015; Zhang *et al*., 2016). Both compounds were reported to expose HIV-1 to the restrictive action of BST-2 and inhibit the release of HIV-1 virions, thereby strongly suppressing the replication of HIV-1. Additional studies

revealed that neither Lapachol nor 6-aza-2-thiouridine prevented HIV-1 Vpu from binding to BST-2 or β-TrCP; but Lapachol inhibited the lysosomal degradation of BST-2 by interfering with the sorting of the restriction factor into lysosomes, while 6-aza-2-thiouridine reduced the HIV-1 Vpu-induced BST-2 ubiquitination levels. Although the mechanisms by which both these compounds block BST-2 degradation and restore the BST-2 surface levels are not completely clear, their discovery further supports the notion of using small molecule compounds to block the antagonist function of HIV-1 Vpu and thereby expose HIV-1 to restriction by BST-2.

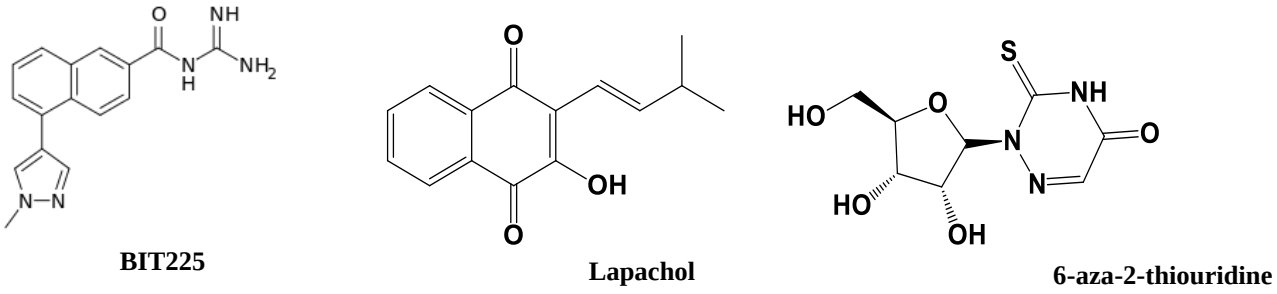

Figure 1.7: Chemical structures of BIT225, Lapachol and 6-aza-2-thiouridine, the three compounds that have been shown to inhibit the activity of HIV-1 Vpu.

1.11 Project Rationale and Motivation

Antiretrovirals against HIV-1 have mostly been successful in turning the infection into a chronic condition when the treatment is available. However, even with the multiple classes of FDA approved antiretrovirals and the positive impact of cART; development of drug resistance is inevitable for this rapidly mutating virus. This makes identification of new therapeutic targets a high priority in HIV-1 research. Over the past years, one of the major focuses in HIV-1 research has been the understanding of the interactions that occur between HIV-1 and the host cell during viral replication. Encoding only 15 proteins, HIV-1 uses factors present in host cells to complete its replication cycle. Since these host-viral interactions directly mediate viral replication and disease progression, their specific disruption can provide alternative targets for therapeutic intervention. Any interaction between viral proteins and host cofactors has the potential to be a target for drug design (Taltynov *et al*., 2012).

The CCR5 antagonist, Maraviroc, mentioned above was the first approved antiretroviral drug to target a host-virus interaction (Dorr *et al*., 2005; Sayana *et al*., 2009). The successful targeting of this interaction demonstrated that HIV-1 therapeutic drug targets are not only limited to virus-encoded enzymes but understanding of the virus-host interactions can provide the basis for future anti-HIV therapeutics. Furthermore, the interaction between IN and its host nuclear binding partner, LEDGF, has also been identified as a potential drug target (Christ *et al*., 2010). Promising compounds, like Tert-butoxy-(4-phenyl-quinolin-3yl)-acetic acids (tBPQAs) and related analogues, 2-(quinolin-3-yl) acetic acid derivatives (LEDGINs) and BB22678, have been identified as inhibitors for the IN-LEDGF interaction (Christ *et al*., 2010; Tsiang *et al*., 2012).

Currently, there are no antiretroviral drugs that target the binding of HIV-1 Vpu to BST-2 in the market. Since the binding between these two proteins occurs through their TM domains, designing small molecule compounds that target the TM domain of HIV-1 Vpu, particularly A14, A18, as well as W22, and hinder the binding of HIV-1 Vpu to BST-2 seems logical. Such compounds would competitively bind to HIV-1 Vpu's TM domain, block the binding of HIV-1 Vpu to BST-2 and thereby overcome the HIV-1 Vpu-induced restriction of virion release.

1.12 Research Aim and Objectives

The aim of this study was to purify and characterise HIV-1 Vpu and to identify potential inhibitors of the interaction of HIV-1 Vpu with BST-2. This was accomplished through completion of the following objectives:

1. Overexpression, purification and characterisation of recombinant HIV-1 Vpu.

2. Development of biological assays for the screening and identification of possible inhibitors for the interaction of HIV-1 Vpu with BST-2.

3. Characterisation of the pharmacological properties of the identified inhibitors.

4. Analysis of the binding of the identified inhibitors to HIV-1 Vpu.

1.13 References

Aasa-Chapman, M.M., Holuigue, S., Aubin, K., Wong, M., Jones, N.A., Cornforth, D., Pellegrino, P., Newton, P., Williams, I., Borrow, P. and McKnight, A., 2005. Detection of antibody-dependent complement-mediated inactivation of both autologous and heterologous virus in primary human immunodeficiency virus type 1 infection. *Journal of virology*, *79*(5), pp.2823-2830.

Adamson, C.S. and Freed, E.O., 2007. Human immunodeficiency virus type 1 assembly, release, and maturation. *Advances in pharmacology*, *55*, pp.347-387.

Aiken, C., Konner, J., Landau, N.R., Lenburg, M.E. and Trono, D., 1994. Nef induces CD4 endocytosis: requirement for a critical dileucine motif in the membrane-proximal CD4 cytoplasmic domain. *Cell*, *76*(5), pp.853-864.

Akira, S. and Takeda, K., 2004. Toll-like receptor signalling. *Nature reviews immunology*, *4*(7), pp.499.

Akira, S., Uematsu, S. and Takeuchi, O., 2006. Pathogen recognition and innate immunity. *Cell*, *124*(4), pp.783-801.

Alvarez, R.A., Hamlin, R.E., Monroe, A., Moldt, B., Hotta, M.T., Caprio, G.R., Fierer, D.S., Simon, V. and Chen, B.K., 2014. HIV-1 Vpu antagonism of tetherin inhibits antibody-dependent cellular cytotoxic responses by natural killer cells. *Journal of virology*, pp.JVI-00449.

An, P., Bleiber, G., Duggal, P., Nelson, G., May, M., Mangeat, B., Alobwede, I., Trono, D., Vlahov, D., Donfield, S. and Goedert, J.J., 2004. APOBEC3G genetic variants and their influence on the progression to AIDS. *Journal of virology*, *78*(20), pp.11070-11076.

An, P. and Winkler, C.A., 2010. Host genes associated with HIV/AIDS: advances in gene discovery. *Trends in genetics*, *26*(3), pp.119-131.

Arias, J.F., Iwabi, Y., and Tokunga, K. 2011. Structural basis for the antiviral activity of BST-2/tetherin and its viral antagonism. *Frontiers in Microbiology* **2**: 1-9.

Arias, J.F., Heyer, L.N., von Bredow, B., Weisgrau, K.L., Moldt, B., Burton, D.R., Rakasz, E.G. and Evans, D.T., 2014. Tetherin antagonism by Vpu protects HIV-infected cells from antibody-dependent cell-mediated cytotoxicity. *Proceedings of the National Academy of Sciences*, *111*(17), pp.6425-6430.

Arrildt, K.T., Joseph, S.B. and Swanstrom, R., 2012. The HIV-1 env protein: a coat of many colors. *Current HIV/AIDS Reports*, *9*(1), pp.52-63.

Balzarini, J., 1994. Metabolism and mechanism of antiretroviral action of purine and pyrimidine derivatives. *Pharmacy World and Science*, *16*(2), pp.113-126.

Bannwarth, L., Rose, T., Frutos, S., Giralt, E., Vanderesse, R., Jamart-Grégoire, B., Vidu, A., Ongeri, S., Sicsic, S., Pannecouque, C. and De Clercq, E., 2007. peptidomimetic Dimerization Inhibitors of Hiv-1 Protease: Further Insights into Structural Variations and Mechanism of Action: 90. *Antiviral Research*, *74*(3), p.A64.

Baum, L.L., Cassutt, K.J., Knigge, K., Khattri, R., Margolick, J., Rinaldo, C., Kleeberger, C.A., Nishanian, P., Henrard, D.R. and Phair, J., 1996. HIV-1 gp120-specific antibody-dependent cell-mediated cytotoxicity correlates with rate of disease progression. *The Journal of Immunology*, *157*(5), pp.2168-2173.

Becker-Herman, S., Arie, G., Medvedovsky, H., Kerem, A. and Shachar, I., 2005. CD74 is a member of the regulated intramembrane proteolysis-processed protein family. *Molecular biology of the cell*, *16*(11), pp.5061-5069.

Benson, R.E., Sanfridson, A., Ottinger, J.S., Doyle, C. and Cullen, B.R., 1993. Downregulation of cell-surface CD4 expression by simian immunodeficiency virus Nef prevents viral super infection. *Journal of Experimental Medicine*, *177*(6), pp.1561-1566.

Besnard-Guerin, C., Belaïdouni, N., Lassot, I., Segeral, E., Jobart, A., Marchal, C. and Benarous, R., 2004. HIV-1 Vpu sequesters β-transducin repeat-containing protein (βTrCP) in the cytoplasm and provokes the accumulation of β-catenin and other SCFβTrCP substrates. *Journal of Biological Chemistry*, *279*(1), pp.788-795.

Binette, J., Dubé, M., Mercier, J., Halawani, D., Latterich, M. and Cohen, É.A., 2007. Requirements for the selective degradation of CD4 receptor molecules by the human immunodeficiency virus type 1 Vpu protein in the endoplasmic reticulum. *Retrovirology*, *4*(1), p.75.

Bolduan, S., Votteler, J., Lodermeyer, V., Greiner, T., Koppensteiner, H., Schindler, M., Thiel, G. and Schubert, U., 2011. Ion channel activity of HIV-1 Vpu is dispensable for counteraction of CD317. *Virology*, *416*(1-2), pp.75-85.

Bomsel, M., Tudor, D., Drillet, A.S., Alfsen, A., Ganor, Y., Roger, M.G., Mouz, N., Amacker, M., Chalifour, A., Diomede, L. and Devillier, G., 2011. Immunization with HIV-1 gp41 subunit virosomes induces mucosal antibodies protecting nonhuman primates against vaginal SHIV challenges. *Immunity*, *34*(2), pp.269-280.

Bottino, C., Falco, M., Parolini, S., Marcenaro, E., Augugliaro, R., Sivori, S., Landi, E., Biassoni, R., Notarangelo, L.D., Moretta, L. and Moretta, A., 2001. Gntb-A, a Novel Sh2d1a-Associated Surface Molecule Contributing to the Inability of Natural Killer Cells to Kill Epstein-Barr Virus–Infected B Cells in X-Linked Lymphoproliferative Disease. *Journal of Experimental Medicine*, *194*(3), pp.235-246.

Bour, S., Perrin, C., Akari, H. and Strebel, K., 2001. The human immunodeficiency virus type 1 Vpu protein inhibits NF-κB activation by interfering with βTrCP-mediated degradation of IκB. *Journal of Biological Chemistry*, *276*(19), pp.15920-15928.

Briz, V., Poveda, E. and Soriano, V., 2006. HIV entry inhibitors: mechanisms of action and resistance pathways. *Journal of Antimicrobial Chemotherapy*, *57*(4), pp.619-627.

Capon, D.J. and Ward, R.H., 1991. The CD4-gpl20 interaction and AIDS pathogenesis. *Annual review of immunology*, *9*(1), pp.649-678.

Carpenter, C.C., Fischl, M.A., Hammer, S.M., Hirsch, M.S., Jacobsen, D.M., Katzenstein, D.A., Montaner, J.S., Richman, D.D., Saag, M.S., Schooley, R.T. and Thompson, M.A., 1997. Antiretroviral therapy for HIV infection in 1997: updated recommendations of the International AIDS Society—USA Panel. *Jama*, *277*(24), pp.1962-1969.

Casartelli, N., Sourisseau, M., Feldmann, J., Guivel-Benhassine, F., Mallet, A., Marcelin, A.G., Guatelli, J. and Schwartz, O., 2010. Tetherin restricts productive HIV-1 cell-to-cell transmission. *PLoS pathogens*, *6*(6), p.e1000955.

Chen, R.Y., Kilby, J.M. and Saag, M.S., 2002. Enfuvirtide. *Expert opinion on investigational drugs*, *11*(12), pp.1837-1843.

Chen, L., Do Kwon, Y., Zhou, T., Wu, X., O'Dell, S., Cavacini, L., Hessell, A.J., Pancera, M., Tang, M., Xu, L. and Yang, Z.Y., 2009. Structural basis of immune evasion at the site of CD4 attachment on HIV-1 gp120. *Science*, *326*(5956), pp.1123-1127.

Chen, N.Y., Zhou, L., Gane, P.G., Price, A., Zufferey, M., Luban, J., James, L., Selwood, D. and Fassati, A., 2013. HIV-1 uncoating in human CD4+ T cells: kinetic and functional analyses. *Retrovirology*, *10*(S1), p.P13.

Christ, F., Voet, A., Marchand, A., Nicolet, S., Desimmie, B.A., Marchand, D., Bardiot, D., Van der Veken, N.J., Van Remoortel, B., Strelkov, S.V. and De Maeyer, M., 2010. Rational design of small-molecule inhibitors of the LEDGF/p75-integrase interaction and HIV replication. *Nature chemical biology*, *6*(6), p.442.

Chung, A., Rollman, E., Johansson, S., Kent, S.J. and Stratov, I., 2008. The utility of ADCC responses in HIV infection. *Current HIV research*, *6*(6), pp.515-519.

Chung, A.W., Rollman, E., Center, R.J., Kent, S.J. and Stratov, I., 2009. Rapid degranulation of NK cells following activation by HIV-specific antibodies. *The Journal of Immunology*, *182*(2), pp.1202-1210.

Cocchi, F., DeVico, A.L., Garzino-Demo, A., Arya, S.K., Gallo, R.C. and Lusso, P., 1995. Identification of RANTES, MIP-1α, and MIP-1β as the major HIV-suppressive factors produced by CD8+ T cells. *Science*, *270*(5243), pp.1811-1815.

Cocka, L.J. and Bates, P., 2012. Identification of alternatively translated Tetherin isoforms with differing antiviral and signaling activities. *PLoS pathogens*, *8*(9), p.e1002931.

Cohen, E.A., Terwilliger, E.F., Sodroski, J.G. and Haseltine, W.A., 1988. Identification of a protein encoded by the vpu gene of HIV-1. *Nature*, *334*(6182), p.532.

Cooper, M.D. and Alder, M.N., 2006. The evolution of adaptive immune systems. *Cell*, *124*(4), pp.815-822.

Coren, L.V., Trivett, M.T., Jain, S., Ayala, V.I., Del Prete, G.Q., Ohlen, C. and Ott, D.E., 2015. Potent restriction of HIV-1 and SIV mac239 Replication by African Green Monkey TRIM5α. *Retrovirology*, *12*(1), p.11.

Cortes, M.J., Wong-Staal, F. and Lama, J., 2001. Cell-surface CD4 interferes with the infectivity of HIV-1 particles released from T cells. *Journal of Biological Chemistry*.

Cullen, B.R., 1991. Regulation of HIV-1 gene expression. *The FASEB Journal*, *5*(10), pp.2361-2368.

De Clercq, E., 2004. Non-nucleoside reverse transcriptase inhibitors (NNRTIs): past, present, and future. *Chemistry & biodiversity*, *1*(1), pp.44-64.

De Clercq, E. and Neyts, J., 2009. Antiviral agents acting as DNA or RNA chain terminators. In *Antiviral Strategies* (pp. 53-84). Springer, Berlin, Heidelberg.

Degli-Esposti, M.A. and Smyth, M.J., 2005. Close encounters of different kinds: dendritic cells and NK cells take centre stage. *Nature Reviews Immunology*, *5*(2), p.112.

Doores, K.J., 2015. The HIV glycan shield as a target for broadly neutralizing antibodies. *The FEBS journal*, *282*(24), pp.4679-4691.

Dorr, P., Westby, M., Dobbs, S., Griffin, P., Irvine, B., Macartney, M., Mori, J., Rickett, G., Smith-Burchnell, C., Napier, C. and Webster, R., 2005. Maraviroc (UK-427,857), a potent, orally bioavailable, and selective small-molecule inhibitor of chemokine receptor CCR5 with broad-spectrum anti-human immunodeficiency virus type 1 activity. *Antimicrobial agents and chemotherapy*, *49*(11), pp.4721-4732.

Douglas, J.L., Viswanathan, K., McCarroll, M.N., Gustin, J.K., Früh, K. and Moses, A.V., 2009. Vpu directs the degradation of the human immunodeficiency virus restriction factor BST-2/Tetherin via a βTrCP-dependent mechanism. *Journal of virology*, *83*(16), pp.7931-7947.

Dragic, T., Trkola, A., Thompson, D.A., Cormier, E.G., Kajumo, F.A., Maxwell, E., Lin, S.W., Ying, W., Smith, S.O., Sakmar, T.P. and Moore, J.P., 2000. A binding pocket for a small molecule inhibitor of HIV-1 entry within the transmembrane helices of CCR5. *Proceedings of the National Academy of Sciences*, *97*(10), pp.5639-5644.

Dubé, M., Roy, B.B., Guiot-Guillain, P., Mercier, J., Binette, J., Leung, G. and Cohen, É.A., 2009. Suppression of tetherin-restricting activity on HIV-1 particle release correlates with localization of Vpu in the trans-Golgi network. *Journal of Virology*.

Dubé, M., Roy, B.B., Guiot-Guillain, P., Binette, J., Mercier, J., Chiasson, A. and Cohen, É.A., 2010a. Antagonism of tetherin restriction of HIV-1 release by Vpu involves binding and sequestration of the restriction factor in a perinuclear compartment. *PLoS pathogens*, *6*(4), p.e1000856.

Dubé, M., Bego, M.G., Paquay, C. and Cohen, É.A., 2010b. Modulation of HIV-1-host interaction: role of the Vpu accessory protein. *Retrovirology*, *7*(1), p.114.

Engelman, A. and Cherepanov, P., 2012. The structural biology of HIV-1: mechanistic and therapeutic insights. *Nature Reviews Microbiology*, *10*(4), p.279.

Ewart, G.D., Sutherland, T., Gage, P.W. and Cox, G.B., 1996. The Vpu protein of human immunodeficiency virus type 1 forms cation-selective ion channels. *Journal of virology*, *70*(10), pp.7108-7115.

Ewart, G.D., Nasr, N., Naif, H., Cox, G.B., Cunningham, A.L. and Gage, P.W., 2004. Potential new anti-human immunodeficiency virus type 1 compounds depress virus replication in cultured human macrophages. *Antimicrobial agents and chemotherapy*, *48*(6), pp.2325-2330.

Farnet, C.M. and Haseltine, W.A., 1991. Determination of viral proteins present in the human immunodeficiency virus type 1 pre-integration complex. *Journal of virology*, *65*(4), pp.1910-1915.

Federau, T., Schubert, U., Floßdorf, J.O.S.E.F., Henklein, P., Schomburg, D. And Wray, V., 1996. Solution structure of the cytoplasmic domain of the human immunodeficiency virus type 1 encoded virus protein U (Vpu). *International journal of peptide and protein research*, *47*(4), pp.297-310.

Feldherr, C.M. and Feldherr, A.B., 1960. The nuclear membrane as a barrier to the free diffusion of proteins. *Nature*, *185*(4708), p.250.

Fisher, A.G., Ensoli, B., Ivanoff, L., Chamberlain, M., Petteway, S., Ratner, L., Gallo, R.C. and Wong-Staal, F., 1987. The sor gene of HIV-1 is required for efficient virus transmission in vitro. *Science*, *237*(4817), pp.888-893.

Fitzpatrick, K., Skasko, M., Deerinck, T.J., Crum, J., Ellisman, M.H. and Guatelli, J., 2010. Direct restriction of virus release and incorporation of the interferon-induced protein BST-2 into HIV-1 particles. *PLoS pathogens*, *6*(3), p.e1000701.

Fogli, M., Mavilio, D., Brunetta, E., Varchetta, S., Ata, K., Roby, G., Kovacs, C., Follmann, D., Pende, D., Ward, J. and Barker, E., 2008. Lysis of endogenously infected CD4+ T cell blasts by rIL-2 activated autologous natural killer cells from HIV-infected viremic individuals. *PLoS pathogens*, *4*(7), p.e1000101.

Forthal, D., Hope, T. and Alter, G., 2013. New paradigms for functional HIV-specific non-neutralizing antibodies. *Current opinion in HIV and AIDS*, *8*(5), p.393.

Freed, E.O. 1998. HIV-1 gag proteins: diverse functions in the virus life cycle. *Virology*, *251*(1), pp.1-15.

Friborg, J., Ladha, A., Göttlinger, H., Haseltine, W.A. and Cohen, E.A., 1995. Functional analysis of the phosphorylation sites on the human immunodeficiency virus type 1 Vpu protein. *Journal of acquired immune deficiency syndromes and human retrovirology: official publication of the International Retrovirology Association*, *8*(1), pp.10-22.

Fritz, J.V., Tibroni, N., Keppler, O.T. and Fackler, O.T., 2012. HIV-1 Vpu's lipid raft association is dispensable for counteraction of the particle release restriction imposed by CD317/Tetherin. *Virology*, *424*(1), pp.33-44.

Galão, R.P., Le Tortorec, A., Pickering, S., Kueck, T. and Neil, S.J., 2012. Innate sensing of HIV-1 assembly by Tetherin induces NFκB-dependent proinflammatory responses. *Cell host & microbe*, *12*(5), pp.633-644.

Gelderblom, H.R., 1991. Assembly and morphology of HIV: potential effect of structure on viral function. *Aids*, *5*(6), pp.617-638.

Gilmore, T.D., 2006. Introduction to NF-κB: players, pathways, perspectives. *Oncogene*, *25*(51), p.6680.

Glushakova, S., Münch, J., Carl, S., Greenough, T.C., Sullivan, J.L., Margolis, L. and Kirchhoff, F., 2001. CD4 down-modulation by human immunodeficiency virus type 1 Nef correlates with the efficiency of viral replication and with CD4+ T-cell depletion in human lymphoid tissue ex vivo. *Journal of virology*, *75*(21), pp.10113-10117.

Goh, W.C., Rogel, M.E., Kinsey, C.M., Michael, S.F., Fultz, P.N., Nowak, M.A., Hahn, B.H. and Emerman, M., 1998. HIV-1 Vpr increases viral expression by manipulation of the cell cycle: a mechanism for selection of Vpr in vivo. *Nature medicine*, *4*(1), p.65.

Goldsmith, M.A., Warmerdam, M.T., Atchison, R.E., Miller, M.D. and Greene, W.C., 1995. Dissociation of the CD4 downregulation and viral infectivity enhancement functions of human immunodeficiency virus type 1 Nef. *Journal of virology*, *69*(7), pp.4112-4121.

Göttlinger, H.G., Dorfman, T., Sodroski, J.G. and Haseltine, W.A., 1991. Effect of mutations affecting the p6 gag protein on human immunodeficiency virus particle release. *Proceedings of the National Academy of Sciences*, *88*(8), pp.3195-3199.

Hammonds, J., Wang, J.J., Yi, H. and Spearman, P., 2010. Immunoelectron microscopic evidence for Tetherin/BST2 as the physical bridge between HIV-1 virions and the plasma membrane. *PLoS pathogens*, *6*(2), p.e1000749.

Harrich, D. and Hooker, B., 2002. Mechanistic aspects of HIV-1 reverse transcription initiation. *Reviews in medical virology*, *12*(1), pp.31-45.

Harris, R.S., Hultquist, J.F. and Evans, D.T., 2012. The restriction factors of human immunodeficiency virus. *Journal of Biological Chemistry*, *287*(49), pp.40875-40883.

Hazuda, D., Iwamoto, M. and Wenning, L., 2009. Emerging pharmacology: inhibitors of human immunodeficiency virus integration. *Annual review of pharmacology and toxicology*, *49*, pp.377-394.

Heinzinger, N.K., Bukinsky, M.I., Haggerty, S.A., Ragland, A.M., Kewalramani, V., Lee, M.A., Gendelman, H.E., Ratner, L., Stevenson, M. and Emerman, M., 1994. The Vpr protein of human immunodeficiency virus type 1 influences nuclear localization of viral nucleic acids in nondividing host cells. *Proceedings of the National Academy of Sciences*, *91*(15), pp.7311-7315.

Huber, M. and Trkola, A., 2007. Humoral immunity to HIV-1: neutralization and beyond. *Journal of internal medicine*, *262*(1), pp.5-25.

Hussain, A., Wesley, C., Khalid, M., Chaudhry, A. and Jameel, S., 2008. Human immunodeficiency virus type 1 Vpu protein interacts with CD74 and modulates major histocompatibility complex class II presentation. *Journal of virology*, *82*(2), pp.893-902.

Ishikawa, J., Kaisho, T., Tomizawa, H., Lee, B.O., Kobune, Y., Inazawa, J., Oritani, K., Itoh, M., Ochi, T., Ishihara, K. and Hirano, T., 1995. Molecular cloning and chromosomal mapping of a bone marrow stromal cell surface gene, BST2, that may be involved in pre-B-cell growth. *Genomics*, *26*(3), pp.527-534.

Iwabu, Y., Fujita, H., Kinomoto, M., Kaneko, K., Ishizaka, Y., Tanaka, Y., Sata, T. and Tokunaga, K., 2009. HIV-1 accessory protein Vpu internalizes cell-surface BST-2/tetherin through transmembrane interactions leading to lysosomes. *Journal of Biological Chemistry*, pp.jbc-M109.

Janeway Jr, C.A. and Medzhitov, R., 2002. Innate immune recognition. *Annual review of immunology*, *20*(1), pp.197-216.

Janeway, C.A., Travers, P., Walport, M. and Shlomchik, M.J., 2005. Immunobiology: the immune system in health and disease.

Janvier, K., Pelchen–Matthews, A., Renaud, J.B., Caillet, M., Marsh, M. and Berlioz-Torrent, C., 2011. The ESCRT-0 component HRS is required for HIV-1 Vpu-mediated BST-2/tetherin down-regulation. *PLoS pathogens*, *7*(2), p.e1001265.

Joint United Nations Programme on HIV/AIDS, 2017. *2017 report on the global AIDS epidemic*. UNAIDS.

Jones, K.A. and Peterlin, M.B., 1994. Control of RNA initiation and elongation at the HIV-1 promoter. *Annual review of biochemistry*, *63*(1), pp.717-743.

Jouvenet, N., Neil, S.J., Zhadina, M., Zang, T., Kratovac, Z., Lee, Y., McNatt, M., Hatziioannou, T. and Bieniasz, P.D., 2009. Broad-spectrum inhibition of retroviral and filoviral particle release by tetherin. *Journal of virology*, *83*(4), pp.1837-1844.

Jowett, J.B., Planelles, V., Poon, B., Shah, N.P., Chen, M.L. and Chen, I.S., 1995. The human immunodeficiency virus type 1 vpr gene arrests infected T cells in the G2+ M phase of the cell cycle. *Journal of virology*, *69*(10), pp.6304-6313.

Kerkau, T., Bacik, I., Bennink, J.R., Yewdell, J.W., Hünig, T., Schimpl, A. and Schubert, U., 1997. The human immunodeficiency virus type 1 (HIV-1) Vpu protein interferes with an early step in the biosynthesis of major histocompatibility complex (MHC) class I molecules. *Journal of Experimental Medicine*, *185*(7), pp.1295-1306.

Khoury, G., Ewart, G., Luscombe, C., Miller, M. and Wilkinson, J., 2010. Antiviral efficacy of the novel compound BIT225 against HIV-1 release from human macrophages. *Antimicrobial agents and chemotherapy*, *54*(2), pp.835-845.

Kilby, J.M. and Eron, J.J., 2003. Novel therapies based on mechanisms of HIV-1 cell entry. *New England Journal of Medicine*, *348*(22), pp.2228-2238.

Klasse, P.J. and Sattentau, Q.J., 2002. Occupancy and mechanism in antibody-mediated neutralization of animal viruses. *Journal of General Virology*, *83*(9), pp.2091-2108.

Klibanov, O.M., 2009. Elvitegravir, an oral HIV integrase inhibitor, for the potential treatment of HIV infection. *Curr Opin Investig Drugs*, *10*(2), pp.190-200.

Klimkait, T., Strebel, K., Hoggan, M.D., Martin, M.A. and Orenstein, J.M., 1990. The human immunodeficiency virus type 1-specific protein vpu is required for efficient virus maturation and release. *Journal of virology*, *64*(2), pp.621-629.

Kogan, M. and Rappaport, J., 2011. HIV-1 accessory protein Vpr: relevance in the pathogenesis of HIV and potential for therapeutic intervention. *Retrovirology*, *8*(1), p.25.

Kuhl, B.D., Cheng, V., Donahue, D.A., Sloan, R.D., Liang, C., Wilkinson, J. and Wainberg, M.A., 2011. The HIV-1 Vpu viroporin inhibitor BIT225 does not affect Vpu-mediated tetherin antagonism. *PLoS One*, *6*(11), p.e27660.

Kuiken, C., Foley, B., Hahn, B., Marx, P., McCutchan, F., Mellors, J., Wolinsky, S. and Korber, B., 2001. HIV sequence compendium 2001. *Theoretical Biology and Biophysics Group, Los Alamos National Laboratory, Los Alamos, NM*.

Kupzig, S., Korolchuk, V., Rollason, R., Sugden, A., Wilde, A. and Banting, G., 2003. Bst-2/HM1. 24 is a raft-associated apical membrane protein with an unusual topology. *Traffic*, *4*(10), pp.694-709.

Kwong, P.D., Wyatt, R., Robinson, J., Sweet, R.W., Sodroski, J. and Hendrickson, W.A., 1998. Structure of an HIV gp120 envelope glycoprotein in complex with the CD4 receptor and a neutralizing human antibody. *Nature*, *393*(6686), p.648.

Laguette, N., Sobhian, B., Casartelli, N., Ringeard, M., Chable-Bessia, C., Ségéral, E., Yatim, A., Emiliani, S., Schwartz, O. and Benkirane, M., 2011. SAMHD1 is the dendritic-and myeloid-cell-specific HIV-1 restriction factor counteracted by Vpx. *Nature*, *474*(7353), p.654.

Lahouassa, H., Daddacha, W., Hofmann, H., Ayinde, D., Logue, E.C., Dragin, L., Bloch, N., Maudet, C., Bertrand, M., Gramberg, T. and Pancino, G., 2012. SAMHD1 restricts the replication of human immunodeficiency virus type 1 by depleting the intracellular pool of deoxynucleoside triphosphates. *Nature immunology*, *13*(3), p.223.

Lama, J., Mangasarian, A. and Trono, D., 1999. Cell-surface expression of CD4 reduces HIV-1 infectivity by blocking Env incorporation in a Nef-and Vpu-inhibitable manner. *Current Biology*, *9*(12), pp.622-631.

Levesque, K., Zhao, Y.S. and Cohen, É.A., 2003. Vpu exerts a positive effect on HIV-1 infectivity by down-modulating CD4 receptor molecules at the surface of HIV-1 producing cells. *Journal of Biological Chemistry*.

Lewis, P.F. and Emerman, M., 1994. Passage through mitosis is required for oncoretroviruses but not for the human immunodeficiency virus. *Journal of virology*, *68*(1), pp.510-516.

Lu, L., Yu, F., Du, L.Y., Xu, W. and Jiang, S.B., 2013. Tactics used by HIV-1 to evade host innate, adaptive, and intrinsic immunities. *Chin Med J (Engl)*, *126*(12), pp.2374-9.

Luscombe, C.A., Huang, Z., Murray, M.G., Miller, M., Wilkinson, J. and Ewart, G.D., 2010. A novel hepatitis C virus p7 ion channel inhibitor, BIT225, inhibits bovine viral diarrhea virus in vitro and shows synergism with recombinant interferon-α-2b and nucleoside analogues. *Antiviral research*, *86*(2), pp.144-153.

Maenza, J. and Flexner, C., 1998. Combination antiretroviral therapy for HIV infection. *American family physician*, *57*(11), pp.2789-2798.

Magadan, J.G., Perez-Victoria, F.J., Sougrat, R., Ye, Y., Strebel, K. and Bonifacino, J.S., 2010. Multilayered mechanism of CD4 downregulation by HIV-1 Vpu involving distinct ER retention and ERAD targeting steps. *PLoS pathogens*, *6*(4), p.e1000869.

Magri, G., Muntasell, A., Romo, N., Sáez-Borderías, A., Pende, D., Geraghty, D.E., Hengel, H., Angulo, A., Moretta, A. and López-Botet, M., 2010. NKp46 and DNAM-1 NK cell receptors drive the response to human cytomegalovirus infected myeloid dendritic cells overcoming viral immune evasion strategies. *Blood*, pp.blood-2010.

Malim, M.H. and Emerman, M., 2008. HIV-1 accessory proteins—ensuring viral survival in a hostile environment. *Cell host & microbe*, *3*(6), pp.388-398.

Malim, M.H., 2014. HIV: Ringside views. *Nature*, *505*(7482), p.167.

Mangasarian, A. and Trono, D., 1997. The multifaceted role of HIV Nef. *Research in virology*, *148*(1), pp.30-33.

Mangeat, B., Turelli, P., Caron, G., Friedli, M., Perrin, L. and Trono, D., 2003. Broad antiretroviral defence by human APOBEC3G through lethal editing of nascent reverse transcripts. *Nature*, *424*(6944), p.99.

Mangeat, B., Gers-Huber, G., Lehmann, M., Zufferey, M., Luban, J. and Piguet, V., 2009. HIV-1 Vpu neutralizes the antiviral factor Tetherin/BST-2 by binding it and directing its beta-TrCP2-dependent degradation. *PLoS pathogens*, *5*(9), p.e1000574.

Mansky, L.M., Le Rouzic, E., Benichou, S. and Gajary, L.C., 2003. Influence of reverse transcriptase variants, drugs, and Vpr on human immunodeficiency virus type 1 mutant frequencies. *Journal of virology*, *77*(3), pp.2071-2080.

Margottin, F., Bour, S.P., Durand, H., Selig, L., Benichou, S., Richard, V., Thomas, D., Strebel, K. and Benarous, R., 1998. A novel human WD protein, h-βTrCP, that interacts with HIV-1 Vpu connects CD4 to the ER degradation pathway through an F-box motif. *Molecular cell*, *1*(4), pp.565-574.

Marin, M., Rose, K.M., Kozak, S.L. and Kabat, D., 2003. HIV-1 Vif protein binds the editing enzyme APOBEC3G and induces its degradation. *Nature medicine*, *9*(11), p.1398.

Matsuda, A., Suzuki, Y., Honda, G., Muramatsu, S., Matsuzaki, O., Nagano, Y., Doi, T., Shimotohno, K., Harada, T., Nishida, E. and Hayashi, H., 2003. Large-scale identification and characterization of human genes that activate NF-κB and MAPK signaling pathways. *Oncogene*, *22*(21), p.3307.

Matusali, G., Potesta, M., Santoni, A., Cerboni, C. and Doria, M., 2012. The Human Immunodeficiency Virus Type 1 Nef and Vpu Proteins Down-regulate The Natural Killer Cell Activating Ligand PVR. *Journal of virology*, pp.JVI-05788.

Medzhitov, R. and Janeway, C.A., 1997. Innate immunity: the virtues of a nonclonal system of recognition. *Cell*, *91*(3), pp.295-298.

Meusser, B. and Sommer, T., 2004. Vpu-mediated degradation of CD4 reconstituted in yeast reveals mechanistic differences to cellular ER-associated protein degradation. *Molecular cell*, *14*(2), pp.247-258.

Mi, Z., Ding, J., Zhang, Q., Zhao, J., Ma, L., Yu, H., Liu, Z., Shan, G., Li, X., Zhou, J. and Wei, T., 2015. A small molecule compound IMB-LA inhibits HIV-1 infection by preventing viral Vpu from antagonizing the host restriction factor BST-2. *Scientific reports*, *5*, p.18499.

Miller, M.D., Farnet, C.M. and Bushman, F.D., 1997. Human immunodeficiency virus type 1 preintegration complexes: studies of organization and composition. *Journal of virology*, *71*(7), pp.5382-5390.

Mitchell, R.S., Katsura, C., Skasko, M.A., Fitzpatrick, K., Lau, D., Ruiz, A., Stephens, E.B., Margottin-Goguet, F., Benarous, R. and Guatelli, J.C., 2009. Vpu antagonizes BST-2–mediated restriction of HIV-1 release via β-TrCP and endo-lysosomal trafficking. *PLoS pathogens*, *5*(5), p.e1000450.

Moll, M., Andersson, S.K., Smed-Sörensen, A. and Sandberg, J.K., 2010. Inhibition of lipid antigen presentation in dendritic cells by HIV-1 Vpu interference with CD1d recycling from endosomal compartments. *Blood*, pp.blood-2009.

Montal, M., 2003. Structure–function correlates of Vpu, a membrane protein of HIV-1. *FEBS letters*, *552*(1), pp.47-53.

Moore, P.L., Gray, E.S., Wibmer, C.K., Bhiman, J.N., Nonyane, M., Sheward, D.J., Hermanus, T., Bajimaya, S., Tumba, N.L., Abrahams, M.R. and Lambson, B.E., 2012. Evolution of an HIV glycan–dependent broadly neutralizing antibody epitope through immune escape. *Nature medicine*, *18*(11), p.1688.

Nachega, J.B., Marconi, V. C., van Zyl, G. U., Gardner, E.M., Preiser, W., Hong, S.Y., Mills, E.J. and Gross, R., 2011. HIV treatment adherence, drug resistance, virologic failure: evolving concepts. *Infectious Disorders-Drug Targets (Formerly Current Drug Targets-Infectious Disorders)*, *11*(2), pp.167-174.

Neil, S.J., Zang, T. and Bieniasz, P.D., 2008. Tetherin inhibits retrovirus release and is antagonized by HIV-1 Vpu. *Nature*, *451*(7177), p.425.

O'Brien, S.J. and Nelson, G.W., 2004. Human genes that limit AIDS. *Nature genetics*, *36*(6), p.565.

O'Neil, P.K., Sun, G., Yu, H., Ron, Y., Dougherty, J.P. and Preston, B.D., 2002. Mutational analysis of HIV-1 long terminal repeats to explore the relative contribution of reverse transcriptase and RNA polymerase II to viral mutagenesis. *Journal of Biological Chemistry*, *277*(41), pp.38053-38061.

Overbaugh, J. and Morris, L., 2011. The antibody response against HIV-1. *Cold Spring Harbor perspectives in medicine*, p.a007039.

Pacyniak, E., Gomez, M.L., Gomez, L.M., Mulcahy, E.R., Jackson, M., Hout, D.R., Wisdom, B.J. and Stephens, E.B., 2005. Identification of a region within the cytoplasmic domain of the subtype B Vpu protein of human immunodeficiency virus type 1 (HIV-1) that is responsible for retention in the golgi complex and its absence in the Vpu protein from a subtype C HIV-1. *AIDS Research & Human Retroviruses*, *21*(5), pp.379-394.

Palella Jr, F.J., Delaney, K.M., Moorman, A.C., Loveless, M.O., Fuhrer, J., Satten, G.A., Aschman, D.J., Holmberg, S.D. and HIV Outpatient Study Investigators, 1998. Declining morbidity and mortality among patients with advanced human immunodeficiency virus infection. *New England Journal of Medicine*, *338*(13), pp.853-860.

Paolini, R., Bernardini, G., Molfetta, R. and Santoni, A., 2015. NK cells and interferons. *Cytokine & growth factor reviews*, *26*(2), pp.113-120.

Parren, P.W., Moore, J.P., Burton, D.R. and Sattentau, Q.J., 1999. The neutralizing antibody response to HIV-1: viral evasion and escape from humoral immunity. *AIDS (London, England)*, *13*, p.S137.

Pauwels, R., 2004. New non-nucleoside reverse transcriptase inhibitors (NNRTIs) in development for the treatment of HIV infections. *Current Opinion in Pharmacology*, *4*(5), pp.437-446.

Perez-Caballero, D., Zang, T., Ebrahimi, A., McNatt, M.W., Gregory, D.A., Johnson, M.C. and Bieniasz, P.D., 2009. Tetherin inhibits HIV-1 release by directly tethering virions to cells. *Cell*, *139*(3), pp.499-511.

Petersen, J.L., Morris, C.R. and Solheim, J.C., 2003. Virus evasion of MHC class I molecule presentation. *The Journal of Immunology*, *171*(9), pp.4473-4478.

Petit, S.J., Blondeau, C. and Towers, G.J., 2011. Analysis of the human immunodeficiency virus type 1 M group Vpu domains involved in antagonizing tetherin. *Journal of general virology*, *92*(12), pp.2937-2948.

Pujol, F.M., Laketa, V., Schmidt, F., Mukenhirn, M., Müller, B., Boulant, S., Grimm, D., Keppler, O.T. and Fackler, O.T., 2016. HIV-1 Vpu antagonizes CD317/tetherin by adaptor protein-1-mediated exclusion from virus assembly sites. *Journal of virology*, pp.JVI-00504.

Purcell, D.F. and Martin, M.A., 1993. Alternative splicing of human immunodeficiency virus type 1 mRNA modulates viral protein expression, replication, and infectivity. *Journal of virology*, *67*(11), pp.6365-6378.

Richard, J. and Cohen, É.A., 2010. HIV-1 Vpu disarms natural killer cells. *Cell host & microbe*, *8*(5), pp.389-391.

Richardson, M.W., Guo, L., Xin, F., Yang, X. and Riley, J.L., 2014. Stabilized human TRIM5α protects human T cells from HIV-1 infection. *Molecular Therapy*, *22*(6), pp.1084-1095.

Rogel, M.E., Wu, L.I. and Emerman, M., 1995. The human immunodeficiency virus type 1 vpr gene prevents cell proliferation during chronic infection. *Journal of Virology*, *69*(2), pp.882-888.

Rollason, R., Korolchuk, V., Hamilton, C., Schu, P. and Banting, G., 2007. Clathrin-mediated endocytosis of a lipid-raft-associated protein is mediated through a dual tyrosine motif. *Journal of cell science*, *120*(21), pp.3850-3858.

Roos, M.T., Claessen, F.A., Huisman, H.G., Kootstra, N.A., Meyaard, L., Schellekens, P.T., Schuitemaker, H. and Miedema, F., 1994. Viro-immunological studies in acute HIV-1 infection. *AIDS (London, England)*, *8*(11), pp.1533-1538.

Rubbert, A., Behrens, G. and Ostrowski, M., 2007. Pathogenesis of HIV-1 infection. *HIV medicine*, *3*, pp.59-63.

Ruben, S., Perkins, A., Purcell, R., Joung, K., Sia, R., Burghoff, R., Haseltine, W.A. and Rosen, C.A., 1989. Structural and functional characterization of human immunodeficiency virus tat protein. *Journal of virology*, *63*(1), pp.1-8.

Santana, M.A. and Esquivel-Guadarrama, F., 2006. Cell biology of T cell activation and differentiation. *International review of cytology*, *250*, pp.217-274.

Sayana, S. and Khanlou, H., 2009. Maraviroc: a new CCR5 antagonist. *Expert review of anti-infective therapy*, *7*(1), pp.9-19.

Schubert, U., Henklein, P., Boldyreff, B., Wingender, E., Strebel, K. and Porstmann, T., 1994. The human immunodeficiency virus type 1 encoded Vpu protein is phosphorylated by casein kinase-2 (CK-2) at positions Ser52 and Ser56 within a predicted α-helix-turn-α-helix-motif.

Schubert, U., Ferrer-Montiel, A.V., Oblatt-Montal, M., Henklein, P., Strebel, K. and Montal, M., 1996. Identification of an ion channel activity of the Vpu transmembrane domain and its involvement in the regulation of virus release from HIV-1-infected cells. *FEBS letters*, *398*(1), pp.12-18.

Schubert, U., Antón, L.C., Bačík, I., Cox, J.H., Bour, S., Bennink, J.R., Orlowski, M., Strebel, K. and Yewdell, J.W., 1998. CD4 glycoprotein degradation induced by human immunodeficiency virus type 1 Vpu protein requires the function of proteasomes and the ubiquitin-conjugating pathway. *Journal of virology*, *72*(3), pp.2280-2288.

Schwartz, O., Maréchal, V., Le Gall, S., Lemonnier, F. and Heard, J.M., 1996. Endocytosis of major histocompatibility complex class I molecules is induced by the HIV–1 Nef protein. *Nature medicine*, *2*(3), pp.338-342.

Seelamgari, A., Maddukuri, A., Berro, R., de la Fuente, C., Kehn, K., Deng, L., Dadgar, S., Bottazzi, M.E., Ghedin, E., Pumfery, A. and Kashanchi, F., 2004. Role of viral regulatory and accessory proteins in HIV-1 replication. *Front Biosci*, *9*(9), pp.2388-2413.

Serrao, E., Odde, S., Ramkumar, K. and Neamati, N., 2009. Raltegravir, elvitegravir, and metoogravir: the birth of" me-too" HIV-1 integrase inhibitors. *Retrovirology*, *6*(1), p.25.

Shah, A.H., Sowrirajan, B., Davis, Z.B., Ward, J.P., Campbell, E.M., Planelles, V. and Barker, E., 2010. Degranulation of natural killer cells following interaction with HIV-1-infected cells is hindered by downmodulation of NTB-A by Vpu. *Cell host & microbe*, *8*(5), pp.397-409.

Sheehy, A.M., Gaddis, N.C., Choi, J.D. and Malim, M.H., 2002. Isolation of a human gene that inhibits HIV-1 infection and is suppressed by the viral Vif protein. *Nature*, *418*(6898), p.646.

Sheehy, A.M., Gaddis, N.C. and Malim, M.H., 2003. The antiretroviral enzyme APOBEC3G is degraded by the proteasome in response to HIV-1 Vif. *Nature medicine*, *9*(11), p.1404.

Sherman, M.P., Schubert, U., Williams, S.A., de Noronha, C.M., Kreisberg, J.F., Henklein, P. and Greene, W.C., 2002. HIV-1 Vpr displays natural protein-transducing properties: implications for viral pathogenesis. *Virology*, *302*(1), pp.95-105.

Shibuya, A., Campbell, D., Hannum, C., Yssel, H., Franz-Bacon, K., McClanahan, T., Kitamura, T., Nicholl, J., Sutherland, G.R., Lanier, L.L. and Phillips, J.H., 1996. DNAM-1, a novel adhesion molecule involved in the cytolytic function of T lymphocytes. *Immunity*, *4*(6), pp.573-581.

Shun, M.C., Raghavendra, N.K., Vandegraaff, N., Daigle, J.E., Hughes, S., Kellam, P., Cherepanov, P. and Engelman, A., 2007. LEDGF/p75 functions downstream from preintegration complex formation to effect gene-specific HIV-1 integration. *Genes & development*, *21*(14), pp.1767-1778.

Skaug, B., Jiang, X. and Chen, Z.J., 2009. The role of ubiquitin in NF-κB regulatory pathways. *Annual review of biochemistry*, *78*, pp.769-796.

Stonos, N., Wootton, S. and Karrow, N., 2014. Immunogenetics of small ruminant lentiviral infections. *Viruses*, *6*(8), pp.3311-3333.

Stopak, K., de Noronha, C., Yonemoto, W. and Greene, W.C., 2003. HIV-1 Vif blocks the antiviral activity of APOBEC3G by impairing both its translation and intracellular stability. *Molecular cell*, *12*(3), pp.591-601.

Strebel, K., Klimkait, T. and Martin, M.A., 1988. A novel gene of HIV-1, vpu, and its 16-kilodalton product. *Science*, *241*(4870), pp.1221-1223.

Strebel, K., 1996. Structure and function of HIV-1 Vpu. *Human retroviruses and AIDS*.

Strebel, K., 2014. HIV-1 Vpu—an ion channel in search of a job. *Biochimica et Biophysica Acta (BBA)-Biomembranes*, *1838*(4), pp.1074-1081.

Sugden, S., Bego, M., Pham, T. and Cohen, É., 2016. Remodeling of the host cell plasma membrane by HIV-1 Nef and Vpu: a strategy to ensure viral fitness and persistence. *Viruses*, *8*(3), p.67.

Tahara-Hanaoka, S., Shibuya, K., Onoda, Y., Zhang, H., Yamazaki, S., Miyamoto, A., Honda, S.I., Lanier, L.L. and Shibuya, A., 2004. Functional characterization of DNAM-1 (CD226) interaction with its ligands PVR (CD155) and nectin-2 (PRR-2/CD112). *International immunology*, *16*(4), pp.533-538.

Taltynov, O., Desimmie, B.A., Demeulemeester, J., Christ, F. and Debyser, Z., 2012. Cellular cofactors of lentiviral integrase: from target validation to drug discovery. *Molecular biology international*, *2012*.

Tanaka, M., Ueno, T., Nakahara, T., Sasaki, K., Ishimoto, A. and Sakai, H., 2003. Downregulation of CD4 is required for maintenance of viral infectivity of HIV-1. *Virology*, *311*(2), pp.316-325.

Temesgen, Z., Cainelli, F., Poeschla, E.M., Vlahakis, S.A. and Vento, S., 2006. Approach to salvage antiretroviral therapy in heavily antiretroviral-experienced HIV-positive adults. *The Lancet Infectious Diseases*, *6*(8), pp.496-507.

Terwilliger, E.F., Cohen, E.A., Lu, Y.C., Sodroski, J.G. and Haseltine, W.A., 1989. Functional role of human immunodeficiency virus type 1 vpu. *Proceedings of the National Academy of Sciences*, *86*(13), pp.5163-5167.

Tokarev, A., Suarez, M., Kwan, W., Fitzpatrick, K., Singh, R. and Guatelli, J., 2012. Stimulation of NF-κB activity by the HIV restriction factor BST2. *Journal of virology*, pp.JVI-02272.

Tomasec, P., Wang, E.C., Davison, A.J., Vojtesek, B., Armstrong, M., Griffin, C., McSharry, B.P., Morris, R.J., Llewellyn-Lacey, S., Rickards, C. and Nomoto, A., 2005. Downregulation of natural killer cell–activating ligand CD155 by human cytomegalovirus UL141. *Nature immunology*, *6*(2), p.181.

Tsiang, M., Jones, G.S., Niedziela-Majka, A., Kan, E., Lansdon, E.B., Huang, W., Hung, M., Samuel, D., Novikov, N., Xu, Y. and Mitchell, M., 2012. New class of HIV-1 integrase (IN) inhibitors with a dual mode of action. *Journal of Biological Chemistry*, pp.jbc-M112.

Turner, B.G. and Summers, M.F., 1999. Structural biology of HIV1. *Journal of molecular biology*, *285*(1), pp.1-32.

Veillette, M., Désormeaux, A., Medjahed, H., Gharsallah, N.E., Coutu, M., Baalwa, J., Guan, Y., Lewis, G., Ferrari, G., Hahn, B.H. and Haynes, B.F., 2013. Interaction with cellular CD4 exposes HIV-1 envelope epitopes targeted by antibody-dependent cell-mediated cytotoxicity. *Journal of virology*, pp.JVI-03230.

Veillette, M., Coutu, M., Richard, J., Batraville, L.A., Dagher, O., Bernard, N., Tremblay, C., Kaufmann, D.E., Roger, M. and Finzi, A., 2014. The HIV-1 gp120 CD4-bound conformation is preferentially targeted by ADCC-mediating antibodies in sera from HIV-1-infected individuals. *Journal of virology*, pp.JVI-02868.

Vigan, R. and Neil, S.J., 2010. Determinants of tetherin antagonism in the transmembrane domain of the human immunodeficiency virus type 1 Vpu protein. *Journal of virology*, *84*(24), pp.12958-12970.

Vittinghoff, E., Scheer, S., O'malley, P., Colfax, G., Holmberg, S.D. and Buchbinder, S.P., 1999. Combination antiretroviral therapy and recent declines in AIDS incidence and mortality. *The Journal of infectious diseases*, *179*(3), pp.717-720.

Wang, X., Ao, Z., Chen, L., Kobinger, G., Peng, J. and Yao, X., 2012. The cellular antiviral protein APOBEC3G interacts with HIV-1 reverse transcriptase and inhibits its function during viral replication. *Journal of virology*, pp.JVI-06594.

Ward, J., Bonaparte, M., Sacks, J., Guterman, J., Fogli, M., Mavilio, D. and Barker, E., 2007. HIV modulates the expression of ligands important in triggering natural killer cell cytotoxic responses on infected primary T-cell blasts. *Blood*, *110*(4), pp.1207-1214.

Wei, X., Decker, J.M., Wang, S., Hui, H., Kappes, J.C., Wu, X., Salazar-Gonzalez, J.F., Salazar, M.G., Kilby, J.M., Saag, M.S. and Komarova, N.L., 2003. Antibody neutralization and escape by HIV-1. *Nature*, *422*(6929), p.307.

Weiss, K.K., Bambara, R.A. and Kim, B., 2002. Mechanistic role of residue Gln151 in error prone DNA synthesis by human immunodeficiency virus type 1 (HIV-1) reverse transcriptase (RT) Pre-steady state kinetic study of the Q151N HIV-1 RT mutant with increased fidelity. *Journal of Biological Chemistry*, *277*(25), pp.22662-22669.

Weller, I.V. and Williams, I.G., 2001. ABC of AIDS: Antiretroviral drugs. *BMJ: British Medical Journal*, *322*(7299), p.1410.

Wensing, A.M., van Maarseveen, N.M. and Nijhuis, M., 2010. Fifteen years of HIV Protease Inhibitors: raising the barrier to resistance. *Antiviral research*, *85*(1), pp.59-74.

Wild, C., Greenwell, T. and Matthews, T., 1993. A synthetic peptide from HIV-1 gp41 is a potent inhibitor of virus-mediated cell—cell fusion. *AIDS research and human retroviruses*, *9*(11), pp.1051-1053.

Wildum, S., Schindler, M., Münch, J. and Kirchhoff, F., 2006. Contribution of Vpu, Env, and Nef to CD4 down-modulation and resistance of human immunodeficiency virus type 1-infected T cells to superinfection. *Journal of virology*, *80*(16), pp.8047-8059.

Witmer, M. and Danovich, R., 2009. Selection and analysis of HIV-1 integrase strand transfer inhibitor resistant mutant viruses. *Methods*, *47*(4), pp.277-282.

Wray, V., Federau, T., Henklein, P., Klabunde, S., Kunert, O., Schomburg, D. and Schubert, U., 1995. Solution structure of the hydrophilic region of HIV-1 encoded virus protein U (Vpu) by CD and lH NMR spectroscopy. *International journal of peptide and protein research*, *45*(1), pp.35-43.

Xu, H., Franks, T., Gibson, G., Huber, K., Rahm, N., De Castillia, C.S., Luban, J., Aiken, C., Watkins, S., Sluis-Cremer, N. and Ambrose, Z., 2013. Evidence for biphasic uncoating during HIV-1 infection from a novel imaging assay. *Retrovirology*, *10*(1), p.70.

Yewdell, J.W. and Hill, A.B., 2002. Viral interference with antigen presentation. *Nature immunology*, *3*(11), p.1019.

Zhang, S., Feng, Y., Narayan, O. and Zhao, L.J., 2001. Cytoplasmic retention of HIV-1 regulatory protein Vpr by protein-protein interaction with a novel human cytoplasmic protein VprBP. *Gene*, *263*(1), pp.131-140.

Zhang, H., Yang, B., Pomerantz, R.J., Zhang, C., Arunachalam, S.C. and Gao, L., 2003. The cytidine deaminase CEM15 induces hypermutation in newly synthesized HIV-1 DNA. *Nature*, *424*(6944), p.94.

Zhang, Q., Mi, Z., Huang, Y., Ma, L., Ding, J., Wang, J., Zhang, Y., Zhou, J., Guo, F., Li, X. and Cen, S., 2016. 2-thio-6-azauridine inhibits Vpu mediated BST-2 degradation. *Retrovirology*, *13*(1), p.13.

Chapter 2: Materials and Methods

2.1 Materials

2.1.1 HIV-1 Vpu Expression plasmid

Most of the specialised reagents used in this study were obtained through the National Institute of Health's (NIH) AIDS Reagent Program, Division of AIDS, National Institute of Allergy and Infectious Diseases (NIAID). These reagents were used extensively in this study and the NIH AIDS Reagent Program catalogue number, contributors and cited references are listed in Table 2.1 below.

Table 2.1: Reagents from the NIH AIDS Reagent Program used within this study

Catalogue Number	Reagent	Contributors	Reference
969	Anti-HIV-1 NL4-3 Vpu Polyclonal	K Strebel	Maldarelli *et al.*, 1993
10076	HIV-1 NL4-3 Vpu Optimised Expression Vector (pcDNA-Vphu)	S Bour and K Strebel	Nguyen *et al.*, 2004
11942	Anti-Vpu Rabbit Antiserum (Anti-Vpu_C)	MH Kraus and BH Hahn	Kraus *et al.*, 2010
11721	Anti-Human BST-2 Polyclonal	K Strebel and A Andrew	Migayi *et al.*, 2009
120	MT-4 cells	Dr. Douglas Richman	Larder *et al.*, 1989; Pauwels *et al.*, 1987
349	ACH-2 Cells	Dr. Thomas Folks	Clouse *et al.*, 1989; Folks *et al.*, 1989

The *Escherichia coli (E. coli)* BL21 (DE3) pLysS competent cells were obtained from Lucigen. The dithiothreitol (DTT), isopropyl β-D-1-thiogalactopyranoside (IPTG), lysozyme, DNase I, urea and ampicillin were obtained from Merck. The compounds 6-aza-2-thiouridine and Lapachol were purchased from CarboSynth Limited and Sigma-Aldrich, respectively. The purification columns were purchased from GE Healthcare Life Sciences, while the size exclusion chromatography analytical column was purchased from Bio-Rad. The TGX FastCast premixed gel acrylamide kits and the precision plus unstained protein molecular weight marker were also obtained from Bio-Rad. The BioElisa HIV-1+2 Ag/Ab kit was purchased from BIOKIT, and the 3-(4,5-dimethylthiazol-2-yl)-5-(3-carboxymethoxyphenyl)-2-(4-sulfophenyl)-2H-tetrazolium (MTS) dye was from Promega. All other reagents used were of analytical grade.

2.2 Methodology

2.2.1 Verification of the plasmid DNA sample

The cDNA sample encoding the HIV-1 Vpu protein was sequenced to confirm the presence of the insert in the plasmid. DNA sequencing was performed by Inqaba Biotech (Pretoria, South Africa; www.inqababiotec.co.za) using the Sanger DNA sequencing method. The *Vphu* subtype B gene was sequenced using the T7 promoter forward primer (5' TAATACGACTCACTATAGGG 3') and the T7 terminator reverse primer (5' GCTAGTTATTGCTCAGCGG 3'). The resultant DNA sequences were translated into amino acid sequences using the ExPASy Translate tool (https://web.expasy.org/translate/) and subsequently analysed using the protein Basic Alignment Search Tool (BLAST) from the National Center for Biotechnology Information (NCBI; https://blast.ncbi.nlm.nih.gov/Blast.cgi).

2.2.2 Heterologous Overexpression, Solubilisation and Purification of HIV-1 Vpu

2.2.2.1 HIV-1 Vpu expression in *E. coli* cells

HIV-1 Vpu was overexpressed using the codon-optimised expression vector, pcDNA-Vphu (plasmid map shown in Figure A.1, Appendix A), in *E. coli* BL21 (DE3) cells containing the pLysS plasmid (Lucigen Corporation) to reduce basal expression of the recombinant gene. The *E. coli* BL21 (DE3) pLysS cells were transformed with the recombinant plasmid using the heat shock method described by Chung *et al.* (1989). Briefly, 50 µL of competent *E. coli* BL21 (DE3) cells were thawed on ice, and 1 µL (100 ng) of the pcDNA-Vphu plasmid DNA was added to the cells. Following a 30 minutes incubation of the reaction mixture on ice, the cells were heat shocked at 42 °C for 45 seconds, and rapidly transferred to ice for 2 minutes. Super Optimal broth with Catabolite repression (SOC; 950 µL; 2% Tryptone, 0.5% Yeast Extract, 10 mM NaCl, 2.5 mM KCl, 10 mM $MgCl_2$, 20 mM Glucose) was added to the reaction mixture and incubated in a shaking incubator at 250 rpm for an hour at 37 °C. Transformants were selected by plating the cells on Luria Broth (LB) agar plates (10 g/L NaCl, 10 g/L Tryptone, 5 g/L Yeast Extract and 15 g/L Agar) supplemented with ampicillin (100 µg/mL) and chloramphenicol (35 µg/mL) and incubated at 37 °C for 16 – 20 hours. Five colonies were randomly selected and grown in LB medium containing ampicillin (100 µg/mL) and chloramphenicol (35 µg/mL) at 37 °C for 16 – 20 hours overnight. Overnight

cultures were subsequently diluted 100–fold into fresh LB medium containing the respective antibiotics. The culture was allowed to grow under continuous shaking for 3 hours at 37 °C. When the optical density (OD) of the culture, measured at 600 nm, reached 0.6 – 0.7 (known as the mid-log phase), the overexpression of HIV-1 Vpu was induced using IPTG to a final concentration of 1 mM. The culture was further grown at 37 °C, with samples collected at 1-, 2-, 3-, 4-, 5- and 16-hours post–induction. The degree of expression at each time point was evaluated using sodium dodecyl sulphate–polyacrylamide gel electrophoresis (SDS–PAGE).

2.2.2.2 HIV-1 Vpu extraction and solubilisation

After 3 hours of induction at 37 °C, the cells were harvested by centrifugation at 3220 x g for 30 minutes at 4 °C. The supernatant was discarded, and the pellet was stored at -80 °C. The 13.4 g pellet from 1L bacterial culture was resuspended in 20 mL ice-cold lysis buffer (20 mM Tris-Cl pH 8.0, 50 mM NaCl, 1 mM DTT, 1 mM Phenylmethylsulphonyl fluoride (PMSF)) and the cells were incubated at 4 °C for an hour with gentle shaking to ensure thorough lysis. The cells were disrupted by sonication at 75 Hz and 0.6 cycles on ice using the Labsonic M ultrasonic processor (Sartorius). DNase I (Sigma Aldrich), to a final concentration of 5 µg/mL, was then added to the cell lysate. The lysate was incubated at 4 °C with shaking for an additional 30 minutes. When the viscosity of the sample had decreased, the lysate was centrifuged at 16 000 x g at 4 °C for 30 minutes, and the supernatant and pellet were analysed for the presence of HIV-1 Vpu. The HIV-1 Vpu, however, was insoluble and present primarily in the inclusion bodies. To solubilise the inclusion bodies, the resulting pellet was resuspended in solubilisation buffer containing 20 mM Tris-Cl pH 8.0, 50 mM NaCl, 1 mM DTT, 8 M urea and incubated at 4 °C for 2 hours with gentle shaking. The lysate was cleared of cell debris and un-solubilised material using centrifugation at 16 000 x g for 30 minutes, after which the supernatant was collected and further analysed for the presence of HIV-1 Vpu using SDS-PAGE.

2.2.2.3 Purification and refolding of the solubilised HIV-1 Vpu

HIV-1 Vpu was purified using a combination of cation and anion exchange chromatography as detailed below.

2.2.2.3.1 Cation exchange filtration

The solubilised HIV-1 Vpu from the inclusion bodies was loaded on a SP-Sepharose Fast Flow cation exchange column (GE HealthCare) connected to an ÄKTAprime Plus system

(GE HealthCare). The column was equilibrated with five column volumes of 20 mM Tris-Cl pH 8.0, 50 mM NaCl, 1 mM DTT and 8 M urea as the equilibration buffer. The supernatant containing HIV-1 Vpu was loaded onto the column at a flow rate of 1 mL/min, and the column was subsequently washed with three column volumes of the equilibration buffer. With an isoelectric point (pI) of 4.69, HIV-1 Vpu is negatively charged at pH 8 and could not bind to the cation exchange column and was thus collected in the flow-though.

2.2.2.3.2 Refolding of HIV-1 Vpu

The HIV-1 Vpu from above was refolded by step-wise dialysis into decreasing concentrations of urea (4 and 0 M, respectively) in 20 mM Tris-Cl pH 8.0, 50 mM NaCl, and 1 mM DTT using SnakeSkin dialysis tubing with a molecular weight cut-off of 3500 Daltons (Life Technologies) at 4 °C. The protein sample was centrifuged at 16 000 x g for 30 minutes to remove any possible precipitates.

2.2.2.3.3 Anion exchange chromatography

The refolded HIV-1 Vpu was further purified using a Q-Sepharose Fast Flow anion exchange column (GE HealthCare, UK) connected to the ÄKTA Prime Plus system. The column was pre-equilibrated with five column volumes of 20 mM Tris-Cl pH 8.0, 50 mM NaCl and 1 mM DTT. HIV-1 Vpu was loaded onto the column at a flow rate of 1 mL/min, and the column was subsequently washed with five column volumes of the equilibration buffer. The recombinant protein was eluted at a gradient with the equilibration buffer as the starting buffer, and a set final target of 100% elution buffer (20 mM Tris-Cl pH 8.0, 250 mM NaCl, and 1 mM DTT). The elution fractions were collected at a flow rate of 3 mL/min and 3 mL per fraction. The elution fractions were analysed for the presence of HIV-1 Vpu, and the fractions containing HIV-1 Vpu were pooled together and concentrated under nitrogen gas using a stirred ultrafiltration cell in conjunction with a 3 kDa cut-off membrane (Millipore). Glycerol and sodium azide (NaN_3) were added to the purified HIV-1 Vpu to final concentrations of 10% (v/v) and 1 mM, respectively. The protein was subsequently stored at -80 °C for future use.

2.2.3 Determination of protein concentration

The concentration of the purified recombinant protein was determined spectrophotometrically at 280 nm by applying the Beer-Lambert Law:

$$A = \varepsilon_{\lambda} c.l$$

where ***A*** is the absorbance at 280 nm as measured using the NanoDrop 2000 spectrophotometer (Thermo Fisher Scientific), $\boldsymbol{\varepsilon_{\lambda}}$ is the molar absorption coefficient of the recombinant protein at a given wavelength ($M^{-1}.cm^{-1}$), ***c*** is the concentration of the protein solution (M) and ***l*** is the path length of light through the solution in the sample retention (cm).

The molar extinction coefficient of HIV-1 Vpu at 280 nm was determined using the extinction coefficients of tryptophan (550 $M^{-1}.cm^{-1}$), tyrosine (1490 $M^{-1}.cm^{-1}$) and cysteine (125 $M^{-1}.cm^{-1}$) residues using the following equation (Pace *et al.*, 1995).

$$\varepsilon_{(280)}\ (M^{-1}.cm^{-1}) = (\Sigma\ Trp)\ (5500) + (\Sigma\ Tyr)\ (1490) + (\Sigma\ Cys)\ (125)$$
$$= (2)\ (5500) + (1)\ (1490) + (0)\ (125)$$
$$= 12\ 490\ M^{-1}.cm^{-1}$$

where $\boldsymbol{\varepsilon_{(280)}}$ refers to the molar extinction coefficient of the protein at 280 nm. The molar extinction coefficient value of HIV-1 Vpu at 280 nm was determined to be $\varepsilon_{280} = 12\ 490\ M^{-1}\ cm^{-1}$.

2.2.4 Biochemical analysis of the purified recombinant HIV-1 Vpu

2.2.4.1 Sodium dodecyl sulphate–polyacrylamide gel electrophoresis

Samples collected from each stage of the HIV-1 Vpu expression and purification processes were analysed for the presence and purity of the recombinant protein using the discontinuous SDS–PAGE system of Laemmli (1970) under reducing conditions. The protein samples were diluted four-fold with 4X sample buffer (Bio-Rad) and boiled for 5 minutes to ensure that the proteins were denatured. The samples were loaded onto SDS-polyacrylamide separating gels consisting of a 4% (w/v) acrylamide stacking gel, and a 12% (w/v) acrylamide separating gel (TGX stain-free FastCast gels, Bio-Rad). The gels were run at 200 volts in SDS tank buffer containing 25 mM Tris (pH 8.6), 192 mM Glycine and 0.1% SDS (w/v), for 45 minutes to achieve separation of the proteins. The proteins were run alongside protein molecular weight markers with the following molecular weights: 250, 150, 100, 75, 50, 37, 25, 15 and 10 kDa. Following completion of the electrophoretic runs, the gels were viewed on the gel capture imager (ChemiDoc™ MP System (Bio-Rad)).

2.2.4.2 Chemiluminescence-based Western blot analysis

To verify the identity of the expressed and purified protein, Western blot analysis was conducted. Proteins separated by SDS-PAGE were transferred to nitrocellulose membranes using the iBlot dry transfer system (Life Technologies) along with the iBlot gel transfer stacks (Life Technologies). The membranes were blocked with blocking buffer (5% casein peptone in Tris-buffered saline (TBS; 20 mM Tris pH 7.6, 150 mM NaCl)) overnight to prevent non-specific antibody binding. After washing the membranes with TBS containing Tween-20 (TBS-T; 20 mM Tris, 150 mM NaCl, 0.1% Tween-20), incubation of membranes with 10 000 times dilutions the rabbit anti-Vpu antibody (NIH) made up in blocking buffer, for 2 hours was conducted. To remove unbound primary antibodies, the membranes were washed with TBS-T before incubating with 10 000 times dilutions of horseradish peroxidase (HRP)-conjugated goat anti-rabbit IgG (KPL) secondary antibody made up in blocking buffer. The membranes were once again washed with TBS-T, developed using the Clarity Western ECL substrate reagent (BioRad), and subsequently viewed on the ChemiDoc™ MP System by exposure for one minute.

2.2.4.3 Qualitative analysis of the purified HIV-1 Vpu using ELISA

Specific detection of the purified recombinant HIV-1 Vpu by HIV-1 Vpu specific antibodies (i.e. rabbit anti-Vpu) was investigated. ELISA also provided the means to further confirm the identity and determine the biological integrity of the purified proteins. For this assay, 96-well microtiter maxisorp surface plates (Nunc) were coated with the purified proteins and ELISA was performed using anti-Vpu in order to detect reactivity. Briefly, the proteins were diluted to the following concentrations: 100, 50, 25, 12.5, 6.25, 3.125 and 1.562 µg/mL in coating buffer (15 mM Na_2CO_3, 35 mM $NaHCO_3$, pH 9.6). The protein solutions were coated onto microtiter plates at 100 µL/well alongside negative coating buffer controls. After an overnight incubation at 4 °C, the coating solution was aspirated, followed by three washing steps with 300 µL/well TBS-T. Blocking of non-specific binding with TBS containing 5% casein peptone was conducted for 2 hours at 37 °C, followed by washing as above. The anti-Vpu primary antibody was diluted 1:5000 in blocking buffer and applied to the wells at 100 µL/well. After 2 hours at 37 °C and three additional washing steps, the wells were incubated with 100 µL HRP-conjugated secondary anti-rabbit antibody diluted to 1:10 000 in blocking buffer for an hour at 37 °C. After washing the wells, HRP activity was detected using the 3,3',5,5'-Tetramethylbenzidine (TMB) substrate, and the reaction was terminated by addition

of 10% (v/v) sulfuric acid in distilled deionised water (ddH_2O) 30 minutes after the addition of the substrate. The colour change was measured spectrophotometrically at a wavelength of 450 nm using an xMark microplate reader (BioRad).

2.2.5 Structural Characterisation of HIV-1 Vpu

2.2.5.1 Far-UV circular dichroism of HIV-1 Vpu

Circular dichroism (CD) is a spectroscopic technique that measures the difference in the absorption of left- and right-circularly polarised light by optically active molecules. In proteins, optical activity arises from the disulphide groups, aromatic side chains, and the peptide backbone (Woody, 1995). Disulphide groups and aromatic amino acids have characteristic absorption bands in the near-UV region (250 - 300 nm), while the peptide backbone is the predominant signal in the far-UV region (170 - 250 nm). For this reason, far-UV CD is widely used as a tool in protein studies to determine the secondary structural elements of proteins. Proteins with a high α-helical content show distinctive troughs at 208 and 222 nm and a strong positive peak near 190 nm, while those high in β-sheets display a single trough at 218 nm and a positive peak in the 195 – 200 nm region (Woody, 1995). However, as a result of a high noise to signal ratio of some buffers, data at wavelengths below 210 nm is usually noisy, making it difficult to read.

After the identity of the purified and refolded protein was confirmed to be HIV-1 Vpu (through the use of Vpu-specific antibodies), CD spectra in the far-UV region (250 – 190 nm) was used to analyse the secondary structure of the protein. For this analysis, HIV-1 Vpu was first dialysed against 20 mM Tris-Cl (pH 7.4), 50 mM NaCl and 1 mM DTT, and centrifuged at 16 000 x g for 30 minutes to remove any aggregates. The CD spectra were measured in a quartz cuvette with a 0.2 cm path length using a J-1500 CD spectrometer (Jasco). A data pitch of 0.5 nm with a scanning speed of 100 nm/min and a band width of 2 nm were used. The protein concentration used varied from 10 - 16 µM, and the spectra were recorded at 20 °C. Spectra were averages of 10 scans, with the buffer control subtracted from 250 to 190 nm. The obtained ellipticity values were converted to mean residue ellipticity [θ] ($mdeg.cm^2.dmol^{-1}$) using the equation:

$$[\theta] = \frac{100\ x\ \theta}{Cnl}$$

where $\boldsymbol{\theta}$ is the measured ellipticity in millidegrees (m.deg), $\boldsymbol{C}$ is the protein concentration in millimolar (mM), $\boldsymbol{n}$ is the number of amino acid residues in the protein and $\boldsymbol{l}$ is the path length of the cuvette in centimetres.

2.2.5.2 Intrinsic Fluorescence

Fluorescence occurs when a fluorophore within a molecule absorbs light at a specific wavelength. The absorbed light results in excitation of electrons to a higher energy level, and when the electrons return to lower energy levels, also known as the ground state, light is emitted (Lakowicz, 1983). During the excited state, energy is lost through vibrational and conformational changes, which means that the emitted light will be of lower energy and greater wavelength compared to the absorbed light. The energy lost between excitation and emission is known as Stoke's shift (Lakowicz, 1983).

In proteins, naturally occurring fluorophores include the aromatic amino acid residues, namely tryptophan, tyrosine and phenylalanine. However, the fluorescence of most proteins is generally dominated by tryptophan residues as both their absorbance at the wavelength of excitation and their quantum yields are much greater than the values for tyrosine and phenylalanine (Lakowicz, 1983). Tryptophan residues are generally more sensitive than tyrosine and phenylalanine residues, and this is because tryptophan has a molar extinction coefficient of 5500 $M^{-1}.cm^{-1}$ at 280 nm, while tyrosine and cysteine are 1490 $M^{-1}.cm^{-1}$ and 125 $M^{-1}.cm^{-1}$, respectively (Pace, 1995). Furthermore, fluorescence of the indole ring of tryptophan is sensitive to changes in its local environment and can thus be used as a valuable probe to monitor local tertiary structural changes that occur in the protein.

The fluorescence measurements were recorded in a quartz cuvette with a 1 cm path-length using a Jasco FP-8200 spectrometer (Jasco Inc., Tokyo, Japan) with the Spectra Manager software (v1.5.00). The experiments were carried out using 5 – 10 µM HIV-1 Vpu in 20 mM Tris (pH 8), 50 mM NaCl and 1 mM DTT. The fluorescence emission spectra of the protein were obtained by selectively exciting the tryptophan residues at 295nm, and tyrosine and tryptophan residues at 280 nm. The emission spectra were recorded from 280 to 500 nm with the excitation and emission slit widths kept at 5 nm. The spectra were recorded at room temperature, buffer blank corrected, and are an average of three accumulations at a scan speed of 200 nm/min.

2.2.5.3 Size Exclusion Chromatography

The size and homogeneity of the purified HIV-1 Vpu was assessed using size exclusion chromatography (SEC). The protein was analysed using an Enrich SEC 70 size exclusion column (Bio-Rad), with a resolution of up to 70 kDa, connected to the NGC Medium-Pressure Liquid *Chromatography* system (Bio-Rad).

The column was equilibrated with 20 mM Tris (pH 8), 250 mM NaCl, 1 mM DTT, and subsequently loaded with 240 µL of 200 µM HIV-1 Vpu. The protein was eluted at a flow rate of 0.5 mL/min using the equilibration buffer, and the elution of the protein was monitored through absorbance at 280 nm. A set of protein standards (GE healthcare low range gel filtration calibration kit) was run according to the manufacturer's instructions using the same conditions as the HIV-1 Vpu. The following protein standards: Conalbumin (75 kDa), Carbonic Anhydrous (29 kDa), Ribonuclease A (13.7 kDa) and Aprotinin (6.5 kDa) were used to construct a standard curve.

2.2.6 Analysis of the protein-protein interaction between HIV-1 Vpu and BST-2

2.2.6.1 <u>In vitro ELISA test for the binding of HIV-1 Vpu to BST-2</u>

The binding between HIV-1 Vpu and BST-2 was analysed using the Enzyme-linked immunosorbent assay (ELISA) with the purified recombinant HIV-1 Vpu and a commercial BST-2 sandwich ELISA kit (Uscn Life Science). The assay was carried out according to the kit instructions, and all reagents used (with the exception of the HIV-1 Vpu) were provided with the kit. Briefly, 100 µL of BST-2, at a concentration of 5 ng/mL, was added on a 96-well microtitre plate that was pre-coated with an anti-BST-2 antibody and the plate was incubated at 37 °C for an hour. Excess BST-2 was discarded and 100 µL of the recombinant HIV-1 Vpu was introduced at 5 and 10 ng/mL. The plate was incubated at 37 °C for another hour, after which 100 µL of a biotin-conjugated anti-BST-2 antibody was added. After an hour incubation at 37 °C, the plate was washed three times with the kit's wash buffer, and 100 µL of Streptavidin conjugated to HRP was added. Following a 30 minutes incubation at 37 °C, the plate was washed again, and the activity of the HRP enzyme was detected using 100 µL of the TMB substrate solution. The enzyme-substrate reaction was terminated through addition of 50 µL of the stop solution (10% sulphuric acid) 30 minutes after the addition of

the substrate, and the absorbance was measured spectrophotometrically at 450 nm using the xMark microplate reader.

2.2.6.2 Analysis of the HIV-1 Vpu/BST-2 interaction using AlphaScreen

The Amplified Luminescent Proximity Homogeneous Assay Screen (AlphaScreen) is a bead-based assay that is used to study biomolecular interactions in a microtiter plate format (PerkinElmer, 2004). The basis of the assay is a proximity-dependent transfer of singlet oxygen (molecular oxygen with a single excited electron) between two types of beads, namely Donor and Acceptor beads. Donor beads contain phthalocyanine, a photosensitiser that converts ambient oxygen to an excited form upon illumination at 680 nm, while the Acceptor beads contain a thioxene derivative that allows for emission of light between 520 and 620 nm. The singlet oxygen has a half-life if 4 µsec and can diffuse up to 200 nm in solution. If an Acceptor bead is within this distance, energy is transferred from the singlet oxygen to the thioxene derivatives within the Acceptor bead, resulting in the production of light (as illustrated in Figure 2.1). However, if the Acceptor bead is not within 200 nm of the Donor bead, the singlet oxygen falls to ground state and no signal is produced.

When measuring protein-protein interactions, one protein is captured on the Donor beads, and the other protein is captured on the Acceptor beads. When the two proteins interact, the Donor and Acceptor beads are brought into proximity (< 200 nm) and energy gets transferred from the singlet oxygen in the Donor beads to the Acceptor beads, thereby resulting in signal generation. In case of no interaction between the two proteins, the singlet oxygen falls back into ground state resulting in no signal production.

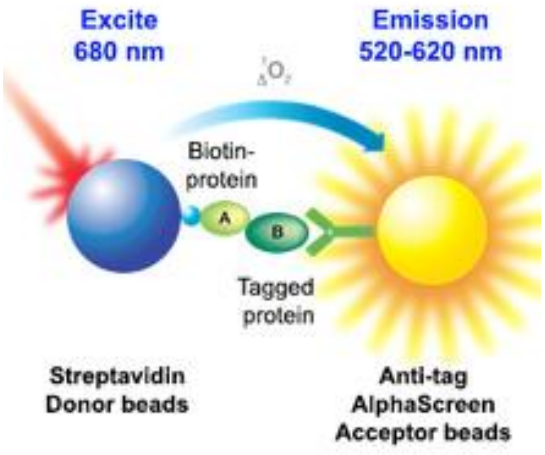

Figure 2.1: Schematic representation of the HIV-1 Vpu/BST-2 interaction in the AlphaScreen assay. The streptavidin Donor bead links to the biotin labelled HIV-1 Vpu which in turn interacts with the GST tagged BST-2 bound to the anti-GST conjugated Acceptor bead.

Chemical Biotinylation of HIV-1 Vpu

HIV-1 Vpu was biotinylated for use in the AlphaScreen Assay. The biotinylation process was conducted using a biotin protein labelling kit (Roche Diagnostics) as per the manufacturer's instructions. Briefly, the purified recombinant HIV-1 Vpu was buffer exchanged *via* dialysis into phosphate buffered saline (PBS; 137 mM NaCl, 2.7 mM KCl, 8 mM Na_2HPO_4, 2 mM KH_2PO_4, pH 7.4) using a 3 kDa MWCO snake skin dialysis tubing. The biotin reagent (D-biotinoyl-ϵ-aminocaproic- acid-N-hydroxysuccinimide) was dissolved in Dimethylsulfoxide (DMSO) to a final concentration of 20 mg/mL. A dilution of HIV-1 Vpu with the biotin reagent at a 1:10 molar ratio (HIV-1 Vpu: biotin) was made and incubated at room temperature for 2 hours with gentle shaking. To remove excess biotin, the HIV-1 Vpu-biotin solution was loaded onto a G25 gel filtration column, which was previously blocked with the blocking reagent (Roche Diagnostics) and equilibrated with PBS. The protein was eluted using PBS through gravity feed and elution fractions of 0.5 mL were collected. The concentration of the protein in each sample was quantified using the Nanodrop 2000 spectrophotometer and samples containing the biotinylated HIV-1 Vpu were pooled together and concentrated using the stirred ultrafiltration cell and a 3 kDa cut-off membrane. DTT and glycerol were added prior to storing the protein at -80 °C for future use.

Verification of the biotinylation of HIV-1 Vpu

To test the efficiency of the biotinylation conducted above, a sandwich ELISA test was developed using the EvenCoat streptavidin coated 96-well microtiter plates (R & D Systems). In brief, serial dilutions of the biotinylated HIV-1 Vpu to the following concentrations: 50, 25, 12.5, 6.25, 3.125 and 1.562 µg/mL were prepared in PBS. The protein was coated at 100 µL per well alongside untagged HIV-1 Vpu and PBS as negative controls. After 1-hour incubation at room temperature, excess protein was discarded, followed by three washing steps with 350 µL TBS-T in each well. Blocking of non-specific binding with TBS containing 5% casein peptone was conducted for 2 hours at room temperature, followed by washing as above. A 1: 5000 dilution of the anti-Vpu primary antibody was prepared in the blocking solution and applied to the plate at 100 µL per well. After 2 hours of incubation at room temperature and three additional washing steps, 100 µL of the HRP-conjugated anti-rabbit secondary antibody diluted to 1:10 000 in blocking buffer was added. The plate was incubated at room temperature for an hour, afterwhich the wells were washed as outlined above, and the activity of the HRP enzyme detected with the TMB substrate. The reaction was terminated using 10% (v/v) sulfuric acid in distilled deionised water (ddH_2O) 30 minutes after the addition of the substrate. The colour change was measured spectrophotometrically at a wavelength of 450 nm using an xMark microplate reader (BioRad).

Development of the HIV-1 Vpu/BST-2 AlphaScreen assay

An AlphaScreen assay for the determination of the interaction of HIV-1 Vpu with BST-2 was developed and used as a secondary assay to confirm the results obtained from the ELISA. The assay was performed using the biotinylated HIV-1 Vpu and a commercial recombinant BST-2 protein with a Glutathione S-transferase (GST) tag (Abcam). HIV-1 Vpu and BST-2 were incubated together at a 1:1 ratio to a final concentration of 100 nM for each protein. Half-area Opti-Plates (Perkin Elmer) were used and the proteins were diluted in an AlphaScreen assay buffer composed of 25 mM HEPES (pH 7.4), 100 mM NaCl, and 0.1% BSA. Following a 2-hour incubation of the proteins at 37 °C, Streptavidin Donor beads and anti-GST conjugated Acceptor beads (Perkin Elmer) were added to a final concentration of 10 µg/mL. The plate was incubated at 30 °C in the dark for an hour and the luminescence response was subsequently read between 520 – 620 nm on the EnSpire Multimode plate reader (Perkin Elmer). The following controls were included in the development of the

assay: beads alone, HIV-1 Vpu alone, BST-2 alone, HIV-1 Vpu and BST-2 alone, and each protein with both beads.

2.2.7 Biochemical screening of inhibitors for the HIV-1 Vpu/BST-2 interaction

2.2.7.1 Computational Docking studies of HIV-1 Vpu and BST-2

Small molecular compounds were designed against the interaction of HIV-1 Vpu with BST-2 using molecular modelling. X-ray structures of the α-helical transmembrane domains of HIV-1 Vpu (code 2GOH, Park *et al*., 2006) and BST-2 (code 2LK9, Skasko *et al*., 2012) were obtained from the protein databank (PDB) and were used to generate a HIV-1 Vpu/BST-2 complex using the ZDOCK program in the Accelrys Discovery Studio software 4.0 (BIOVIA). The docking resulted in multiple docking poses, and the one with the lowest root-mean-square deviation (RMSD) value of 2.57 Å was chosen as the most favourable model (illustrated in Figure 2.2). Analysis of the HIV-1 Vpu/BST-2 interaction using this model showed that amino acid residues Ala10, Ala14, Ala18 and Trp22 of HIV-1 Vpu and amino acid residues Val30, Ile33, Ile34, Ile37, Leu41 and Thr45 of BST-2 were involved in the interaction. These results are consistent with previous findings by Zhou *et al.* (2012) using mutational analysis. This model of the HIV-1 Vpu/BST-2 transmembrane complex also shows that the two proteins interact in an anti-parallel manner, and this is also in agreement with previous reports (Zhou *et al*., 2012). Furthermore, Ala14, Ala18 and Trp22 of HIV-1 Vpu's TM domain were used as a query in the virtual screening of compounds against the HIV-1 Vpu/BST-2 interaction using the pepMMsMIMIC web-based screening tool (http://mms.dsfarm.unipd.it/pepMMsMIMIC/index.php) (Rashamuse, 2017). The top 24 compounds identified from the *in silico* virtual screening were synthesised in-house and screened for their ability to disrupt the binding of HIV-1 Vpu to BST-2 *in vitro* (details of the screening are described below).

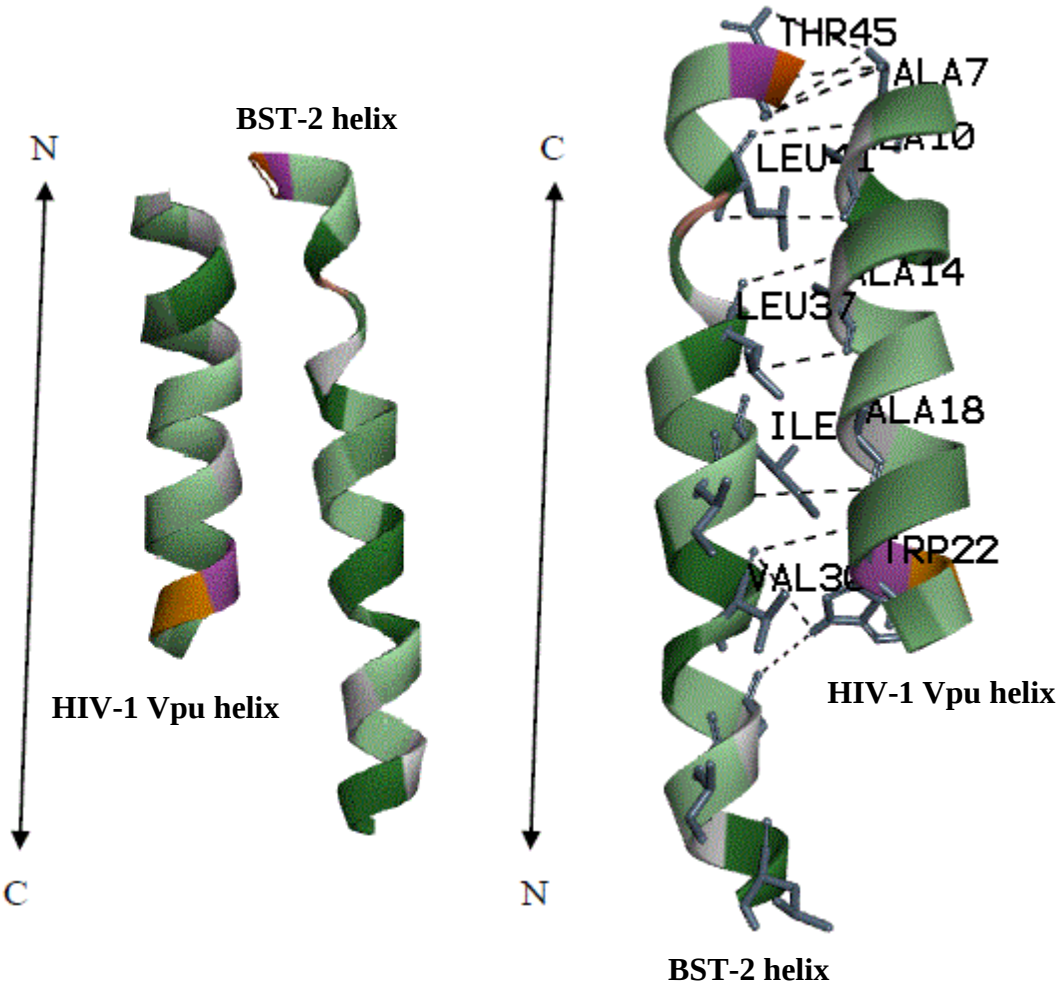

Figure 2.2: Representation of the HIV-1 Vpu in complex with BST-2 through their respective α-helical transmembrane domains. This complex was predicted using the ZDOCK program in the Accelrys Discovery Studio software 4.0 (BIOVIA).

2.2.7.2 Sandwich ELISA

The ELISA test optimised above was used in the screening of the 24 compounds identified to show inhibition against the HIV-1 Vpu/BST-2 interaction *in silico*. For this assay, 5 ng/mL of HIV-1 Vpu was incubated with 100 µM of each compound for 30 minutes at 37 °C with slight shaking, and BST-2, to a final concentration of 5 ng/mL, was coated on a 96-well polysorp plate that was pre-coated with an anti-BST-2 antibody (Uscn Life Science). Following the incubation period, excess BST-2 was discarded and the HIV-1 Vpu/compound solutions were introduced at 100 µL. The plates were incubated at 37 °C for an hour, and a biotin-conjugated anti-BST-2 antibody (Uscn Life Science) was added and incubated at 37

°C for another hour. Following three washes, the Streptavidin conjugated to HRP was added and the plates were incubated at 37 °C for 30 minutes. The plate was washed five times, afterwhich the activity of the HRP enzyme was detected using the TMB substrate, the enzyme-substrate reaction was terminated by addition of sulphuric acid, and the colour change was measured spectrophotometrically at 450 nm. The compounds were tested in duplicate wells and the assay was repeated three times. The inhibition percentage for each of the test compounds was calculated using the following equation:

$$\%\text{Inhibition} = 1 - \frac{Sample - Negative\ Control}{Positive\ Control - Negative\ Control} X100$$

2.2.7.3 AlphaScreen

To validate the compound screening results obtained from the ELISA, the AlphaScreen assay was used to confirm the activity of the compounds in inhibiting the HIV-1 Vpu/BST-2 interaction. For this assay, 400 nM of the biotinylated HIV-1 Vpu was incubated with 100 µM of each compound at 37 °C for 30 minutes. Following the incubation period, the recombinant GST-tagged BST-2 was added to a final concentration of 100 nM and incubated at 37 °C for an hour. Streptavidin Donor and anti-GST conjugated Acceptor beads were added at 10 µg/mL and the plate was incubated at 30 °C in the dark for an hour. The plate was read on the EnSpire Multimode plate reader as detailed above, and the inhibition percentages of the compounds were calculated using the %Inhibition equation used for the ELISA screening above. The compounds were tested in duplicate wells and the assays were repeated three times.

2.2.7.4 Dose-Response Studies

The optimised AlphaScreen assay from above was used to conduct dose-response studies for the compounds that showed highest inhibition in the interaction of HIV-1 Vpu with BST-2. This was done to determine the concentrations of the compounds that caused 50% inhibition (IC_{50}) in the interaction. A total of eight serial dilutions ranging from 200 – 1.56 µM were run for each compound on this assay. Percentage inhibition was calculated for each concentration and plotted against the logarithm of the concentration. The compounds were tested in duplicate at each concentration and the assays were repeated three times. The obtained data was analysed and fitted using Origin 6.0 software.

2.2.8 Determination of the pharmacochemical properties of the inhibitors

2.2.8.1 In silico assessment of the ADME-T properties of the compounds

The compounds that showed good inhibition percentages for the HIV-1 Vpu/BST-2 interaction were analysed for drug-likeness according to Lipinski's rule-of-five (Lipinski *et al*., 1997). The rule-of-five defines the desired physicochemical properties of a compound that allow for oral absorption (Lipinski *et al*., 1997). For a compound to be considered as a 'lead', it should exhibit specific binding towards the target and the absorption, distribution, metabolism, excretion and toxicity (ADME-T) properties of the compound should be known (Wunberg *et al*., 2006). The rule was developed after a pattern in the physicochemical properties was observed following the screening of 2245 compounds from the World Drug Index (Lipinski *et al*., 1997). The majority of screened compounds displayed a molecular mass of less than 500 g/mol, were composed of less than 10 hydrogen bond acceptors (N and O atoms) and 5 hydrogen bond donors (OH and NH groups) and possessed an octanol-water partition coefficient (LogP) value of less than 5 (Lipinski *et al*., 1997). The Accelrys Discovery Studio 4.0 software package (Accelrys) on the other hand was used to determine the water-octanol partitioning co-efficiency (LogP), as well as the number of hydrogen bond donors and acceptors in each compound.

2.2.8.2 Aqueous Solubility analysis of the compounds

Aqueous solubility has been shown to have a large impact on numerous aspects of drug discovery. It has become apparent that low solubility can affect biological assays by reducing the concentration of the compound at the target site, resulting in erroneous structure-activity-relationship (SAR) and ADME-T assessments. For this reason, screening the compounds for their aqueous solubility, in addition to the *in silico* prediction was mandatory. To study the aqueous solubility of the identified inhibitors, a filtration-based assay that includes 96-well filter plates was adapted from Millipore and was conducted according to the manufacturer's instructions. Briefly, compound stocks were prepared in DMSO, and the standards were diluted in an 80:20 PBS: acetonitrile solution. The concentration of DMSO was maintained at 5% in all the standards, and standard concentrations of 500, 200, 50, 12.5 and 3.13 µM were prepared for the construction of a standard curve. The standards were incubated in a 96-well filter plate (Millipore, Merck) at room temperature shaking at 300 rpm overnight (~16 hours). Following vacuum filtration into a deep-well plate, the compounds in solution were

transferred to a UV-Star plate and analysed by UV/Vis spectroscopy using a microplate reader (measured from 200 to 800 nm at 10 nm increments). The inhibitors were tested alongside Chloramphenicol as a positive control.

Following construction of the standard curves, 200 and 100 µM samples of the compounds were prepared in 100% PBS, incubated in a filter plate shaking overnight at room temperature. The plate was vacuum filtered and 80 µL of the compounds transferred to a UV-Star half-area micro plate for analysis. A total of 20 µL acetonitrile was added per sample and the compounds were quantified using UV/Vis spectroscopy at the optimum wavelength for each compound.

The amount of soluble compound in the aqueous sample was quantified using the following equation:

$$Aqueous\ Solubility = (A_{max}\ Filtrate/\ Slope) * 1.25$$

where the maximum absorbance of each compound ($\boldsymbol{A_{max}}$) was divided by the slope of the line from the respective calibration curve and multiplied by a factor of 1.25 to account the dilution with acetonitrile.

2.2.8.3 Cellular toxicity

The toxicity of the test compounds against mammalian cells was evaluated using the MTS cell proliferation assay according to the manufacturer. The method is based on the reduction of the yellow MTS tetrazolium compound by viable cells to generate a purple coloured formazan product with an absorbance maximum of 490 nm. When cells die, they rapidly lose their ability to convert the substrate to product, making this conversion directly proportional to the number of viable cells present.

Briefly, Human T cell leukaemia (MT-4) cells (NIH AIDS Reagents Programme, Division of AIDS, NIAID, NIH: catalogue number: 120) were seeded at a density of $1x10^5$ cells/mL and a final volume of 100 µL/well in 96-well cell culture plates (Sigma Aldrich). The cells were incubated at 37 °C in a humidified atmosphere of 5% CO_2 for 4 hours to allow for stabilisation. Following the incubation period, dose response studies of the test compounds were conducted using 2-fold serial dilutions, with final concentrations ranging from 200 to 1.56 µM in Roswell Park Memorial Institute (RPMI) 1640 medium (Gibco, Life Technologies) containing 10% (v/v) foetal calf serum (FCS, Highveld Biological). Auranofin

(Biomol International) was used as a positive control, and a total of 100 µL compounds were added to the cells. The plates were incubated under standard culture conditions (37 °C and 5% CO_2) for 72 hours, afterwhich the viability of the cells was determined using the MTS dye. The MTS solution, to a volume of 20 µL per well, was added and the plates were incubated at 37 °C for a further 4 hours. The amount of soluble formazan produced was measured spectrophotometrically at 490 nm, and untreated MT-4 cells were used as positive controls. The percentage of viable cells (%Viability) calculated using the following equation:

$$\%\text{Viability} = \frac{Absorbance\ of\ Sample - Absorbance\ of\ Medium}{Absorbance\ of\ Control - Absorbance\ of\ Medium}\ X\ 100$$

The data was then further analysed using Origin 6.0 with the logarithmic value of the compound concentration plotted against the viability percentage to obtain a dose-response curve. From the dose curve, a half maximal cytotoxic concentration (CC_{50}) value for each compound was determined.

2.2.9 Determination of the antiviral activity of the compounds

2.2.9.1 Preparation of virus stocks

Viral stocks of HIV-1 were obtained using HIV-1 chronically infected T-cells, called ACH-2 cells (NIH AIDS Reagents Programme, Division of AIDS, NIAID, NIH; catalogue number: 349). ACH-2 cells are human T-lymphocytic leukemia cells that consist of a single integrated copy of latent HIV-1 proviral DNA of the lymphadenopathy-associated virus (LAV) strain. These cells are CD4-negative, CD5-positive, and transferrin receptor-positive, and are used as a model for chronic HIV infection (Folks *et al*., 1989; Pomerantz *et al*., 1990). Upon treatment with cytokines, viral production from these cells was shown to be enhanced (Folks *et al*., 1989). In this study, ACH-2 cells were seeded in a T-25 flask at a density of $1x10^6$ cells/mL and phorbol 12-myristate 13-acetate (PMA; Sigma Aldrich), at a final concentration of 0.5 ng/mL, was used as a stimulant. The flask was incubated under standard culture conditions for 72 hours, afterwhich the virus containing media was collected from the cells, filtered through 0.22 µm pore-size filters and stored at –80 °C for future use.

2.2.9.2 The anti-HIV-1 activity of the compounds

The antiviral activities of the identified compounds against HIV-1 were investigated using MT-4 cells and the HIV-1 LAV viral strain. Briefly, MT-4 cells ($1x10^5$ cells/mL) were infected using the virus containing supernatant prepared above at a multiplicity of infection (MOI) of 0.1. The cells were plated onto 96-well tissue culture plates at 100 µL/well, and the plates were subsequently incubated at 37 °C in a humidified atmosphere of 5% CO_2 for 90 minutes. Following the incubation period, two-fold serial dilutions of each compound (200 – 1.56 µM) made up in 10% RPMI were added to the cells and the plates were incubated at 37 °C and 5 % CO_2 for 72 hours. The compounds were tested alongside HIV-1 infected cells without any compound treatment, as well as uninfected MT-4 cells as controls. Raltegravir, a known inhibitor of HIV-1, was used as a positive antiretroviral control. After the 72 hour incubation, supernatants were collected from the cells and viral levels were analysed *via* a p24 ELISA test.

Cell supernatants were used to test for the presence of the p24 antigen using the BioElisa HIV-1+2 Ag/AB kit (BIOKIT) according to the manufacturer's instructions. All buffers were prepared according to manufacturer's specifications and the manufacturer's protocol was followed. Briefly, 100 µL of sample diluent buffer and 100 µL of test and control samples were added to the wells of the supplied microplate, coated with monoclonal antibodies against p24. The plate was incubated at 37 °C for an hour, followed by a washing step (5 wash cycles). Conjugate 1 was added to the plate at 200 µL per well and incubated at 37 °C for 30 minutes. The plate was washed (3 wash cycles) and 200 µL per well of conjugate 2 were added to the plate. Following a 30 minute incubation period at 37 °C, the plate was washed (5 cycles) and 150 µL of TMB substrate were added to the wells. The reaction was monitored for up to 30 minutes (until sufficient colour had developed), and 100 µL of the stopping solution was added to stop the reaction. The plates were analysed using UV/Vis spectroscopy at 450 nm.

2.2.10 Analysis of the binding of the compounds to HIV-1 Vpu

2.2.10.1 Binding studies using Intrinsic Fluorescence

The affinities of the identified compounds for the HIV-1 Vpu were determined by measuring the quenching or enhancement of the intrinsic tryptophan fluorescence of the protein upon titration with the different compounds. All fluorescence measurements were performed as detailed in section 2.2.5. HIV-1 Vpu, at a concentration of 5 µM, was titrated with increasing concentrations of the different ligands in quartz cuvettes. The test compounds (at 50 µM increments) were added at each time point, and the final dilution factor was kept below 10% of the initial volume. The protein-ligand solutions were incubated at 20 °C for at least 10 minutes to allow for binding to occur. The tryptophan residues were selectively excited at 295 nm and emission spectra were recorded from 280 to 500 nm. All spectra were recorded at room temperature, corrected for the buffer, and were an average of three accumulations at a scan speed of 200 nm/min. The data was analysed using the Origin 6.0 software.

2.2.10.2 Effects of Ligand Binding on the Thermal Stability of HIV-1 Vpu

Thermal denaturation-based methods are a useful way of characterising the conformational stability of proteins. Methods such as fluorescence and CD are widely used to monitor the thermal induced denaturation of proteins. In this study, the relative stability of HIV-1 Vpu was assessed by monitoring the extent of α-helix denaturation using CD spectroscopy at 222 nm in response to changes in temperature. The samples consisted of 5 μM HIV-1 Vpu in 20 mM Tris (pH 8), 50 mM NaCl, and readings were recorded from 20 °C to 100 °C at a heating rate 1 °C.min^{-1}. The temperature unfolding profiles were normalised by calculating the mean residue ellipticity [θ] in deg.cm^2.dmol^{-1} and the data was used to construct a thermal denaturation curve. The melting temperature (T_m) of HIV-1 Vpu, which is the mid-point of the thermal denaturation curve, was subsequently determined. The reversibility of HIV-1 Vpu after thermal denaturation was assessed by monitoring secondary structural changes at 222 nm as the samples were cooled from 100 °C to 20 °C at 1°.min^{-1} decrements.

Furthermore, since the binding of ligands to proteins causes a shift in the protein's stability, thermal shift assays are gaining recognition in the pharmaceutical industry as a tool to investigate the binding of drug candidates to therapeutic targets. This becomes especially important when the target protein has no enzymatic activity, as is the case with HIV-1 Vpu. A shift in the T_m value of the protein to higher or lower temperatures is indicative of binding,

and potential ligands are usually ranked in terms of the magnitude of the shift in the *Tm* value. The effect of the four test compounds (Compound 1, Compound 8, 6-aza-2-thiouridine and Lapachol) on the thermal stability of HIV-1 Vpu was thus assessed in this study. For this assay, 5 µM HIV-1 Vpu was incubated with 5 µM of each of the identified compounds in 20 mM Tris (pH 8), 50 mM NaCl at 20 °C for 30 minutes. The thermal stability of HIV-1 Vpu in the presence of the compounds was assessed using CD spectroscopy at 222 nm recorded from 20 °C to 100 °C at a heating rate of 1 °C.min^{-1} as outlined above. Thermal denaturation curves were constructed from the data.

2.2.10.3 Isothermal Titration Calorimetry

To assess the binding energetics of the identified ligands to HIV-1 Vpu, an isothermal titration calorimetry (ITC) assay was developed. ITC is used to obtain a detailed thermodynamic profile of molecular associations. To date, it is the most sensitive and rigorous method available for the quantitative measurement of protein–ligand interactions. ITC is capable of directly measuring the heat absorbed or released during the binding process. This technique thus allows for the direct determination of the standard Gibbs free energy change (ΔG), the binding constant (K_a), the enthalpy change (ΔH), the entropy change (ΔS) as well as the stoichiometry (N) of the binding interaction in one experiment (Velazquez-Campoy *et al.*, 2004). K_a and ΔH can be derived directly from the titration profile, and these values can be used to calculate ΔG and ΔS using the following equations (Ladbury and Chowdhry, 1996).

$$\Delta G = - RT \ln K_a$$

Where $\boldsymbol{R}$ is the universal gas constant (8.314 J/mol/K), $\boldsymbol{T}$ is the temperature in Kelvin and $\boldsymbol{K_a}$ is the equilibrium binding constant. ΔG is associated with enthalpy and entropy changes as expressed in the following equation:

$$\Delta G = \Delta H - T \Delta S$$

Performing the same experiments at different temperatures, the change in heat capacity (ΔC_p) of the protein–ligand binding reaction may also be determined.

The ITC experiments in this study were performed using the high precision standard volume Nano isothermal titration calorimeter (TA instruments). Prior to the experiments, HIV-1 Vpu was dialysed against 20 mM Tris (pH 7.4), 150 mM NaCl and the ligands were diluted in the

same dialysate to avoid buffer mismatch. The ligand and protein solutions were degassed for 10 minutes immediately prior to use, and the protein solution was loaded into the sample cell, the ligands were loaded in the syringe, and the reference cell was filled with distilled-deionised water. Varying concentrations ratios of HIV-1 Vpu to the ligands were tested in this study, in an attempt to obtain better binding profiles. Using of 10 µM HIV-1 Vpu, 0.2 mM Lapachol, 0.4 mM 6-aza-2-thiouridine, 0.7 mM Compound 1 and 1 mM of Compound 8 were found to give better binding profiles and allowed for the determination of the binding energetics. The DMSO concentration was maintained below 2% throughout the study, and DMSO was added to the protein solution immediately before the ITC experiment to match the DMSO concentration in the ligand solution. The initial titration volume for each ligand was 2 µL, followed by 30 7.5 µL injections. The temperature and stirring speed were kept constant at 20 °C and 300 rpm, respectively, and the spacing between injections was set to 300 seconds. Control experiments, which included similar injections of the ligands into the buffer solution, were also performed and corrected for from the obtained results. The obtained data were fitted with the NanoAnalyze software (TA Instruments) using the independent model.

2.3 References

Adachi A, Gendelman HE, Koenig S, Folks T, Willey R, Rabson A, Martin MA. 1986. Production of acquired immunodeficiency syndrome-associated retrovirus in human and nonhuman cells transfected with an infectious molecular clone. *Journal of Virology* **59**: 284 – 291.

Birdsall B, King RW, Wheeler MR, Lewis CA, Godde SR, Dunlap RB, Roberts GCK. 1983. Correction for light absorption in fluorescence studies of protein-ligand interactions. *Analytical Biochem*istry **132**: 353 – 361.

Chung CT, Niemela SL, Miller RH. 1989. One-step preparation of competent Escherichia coli: Transformation and storage of bacterial cells in the same solution. *Proceedings of the National Academy of Sciences* **86**: 2172 – 2175.

Clouse, K.A., Powell, D., Washington, I., Poli, G., Strebel, K., Farrar, W., Barstad, P., Kovacs, J., Fauci, A.S. and Folks, T.M., 1989. Monokine regulation of human immunodeficiency virus-1 expression in a chronically infected human T cell clone. *The Journal of Immunology*, *142*(2), pp.431-438.

Eftink MR. 1995. Use of Multiple Spectroscopic Methods to Monitor Equilibrium Unfolding of Proteins. *Methods in Enzymol*ogy **259**: 487 – 512.

Folks, T.M., Clouse, K.A., Justement, J., Rabson, A., Duh, E., Kehrl, J.H. and Fauci, A.S., 1989. Tumor necrosis factor alpha induces expression of human immunodeficiency virus in a chronically infected T-cell clone. *Proceedings of the National Academy of Sciences*, *86*(7), pp.2365-2368.

Kraus MH, Parrish NF, Shaw KS, Decker JM, Keele BF, Salazar-Gonzalez JF, Grayson T, McPherson DT, Ping LH, Anderson JA, Swanstrom R, Williamson C, Shaw GM, Hahn BH. 2010. A Rev1 – Vpu polymorphism unique to HIV-1 subtype A and C strains impairs envelope glycoprotein expression from rev-vpu-env cassettes and reduces virion infectivity in pseudotyping assays. *Virology* **20** 397(2): 346 – 57.

Lackowicz, J.R., Principles of fluorescence spectroscopy. 1983. *Search PubMed*, pp.262-268.

Ladbury JE, Chowdhry BZ. 1996. Sensing the heat: the application of isothermal titration calorimetry to thermodynamic studies of biomolecular interactions. *Chemistry & Biology* **3**: 791 – 801.

Laemmli UK. 1970. Cleavage of structural proteins during assembly of the head bacteriophage T4. *Nature* **227**: 680 – 685.

Larder BA, Darby G, Richman DD. 1989. HIV with reduced sensitivity to zidovudine (AZT) isolated during prolonged therapy. *Science* **243** (4899): 1731 – 1734.

Lin YC, Boone M, Meuris L, Lemmens I, Van Roy N, Soete A, Reumers J, Moisse M, Plaisance S, Drmanac R, Chen J. 2014. Genome dynamics of the human embryonic kidney 293 lineage in response to cell biology manipulations. *Nature Communications* **5**: 4767 – 4779.

Lipinski CA, Lombardo F, Dominy BW, Feeney PJ. 1997. Experimental and computational approaches to estimate solubility and permeability in drug discovery and development settings. *Advanced Drug Delivery Reviews* **23**: 3 – 25.

Maldarelli F, Chen M-Y, Willey RL, Strebel K. 1993. Human immunodeficiency virus type 1 Vpu protein is an oligomeric type 1 integral membrane protein. *Journal of Virology* **67**: 5056 – 5061.

Miyagi E, Andrew A, Kao S, Strebel K. 2009. Vpu enhances HIV-1 virus release in the absence of BST-2 cell surface down-modulation and intracellular depletion. *Proceedings of the National Academy of Sciences* **106**: 2868 – 2873.

Nguyen K-L, Llano M, Akari H, Miyagi E, Poeschla EM, Strebel K, Bour S. 2004. Codon optimization of the HIV-1 vpu and vif genes stabilizes their messenger RNA and allows for highly efficient Rev-independent expression. *Virology* **319**:163.

O'Doherty U, Swiggard WJ, Malim MH. 2000. Human Immunodeficiency Virus Type 1 Spinoculation Enhances Infection through Virus Binding. *Journal of Virology* **74**: 10074 – 10080.

Pace CN, Vajdos F, Fee L, Grimsley G, Gray T. 1995. How to measure and predict the molar absorption coefficient of a protein. *Protein Science* **4**: 2411 – 2423.

Park SH, De Angelis AA, Nevzorov AA, Wu CH, Opella SJ. 2006. Three-dimensional structure of the transmembrane domain of Vpu from HIV-1 in aligned phospholipid Bicelles. *Biophysical Journal* **91**(8): 3032 – 3042.

Pomerantz, R.J., Trono, D., Feinberg, M.B. and Baltimore, D., 1990. Cells nonproductively infected with HIV-1 exhibit an aberrant pattern of viral RNA expression: a molecular model for latency. *Cell*, *61*(7), pp.1271-1276.

Rashamuse, T.J. 2017. Design and synthesis of nitrogen containing heterocyclic fragments via isocyanide chemistry and their biological evaluation as potential inhibitors of HIV-1 replication, viewed 06 March 2019, http://wiredspace.wits.ac.za/handle/10539/23655

Skasko M, Wang Y, Tian Y, Tokarev A, Munguia J, Ruiz A, Stephens EB, Opella SJ, Guatelli J. 2012. HIV-1 Vpu protein antagonizes innate restriction factor BST-2 via lipid-embedded helix-helix interactions. *Journal of Biological Chemistry* **287** (1): 58 – 67.

Schmid FX. 1997. Optical spectroscopy to characterise protein conformation. In Protein structure – a practical approach (2nd Ed.) (Creighton, T.E., ed.), pp. 261-297, Oxford University Press, UK.

Shirley BA. 1995. Urea and guanidine hydrochloride denaturation curves. *Methods in Molecular Biology* **40**: 177 – 190.

Stepanenko AA, Dmitrenko VV. 2015. HEK293 in cell biology and cancer research: phenotype, karyotype, tumorigenicity, and stress-induced genome-phenotype evolution. *Gene* **569** (2): 182 – 190.

Velazquez-Campoy A, Leavitt SA, Freire E. 2004. Characterization of protein – protein interactions by isothermal titration calorimetry. *Methods in Molecular Biology* **261**: 35 – 54.

Woody RW. 1995. Circular dichroism. *Methods in Enzymology* **246**: 34 – 71.

Wunberg T, Hendrix M, Hillisch A, Lobell M, Meier H, Schmeck C, Wild H, Hinzen B. 2006.
Improving the hit-to-lead process: data-driven assessment of drug-like and lead-like screening hits. *Drug Discovery Today* **11**: 175 – 178.

Zhou J, Zhang Z, Mi Z, Wang X, Zhang Q, Li X, Liang C, Cen S. 2012. Characterization of the interface of the bone marrow stromal cell antigen 2-Vpu protein complex via computational chemistry. *Biochemistry* **51:** 1288 – 1296.

Chapter 3: The Overexpression, Purification and Characterisation of HIV-1 Vpu

3.1 Introduction

The involvement of HIV-1 Vpu in manipulating the cellular environment in ways that favour viral replication makes this protein an attractive drug target in the treatment of HIV/AIDS. Before a biological molecule can be pursued as a drug target, intensive research into the structure and function of the molecule is essential, and this requires sufficient quantities of the biomolecule of interest. However, as a membrane bound protein, heterologous overexpression and purification of HIV-1 Vpu does not occur readily. Purification of membrane proteins remains a challenge as a result of their insolubility in aqueous solutions and low yields. The most commonly used method for solubilising membrane proteins is the use of detergents. Detergents, however, are not without their own challenges. Detergents have varying characteristics and finding a detergent and buffer conditions that will provide optimal stability for an individual protein involves trial and error (Tate, 2010; Gutmann *et al*., 2007). The detergent concentration also always has to be maintained above the critical micelle concentration (CMC) to avoid the dissolution of the micelle-protein complex, and this concentration is detergent specific (Tate, 2010). Furthermore, the presence of detergents may have an impact on the stability and downstream characterisation of isolated proteins, and therefore excess detergent should be removed or exchanged for an alternative one prior to subsequent analysis.

This section describes a successful strategy that can be employed in the overexpression, solubilisation and purification of full-length HIV-1 Vpu in sufficient quantities. Biochemical techniques such as SDS-PAGE analysis, Western blot analysis, CD and fluorescence spectroscopy were used in the verification and characterisation of the recombinant protein.

3.2 Verification of the HIV-1 Vpu plasmid DNA

In order to confirm the presence and orientation of the HIV-1 Vpu cDNA insert in the pcDNA-Vphu plasmid, the sample was analysed by DNA sequencing using the T7 promoter and T7 terminator universal primers (Inqaba Biotech, South Africa). The obtained sequence showed 100% identity to the *Vphu* synthetic construct by Nguyen *et al.* (2004) with accession number AAZ08413.1 (results shown in Figure B.1, Appendix B).

3.3 Overexpression and Solubilisation of HIV-1 Vpu

HIV-1 Vpu was overexpressed and purified using the protocol outlined in Njengele *et al.* (2016). The protein was heterologously expressed in *E. coli* BL21 (DE3) pLysS cells using IPTG as an inducer. Induction trials determined that optimum expression of HIV-1 Vpu occurred 3 hours after induction with 1 mM IPTG (lane 5 of Figure 3.1). Also evident from Figure 3.1 (lane 2) is that the uninduced *E. coli* BL21 (DE3) pLysS control cells did not show any detectable expression of HIV-1 Vpu upon analysis by SDS-PAGE. A significant decrease in the amount of HIV-1 Vpu present in the cells was observed ~16 hours post induction, indicating that the cells began breaking down the protein. This could be due to misfolding of the protein at high concentrations, which results in the breakdown of misfolded proteins in the periplasm of the bacterial cells (Baneyx, 1999). Although HIV-1 Vpu is 9 kDa in size, it has been shown to anomalously migrate at 16 kDa in glycine-containing SDS-PAGE gels (Strebel *et al.*, 1988; Schubert *et al.*, 1994), and this corresponds to the size of the overexpressed protein in Figure 3.1.

E. coli BL21 (DE3) pLysS cells that showed successful overexpression of HIV-1 Vpu were lysed as described in section 2.2.5, and the solubility of the protein was assessed *via* SDS-PAGE analysis of the cytosol and pellet fractions. This analysis showed that HIV-1 Vpu was mainly in the pellet fraction, suggesting that the protein was predominantly expressed in the insoluble inclusion bodies. Urea, to a total concentration of 8 M, was successfully used to solubilise the inclusion bodies in order to get most of the HIV-1 Vpu into the soluble fraction (results not shown).

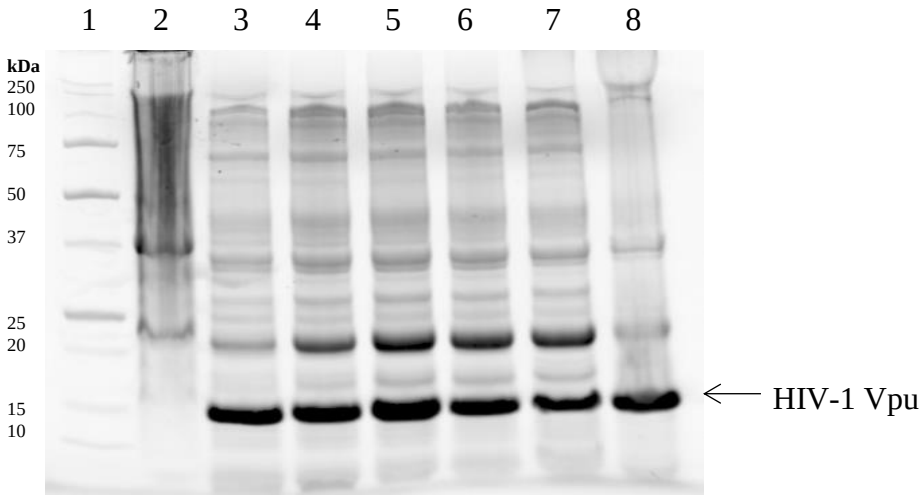

Figure 3.1: SDS–PAGE analysis of the recombinant HIV-1 Vpu protein expressed using *E. coli cells*. The expression was induced by 1 mM IPTG at 37 °C for different time periods. Lane 1: protein molecular weight marker; Lane 2: whole cell lysates before IPTG induction; Lanes 3 – 7: whole cell lysates 1, 2, 3, 4, 5, 6, and 16 hours post IPTG induction, respectively.

3.4 Purification of HIV-1 Vpu

The urea unfolded HIV-1 Vpu protein was first run through a SP-Sepharose fast flow cation exchange chromatography column (GE Healthcare) at pH 8. By virtue of its theoretical isoelectric point (pI = 4.69), estimated using the ExPASy ProtParam tool (http://web.expasy.org/protparam/), HIV-1 Vpu was expected to have an overall negative charge at this pH, and thus not bind the cation exchange resin, while any positively charged proteins at this pH were expected to remain bound to the resin. As shown in Figure 3.3A, lane 6, most of the unwanted protein species that were co-expressed with HIV-1 Vpu remained bound to the SP-Sepharose resin, while HIV-1 Vpu was collected in the flow-through. The protein was refolded by stepwise dialysis into decreasing concentrations of urea (as detailed in section 2.2.5 above), and the refolding of the protein was deemed successful since no indication of precipitation was observed during and/or after the refolding. The HIV-1 Vpu from this step, however, was partially pure, and required further purification.

The refolded sample from the SP-Sepharose column was subsequently purified using a Q-Sepharose fast flow anion exchange chromatography column (GE Healthcare) at pH 8. The protein was eluted using a linear salt gradient from 50 mM to 250 mM. The elution of the

protein was monitored spectrophotometrically at 280 nm, and the elution profile is shown in Figure 3.2 below.

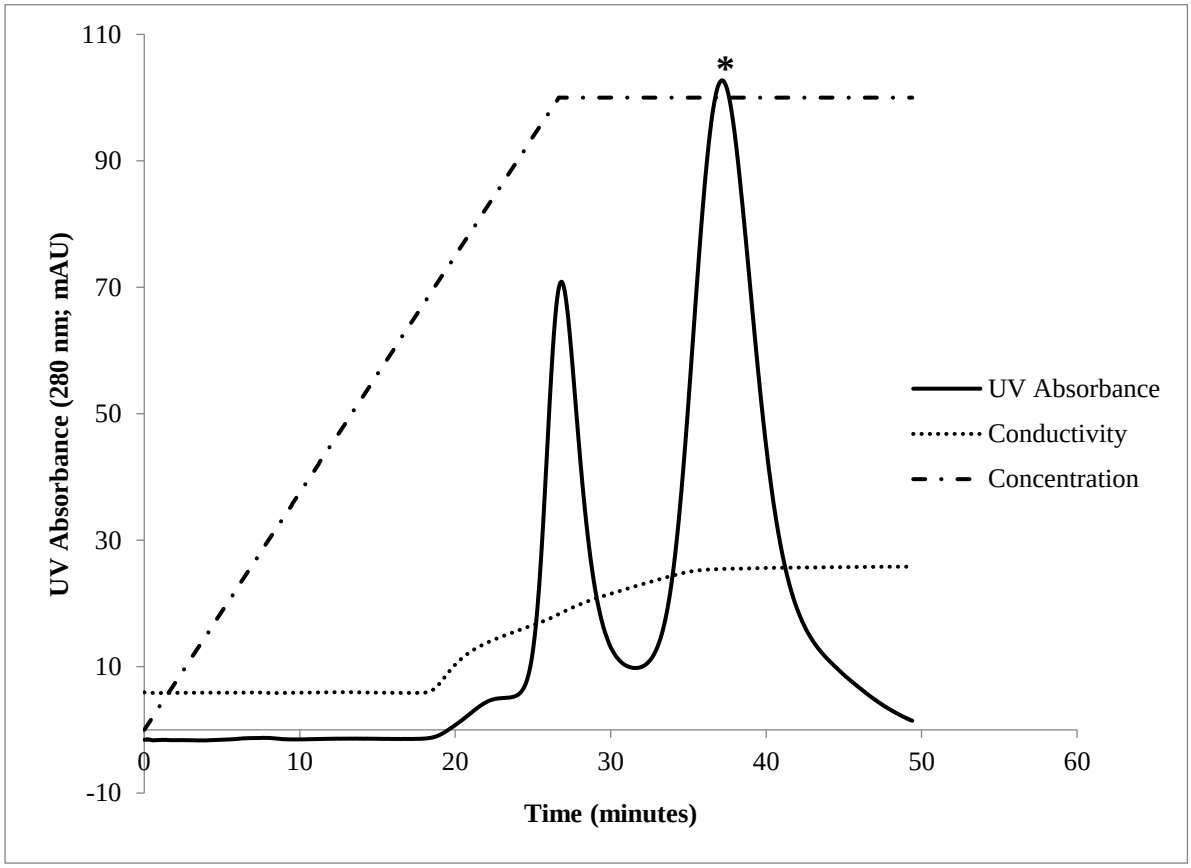

Figure 3.2: The elution profile of HIV-1 Vpu from the Q-Sepharose anion exchange column. The protein was eluted using salt gradient from 0 to 250 mM NaCl. The last peak, marked with an asterisk, contained HIV-1 Vpu.

3.5 Biochemical Analysis of the Purified Recombinant HIV-1 Vpu

3.5.1 SDS-PAGE and Western blot Analysis

The elution fractions collected from the Q-Sepharose purification were analysed for the presence of HIV-1 Vpu using SDS-PAGE and the third peak, marked with an asterisk (Figure 3.2), proved to be HIV-1 Vpu. Fractions corresponding to the HIV-1 Vpu peak were pooled and concentrated, and SDS-PAGE was used to analyse the purity of the protein. Following the second purification step, the SDS-PAGE gel (Figure 3.3 B) shows that the only observable band was at 16 kDa, corresponding to the expected size of full-length HIV-1 Vpu. From the gel, the protein was thus judged to be highly pure, and a total of about 6 mg per litre of bacterial culture was obtained. A calibration curve of the relative mobility of the protein molecular weight standards was constructed from the SDS-PAGE gel in Figure 3.3 B and used to determine the molecular weight of the purified protein (Figure 3.3 D). The calibration curve shows the estimated molecular weight of the purified protein to be approximately 16 kDa, which correlates to the expected size. To further validate the identity of the purified protein, Western blot analysis using HIV-1 Vpu specific antibodies was conducted. The Western blot analysis also showed a 16 kDa band, confirming the identity of the purified recombinant protein to be HIV-1 Vpu (Figure 3.3 C).

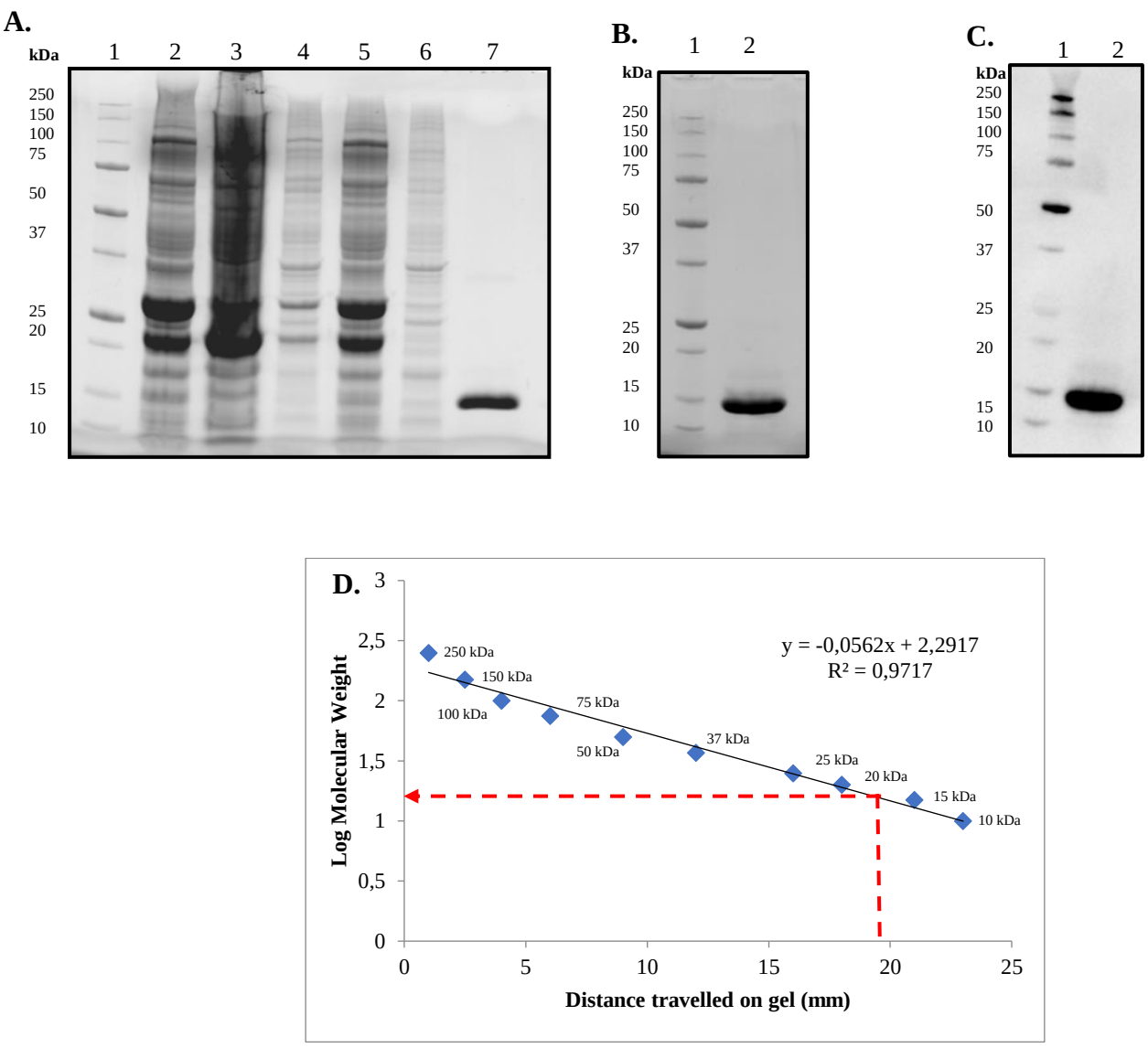

Figure 3.3: Overview of the purification process of HIV-1 Vpu using ion exchange chromatography. The protein was purified by cation and anion exchange chromatography from 1 L culture of *E. coli* BL21 (DE3) pLysS cells transformed with an expression plasmid encoding for HIV-1 Vpu. Samples collected from each step of the purification process were collected and analysed by SDS–PAGE **A.** Lane 1: protein molecular weight marker; Lane 2: whole cell lysate after HIV-1 Vpu expression; Lanes 3: lysate pellet; Lane 4: lysate supernatant; Lane 5: urea solubilised lysate pellet; Lane 6: SP-Sepharose flow-through; Lane 7: Q-Sepharose purified HIV-1 Vpu. **B and C.** SDS-PAGE and Western blot analysis of the purified HIV-1 Vpu using an anti-Vpu antibody, respectively. **D.** Calibration curve constructed using the SDS-PAGE of HIV-1 Vpu and the molecular weight standards. The molecular weight of HIV-1 Vpu was calculated to be ~16 kDa (red arrow).

3.5.2 Qualitative ELISA test

To further analyse the specificity of the detection of the purified recombinant HIV-1 Vpu by the anti-Vpu antibodies, an ELISA was conducted. For this assay, the purified HIV-1 Vpu was coated on microtiter plates at varying concentrations (100, 50, 25, 12.5, 6.25, 3.125, 1.56, 0 µg/mL) to construct a standard curve and the subsequent steps were performed according to the protocol in section 2.2.4. All samples were tested in triplicate, and the average absorbance values for each protein concentration are shown in Figure 3.4 below. Figure 3.4 shows that as the concentration of the protein increased, absorbance readings also increased, indicating a clear positive correlation between the absorbance values and the HIV-1 Vpu concentration. These results suggest specificity of the refolded HIV-1 Vpu recognition by the anti-Vpu antibody, consequently confirming the identity of the protein.

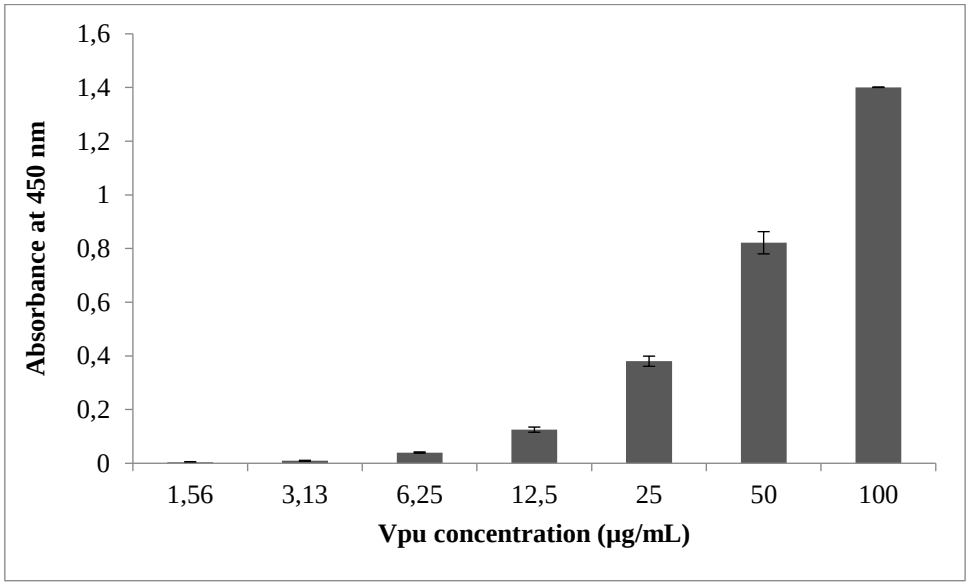

Figure 3.4: Qualitative ELISA analysis of the purified recombinant HIV-1 Vpu. Serial dilutions of HIV-1 Vpu were prepared and detected with anti-Vpu antibodies to confirm the identity and correct presentation of the epitope by the protein. The error bars represent standard errors from three independent experiments.

3.6 Structural Characterisation of HIV-1 Vpu

Following the unfolding and the refolding of HIV-1 Vpu, checking if the protein assumed its correct secondary, tertiary and quaternary structure was of paramount importance. This was conducted using CD spectroscopy, fluorescence spectroscopy and size exclusion chromatography, respectively.

3.6.1 Secondary Structural Characterisation

The secondary structural analysis of the purified recombinant HIV-1 Vpu was conducted using CD spectroscopy in the far-UV region (190 – 250 nm). In this region, α-helices give rise to negative troughs at 222 and 208 nm and a positive peak at 190 nm, while β-sheets produce one trough near 217 nm and a positive peak in the 195 – 200 nm range (Woody, 1995). The CD spectrum obtained for the recombinant HIV-1 Vpu showed two troughs at 208 and 220 nm (Figure 3.5), characteristic of a predominantly α-helical protein.

3.6.2 Tertiary Structural Characterisation

To determine any folding abnormalities that may have occurred during the refolding of HIV-1 Vpu, the protein's tertiary structure was analysed. This was done by means of intrinsic fluorescence spectroscopy of tryptophan and tyrosine residues. Tryptophan residues were selectively excited at 295 nm, while excitation of tryptophan and tyrosine residues was conducted at 280 nm. The refolded HIV-1 Vpu was analysed alongside a denatured HIV-1 Vpu sample. Figure 3.6 shows the fluorescence spectra of the native and denatured HIV-1 Vpu. The fluorescence emission maximum was observed at approximately 340 nm for both the native and the denatured HIV-1 Vpu at both excitation wavelengths (280 and 295 nm). While no wavelength shifts were observed in the spectra of denatured HIV-1 Vpu, a decrease in the fluorescence quantum yield is evident.

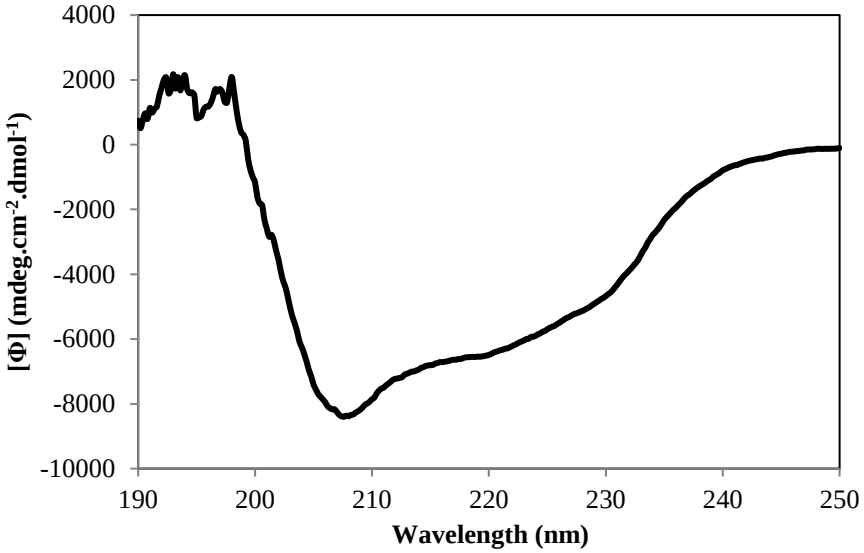

Figure 3.5: Far-UV circular dichroism spectrum of the purified recombinant HIV-1 Vpu. The spectra were determined using 16 µM HIV-1 Vpu in 20 mM Tris-HCl (pH 7.4), 50 mM NaCl. The spectra were an average of 10 scans collected from 250 to 190 nm.

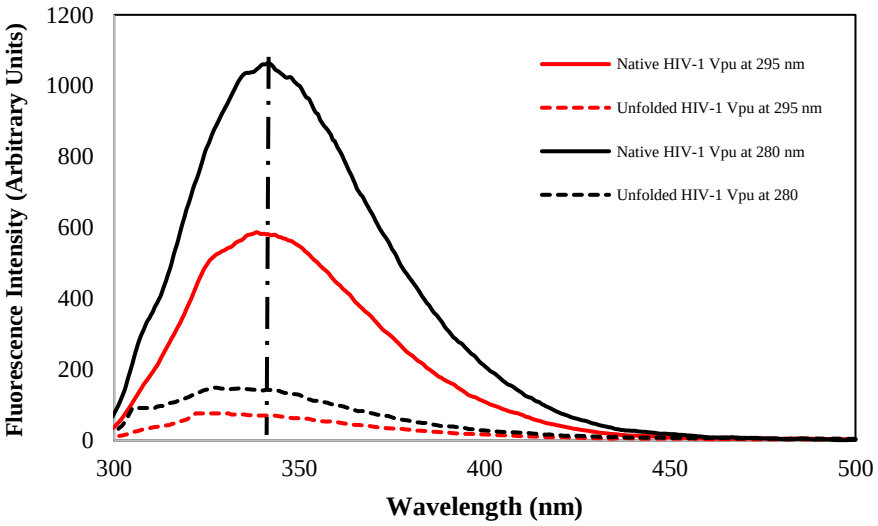

Figure 3.6: Fluorescence emission spectra of HIV-1 Vpu. The spectra were collected using 5 µM HIV-1 Vpu in 20 mM Tris (pH 8.0), 150 mM NaCl. Both the intrinsic tryptophan (red) and the tryptophan and tyrosine emission spectra (black) show emission maxima around 340 nm (presented by the vertical line).

Quaternary Structural Characterisation of HIV-1 Vpu

The quaternary structure of HIV-1 Vpu was analysed using a size exclusion chromatography column coupled to the NGC medium-pressure chromatography system. Prior to loading the protein sample, low molecular weight standards from GE Healthcare were loaded as recommended by the supplier (Mix A: Conalbumin, Carbonic Anhydrous, Ribonuclease A and Aprotinin; Mix B: Ovalbumin, Ribonuclease A and Aprotinin), and the obtained results (Figure 3.7 A) were used in the construction of a standard curve. The logarithm of the molecular weight of each standard was plotted against their respective elution volumes (Figure 3.7 B). A linear regression model with the equation: $y = -0.1856x + 3.4522$ and a R^2 value of 0.9601 was fitted and used to estimate the molecular weight of the purified recombinant HIV-1 Vpu. Both HIV-1 Vpu and the molecular weight standards were analysed under the same conditions, i.e. 20 mM Tris (pH 7.6) and 150 mM NaCl at a flow rate of 0.5 mL/min. HIV-1 Vpu eluted at ~13.3 mL (Figure 3.7 C) and had an estimated hydrodynamic volume of 9.6 kDa as calculated from the molecular weight standard curve.

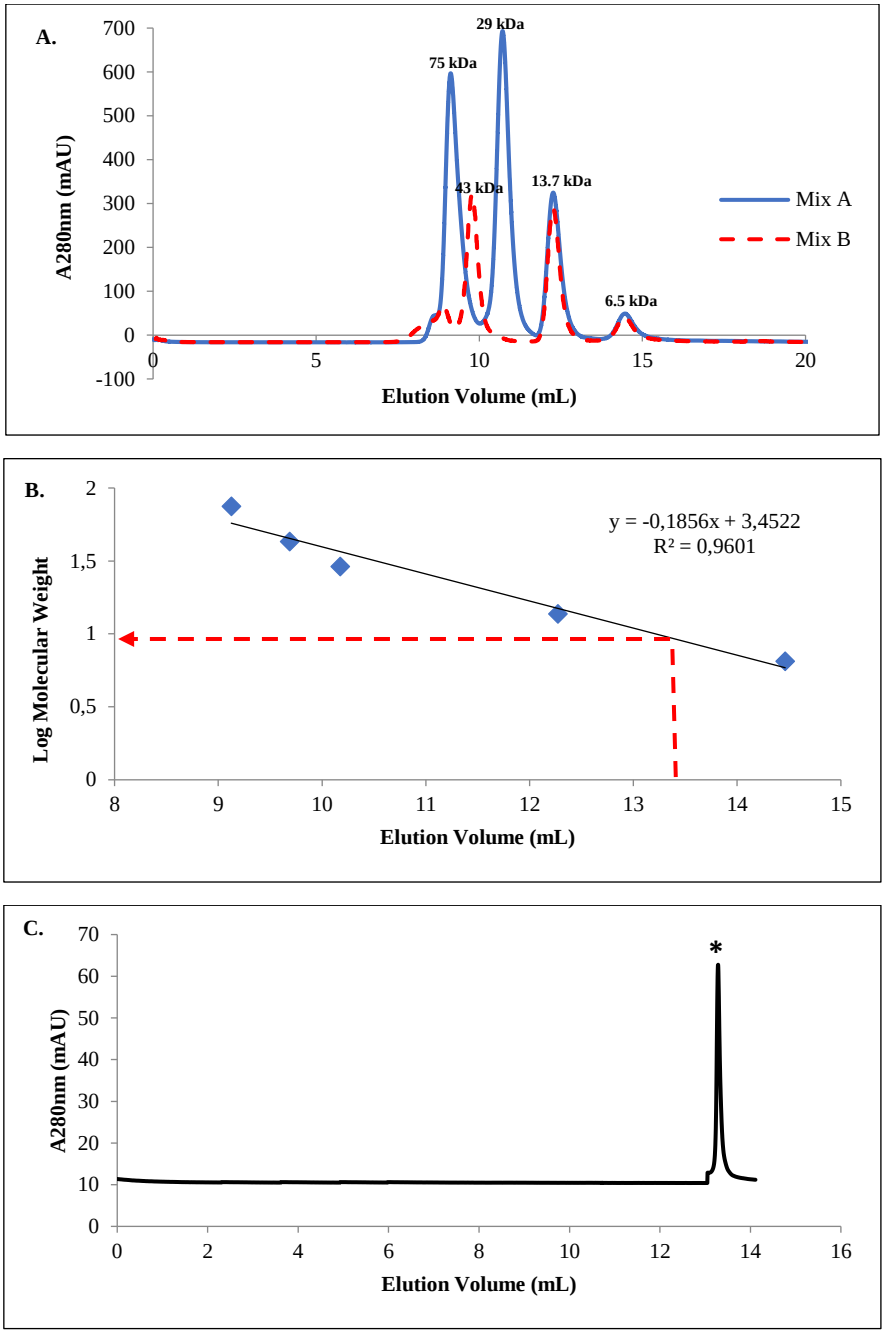

Figure 3.7: Quaternary structural characterisation of HIV-1 Vpu. A. Elution profile of the Low Molecular Weight gel filtration calibration standards from GE Healthcare. The standards, from first eluted, include: Conalbumin (75 kDa); Ovalbumin (43 kDa); Carbonic anhydrase (29 kDa); Ribonuclease A (13.7 kDa) and Aprotinin (6.5 kDa). **B.** Standard curve obtained from the gel filtration standards. The standard curve was constructed by plotting the elution volume of the standards against the logarithm of their molecular weights. A linear regression with a R^2 value of 0.9601 and a line equation of $y = -0.1856x + 3.4522$ was fitted. **C.** Elution profile of 100 µM HIV-1 Vpu from an ENrich size exclusion chromatography. The asterisk in Figure C denotes the position of the HIV-1 Vpu.

3.7 Discussion

In this study, a novel method for the overexpression and purification of full-length HIV-1 Vpu was developed. The method included overexpressing HIV-1 Vpu in bacterial cells and extracting the protein from the insoluble inclusion bodies using urea. The protein was purified using a combination of cation and anion exchange chromatography and refolded using a stepwise dialysis into decreasing concentrations of urea. This method produced a total of ~6 mg of highly purified HIV-1 Vpu per litre of bacterial culture. The yields of HIV-1 Vpu obtained in this study were notably greater than what has been reported in literature for HIV-1 Vpu purification (1 mg of protein from a litre of bacterial culture; Ma *et al*., 2002). Western blot analysis and qualitative ELISA tests of the purified protein with HIV-1 Vpu specific antibodies confirmed the identity of the purified protein to be HIV-1 Vpu.

Following the denaturation (with urea) and subsequent refolding of HIV-1 Vpu, checking if the protein assumed its correct secondary, tertiary and quaternary structure was of paramount importance. The secondary structure of the refolded recombinant HIV-1 Vpu was analysed using Far-UV (190 – 250 nm) CD spectroscopy. The protein showed minima at 208 and 222 nm, characteristic of a predominantly α-helical protein. These results correspond with earlier findings that HIV-1 Vpu consists of three α-helical regions, two in the cytoplasmic domain, and one in the transmembrane domain (Wittlich *et al*., 2009). The overall secondary structural composition of the protein was also estimated to be approximately 65% α-helices, 23% random coils and 10% β-strands using the secondary structure prediction algorithm (SOPMA), available on ExPASy (www.expasy.org/proteomics). The findings proved that the solubilisation, purification and refolding methods used in this study produced a correctly folded recombinant protein.

The tertiary and quaternary structure of HIV-1 Vpu were characterised using intrinsic fluorescence spectroscopy and size exclusion chromatography, respectively. The intrinsic tryptophan spectra of native and denatured HIV-1 Vpu, excited at 295 and 280 nm, showed emission maxima at 340 nm. HIV-1 Vpu consists of two tryptophan residues located in different regions of the protein. The first tryptophan residue (W22) is located in the TM domain, while the second residue (W76) is located in the cytoplasmic domain of the protein. The two tryptophan residues were selectively excited at 295 nm, while excitation at 280 nm excited the tryptophans, along with the single tyrosine residue (Y29) of HIV-1 Vpu, located in the hinge region between helix 1 and 2 (refer to Figure 1.4 in section 1). This protein's

intrinsic fluorescence analysis is thus a good indicator of a global structural integrity as the fluorophores are located across three separate regions of the protein. An emission maximum of 340 nm is indicative of a protein with tryptophan residues that are partially exposed to solvent. These results are consistent with findings that were obtained using the NMR resolved full-length structure of HIV-1 Vpu (Zhang *et al*., 2015) where the tryptophan residues were partially exposed to solvent (~60% exposure). In terms of the quaternary structure of HIV-1 Vpu, the results obtained from the size exclusion chromatography analysis showed that the recombinant protein had a relative hydrodynamic volume of ~9.6 kDa; correlating with the expected size of ~9 kDa for HIV-1 Vpu (Neil *et al.*, 1988). Furthermore, the size exclusion analysis of HIV-1 Vpu shows that the protein eluted as a single peak, confirming the native state of the protein to be monomeric, and that no other molecular species were present in the sample after purification.

3.8 References

Baneyx, F., 1999. Recombinant protein expression in Escherichia coli. *Current opinion in biotechnology*, *10*(5), pp.411-421.

Gutmann, D.A., Mizohata, E., Newstead, S., Ferrandon, S., Henderson, P.J., Van Veen, H.W. and Byrne, B., 2007. A high-throughput method for membrane protein solubility screening: The ultracentrifugation dispersity sedimentation assay. *Protein science*, *16*(7), pp.1422-1428.

Ma, C., Marassi, F.M., Jones, D.H., Straus, S.K., Bour, S., Strebel, K., Schubert, U., Oblatt-Montal, M., Montal, M. and Opella, S.J., 2002. Expression, purification, and activities of full-length and truncated versions of the integral membrane protein Vpu from HIV-1. *Protein science*, *11*(3), pp.546-557.

Njengele, Z., Kleynhans, R., Sayed, Y. and Mosebi, S., 2016. Expression, purification and characterization of a full-length recombinant HIV-1 Vpu from inclusion bodies. *Protein expression and purification*, *128*, pp.109-114.

Park, S.H., De Angelis, A.A., Nevzorov, A.A., Wu, C.H. and Opella, S.J., 2006. Three-dimensional structure of the transmembrane domain of Vpu from HIV-1 in aligned phospholipid bicelles. *Biophysical journal*, *91*(8), pp.3032-3042.

Schubert, U., Henklein, P., Boldyreff, B., Wingender, E., Strebel, K. and Porstmann, T., 1994. The human immunodeficiency virus type 1 encoded Vpu protein is phosphorylated by casein kinase-2 (CK-2) at positions Ser52 and Ser56 within a predicted α-helix-turn-α-helix-motif.

Strebel, K., Klimkait, T. and Martin, M.A., 1988. A novel gene of HIV-1, vpu, and its 16-kilodalton product. *Science*, *241*(4870), pp.1221-1223.

Tate, C.G., 2010. Practical considerations of membrane protein instability during purification and crystallisation. In *Heterologous Expression of Membrane Proteins* (pp. 187-203). Humana Press.

Wittlich, M., Koenig, B.W., Stoldt, M., Schmidt, H. and Willbold, D., 2009. NMR structural characterization of HIV-1 virus protein U cytoplasmic domain in the presence of dodecylphosphatidylcholine micelles. *The FEBS journal*, *276*(22), pp.6560-6575.

Woody, R.W., 1995. [4] Circular dichroism. In *Methods in enzymology* (Vol. 246, pp. 34-71). Academic Press.

Zhang, H., Lin, E.C., Das, B.B., Tian, Y. and Opella, S.J., 2015. Structural determination of virus protein U from HIV-1 by NMR in membrane environments. *Biochimica et Biophysica Acta (BBA)-Biomembranes*, *1848*(11), pp.3007-3018.

Chapter 4: Screening of Inhibitors against the interaction of HIV-1 Vpu with BST-2

4.1 Introduction

BST-2 is one of the host restriction factors that act against HIV-1 replication. BST-2 functions by tethering newly formed HIV-1 virus particles to the membranes of infected cells, inhibiting their release (Neil *et al*., 2008; Van Damme *et al*., 2008). HIV-1 Vpu, however, binds to BST-2 through an interaction that involves the transmembrane domains of the two proteins and induces the down-regulation of BST-2 from the cell surface. In doing so, HIV-1 Vpu removes BST-2 from the virus budding sites, thereby supressing the antiviral activity of BST-2 and enhancing the release of progeny virions (Mitchell *et al*., 2009; Douglas *et al*., 2009; Goffiet *et al*., 2009). Although the exact mechanistic pathway by which HIV-1 Vpu removes BST-2 from the cell surface is still under investigation, the ability of HIV-1 Vpu to interact with BST-2 has been shown to be of crucial importance in the down-regulation of this restriction factor. Mutational analysis studies revealed that the two proteins interact through Ala10, Ala14, Ala18 and Trp22 of HIV-1 Vpu and Val30, Ile33, Ile34, Ile37, Leu41 and Thr45 of BST-2 (Gupta *et al*., 2009; Skasko *et al*., 2012). Blocking the interaction of HIV-1 Vpu with BST-2 could potentially increase cell surface expression levels of BST-2, expose HIV-1 to the antiviral activity BST-2 and consequently hinder the replication of the virus.

Herein, small molecular compounds were virtually screened for the inhibition of the interaction of HIV-1 Vpu with BST-2. The compounds that showed activity in inhibiting the binding of the two proteins *in silico* were chemically synthesised for screening in *in vitro* biological assays. However, for any compound to be considered as a potential drug candidate, it has to be sufficiently active against the target at biologically relevant concentrations, and the absorption, distribution, metabolism, excretion and toxicity (ADME-T) properties of the compound should be known (Wunberg *et al*., 2006). The main objective here was to develop biological assays that are amenable to high throughput screening to screen the small library of compounds *in vitro*. A range of computational, biochemical, biophysical and cell-based assays were employed to gain insight into the drug-likeness and potential activity of the test compounds.

4.2 Confirmation of the binding of HIV-1 Vpu with BST-2

4.2.1 HIV-1 Vpu/BST-2 interaction using ELISA

The interaction between HIV-1 Vpu and BST-2 was verified using the recombinant HIV-1 Vpu purified above, and a commercial BST-2 ELISA kit (Uscn Life Science). As detailed in section 2.2.6 above, the interaction of HIV-1 Vpu with BST-2 was analysed *in vitro* at 1:1 and 1:2 molar ratios of the two proteins. Figure 4.1 shows that a 16% decrease in absorbance was observed (from 1.17 to 0.98) when equimolar concentrations of BST-2 and HIV-1 Vpu were used, and a further 34% decrease (from 0.98 to 0.58) was observed when the molar ratio of BST-2 to HIV-1 Vpu was increased to 1:2. All samples were tested in triplicate, and the results were corrected for buffer blank.

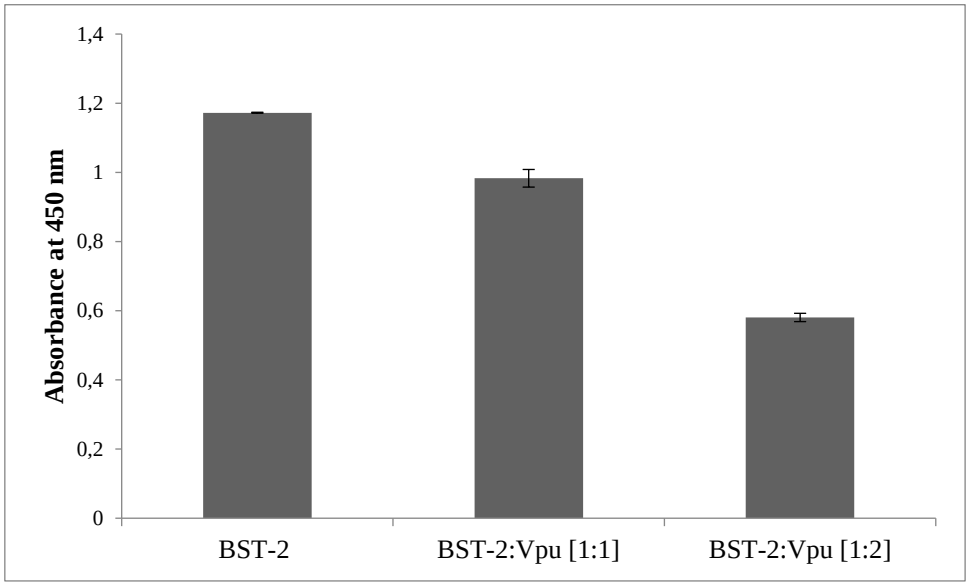

Figure 4.1: HIV-1 Vpu-BST-2 ELISA to confirm the binding of HIV-1 Vpu to BST-2. The interaction between BST-2 (5 ng/mL) and HIV-1 Vpu (5 and 10 ng/mL) is shown. The responses indicate binding between HIV-1 Vpu and BST-2. Values for each molar ratio (1:1 and 1:2) are mean absorbance measurements at 450 nm and the error bars represent standard errors from three independent experiments.

4.2.2 Evaluation of the binding of HIV-1 Vpu with BST-2 using AlphaScreen

4.2.2.1 Chemical Biotinylation of HIV-1 Vpu

Prior to analysing the interaction of HIV-1 Vpu with BST-2 through the AlphaScreen assay, the recombinant HIV-1 Vpu was covalently linked to biotin for use with Streptavidin-coated beads in the assay. The biotinylation process was conducted using a commercial kit (Roche), and the completion of the process was validated using a Streptavidin sandwich ELISA test. For this assay, 50 µg/mL of the biotinylated HIV-1 Vpu was coated on a Streptavidin coated ELISA plate alongside an untagged HIV-1 Vpu at the same concentration as a negative control. Figure 4.2 shows that the response in the wells that contained the biotinylated HIV-1 Vpu was 14-fold higher compared to the wells with the un-biotinylated HIV-1 Vpu sample. These results show a clear binding of the biotinylated HIV-1 Vpu to the Streptavidin, suggesting that the biotinylation was a success, and that the protein could be used in the AlphaScreen assay in conjunction with the Streptavidin-coated beads.

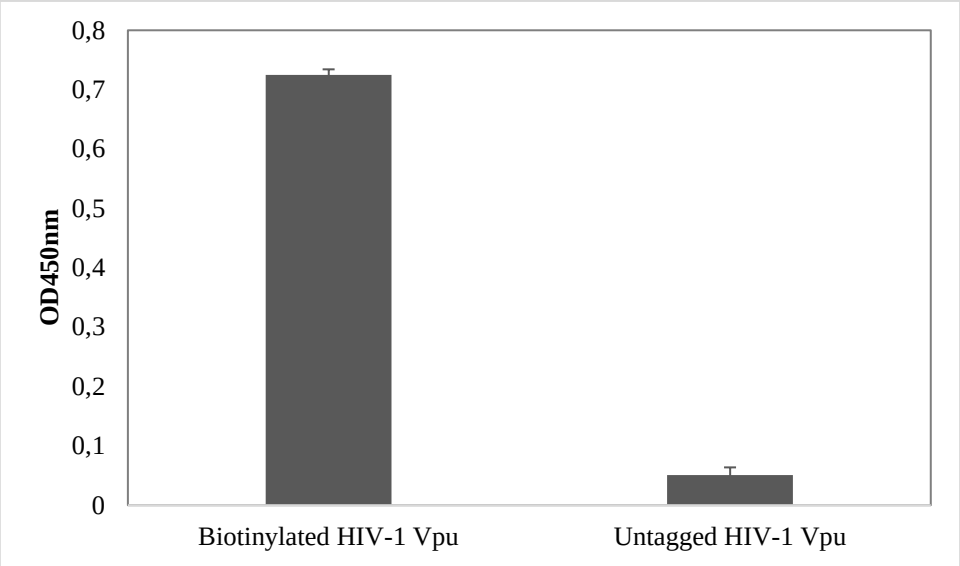

Figure 4.2: Streptavidin ELISA to test the biotinylation of HIV-1 Vpu. Biotinylated HIV-1 Vpu (50 µg/mL) was tested against an untagged HIV-1 Vpu at equimolar concentrations as a negative control. The error bars indicate standard errors from three independent experiments.

4.2.2.2 The HIV-1 Vpu/BST-2 AlphaScreen analysis

An AlphaScreen assay for the analysis of the interaction of HIV-1 Vpu with BST-2 was developed as detailed in section 2.2.6. The assay was conducted using the biotinylated recombinant HIV-1 Vpu from above, in conjunction with a commercial recombinant GST-tagged BST-2 (Abcam). Fixed concentrations of BST-2 (100 nM) bound to anti-GST Acceptor beads were used against varying concentrations of the biotinylated HIV-1 Vpu (200 – 1.56 µM) bound to Streptavidin Donor beads. The obtained results were used to estimate the dissociation constant (K_D) of binding of these two proteins using the Origin 6.0 software, as shown in Figure 4.3. The K_D for the binding of HIV-1 Vpu to BST-2 was determined as the concentration of HIV-1 Vpu at which the AlphaScreen signal was reduced by half, and this value was determined to be 4.7 ± 1.62 nM.

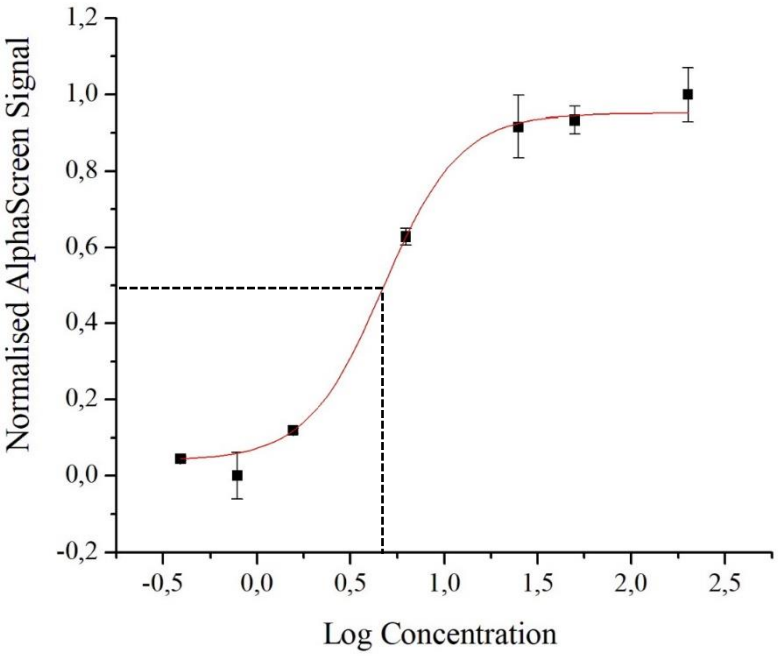

Figure 4.3: Measuring the binding affinity of HIV-1 Vpu for BST-2 using the AlphaScreen assay. The interaction was evaluated using 100 nM of the GST-tagged BST-2 and Biotinylated HIV-1 Vpu at concentrations ranging from 0.39 to 200 nM. A K_D of 4.7 ± 1.62 nM was obtained for this protein-protein interaction and the error bars represent standard errors from three independent experiments.

4.3 Screening of Inhibitors against the HIV-1 Vpu/BST-2 interaction

Virtual screening of compounds that could disrupt the transmembrane interaction of HIV-1 Vpu and BST-2 was conducted using the pepMMsMIMIC database available at: http://mms.dsfarm.unipd.it/pepMMsMIMIC/index.php (Floris *et al.,* 2011). The three-dimensional transmembrane domain structure of HIV-1 Vpu that was resolved using solid-state NMR from the protein data bank was used as a query in the screening of these compounds (PDB ID. 2GOH, Park *et al.*, 2006). This was done to identify promising scaffolds as the starting point for designing and synthesising potentially active compounds against HIV-1 Vpu. The compounds were ranked based on their shape and complementarity (Floris *et al.,* 2011), and the top 200 candidate molecules (with scores ranging between 0.5 and 0.98) were identified by the program. A common feature amongst the identified molecules is that they all contained nitrogen heterocyclic systems such as benzimidazole, benzoxazole and imidazopyridine scaffolds represented in Figure 4.4 (Rashamuse, 2017). Out of the 200 compounds identified as potential inhibitors of the HIV-1 Vpu/BST-2 interaction from the virtual screening, 24 showed scoring values above 0.9, as per the pepMMsMIMIC program scoring, and these were synthesised in-house and screened for their ability to disrupt the HIV-1 Vpu/BST-2 interaction *in vitro* using the sandwich ELISA test. The chemical structures of these compounds, however, cannot be disclosed at this stage for intellectual property protection purposes.

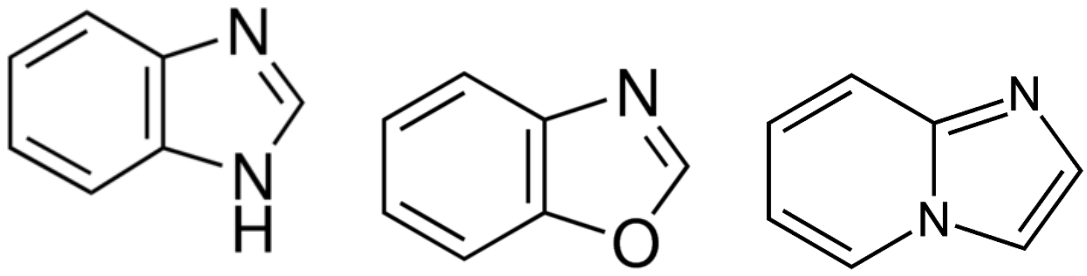

Benzimidazole **Benzoxazole** **Imidazopyridine**

Figure 4.4: Recurring nitrogen heterocyclic scaffolds identified from the virtual screening of novel small molecule compounds against the interaction of HIV-1 Vpu with BST-2 using the pepMMsMIMIC program.

For the ELISA screening assay, HIV-1 Vpu was incubated with 100 µM of each of the 24 test compounds and subsequently added to a BST-2 coated ELISA plate. Inhibition percentage (%Inhibition) of each compound at the different concentrations were calculated using unbound and untreated BST-2 as a positive control and HIV-1 Vpu and BST-2 (with no inhibitor) as a negative control. The results obtained from the screening of these compounds are shown in Figure 4.5. Of the 24 screened compounds, Figure 4.5 shows that compounds 1, 2, 3, 4, 5, 8, 22 and 23 showed promising inhibitory activity (i.e. inhibition percentage greater than 50%) at the single dose of 100 µM. These compounds were further analysed using a secondary screening assay to verify these observations.

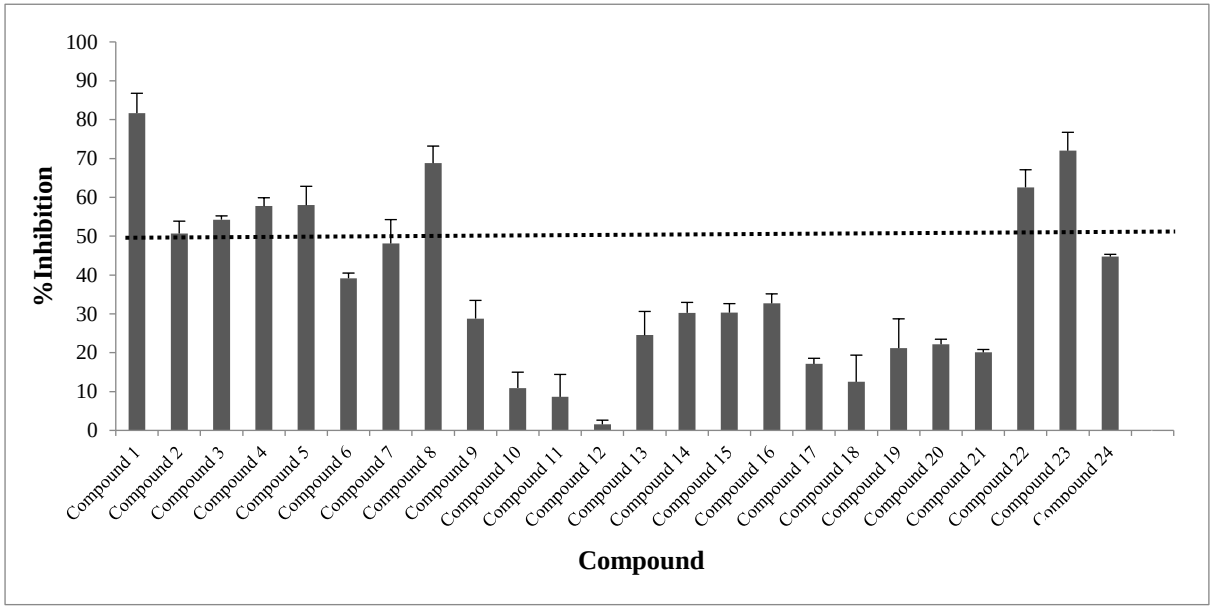

Figure 4.5: Inhibition percentage results obtained for the 24 in-house synthesised compounds against the HIV-1 Vpu/BST-2 interaction using ELISA. The error bars represent standard errors from three independent experiments.

4.4 AlphaScreen as a Secondary Screening Assay

In an attempt to eliminate any false positive hits, the AlphaScreen assay developed above was used as a secondary screening tool to validate the activity of the compounds identified through the ELISA test in inhibiting the interaction of HIV-1 Vpu with BST-2. The eight compounds that showed inhibition percentages of at least 50% at 100 µM in the ELISA test were rescreened using this assay. For this assay, 100 µM of the compounds were incubated

with the biotinylated HIV-1 Vpu, prior to the addition of BST-2 and the AlphaScreen beads. Controls, which included HIV-1 Vpu and BST-2 without any compound, and the Donor and Acceptor beads on their own, were included. Figure 4.6 shows that majority of the results obtained from the AlphaScreen assessment were comparable to those attained though the ELISA test, with the exception of Compound 23, which showed notable variability between the two assays.

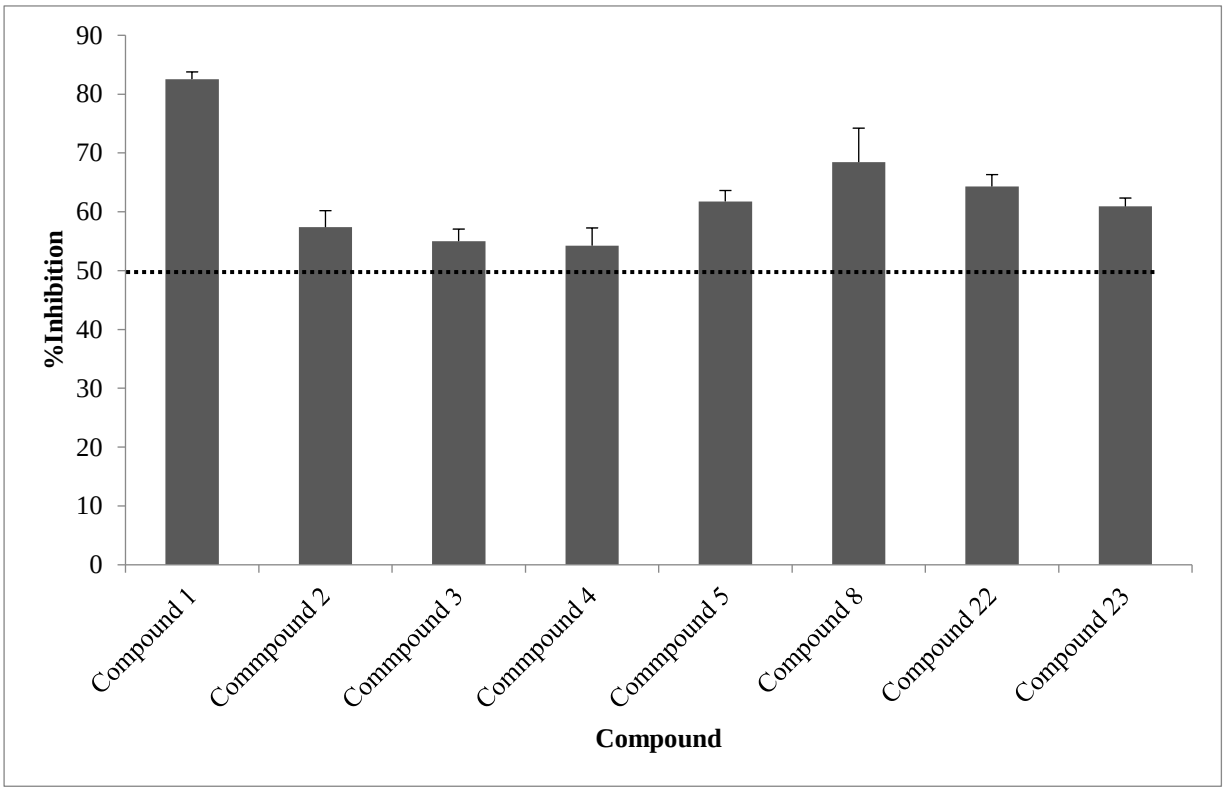

Figure 4.6: Inhibition results obtained for the eight hit compounds that were identified as potential inhibitors for the interaction of HIV-1 Vpu with BST-2 using AlphaScreen. The error bars represent standard errors from three independent experiments.

4.5 Dose-Response analysis of the Compounds

The two compounds that showed high inhibition at a single dose of 100 µM (Compound 1 and 8) were subjected to a dose-response analysis using the optimised AlphaScreen assay to determine their IC_{50} values. The biotinylated HIV-1 Vpu was incubated with varying concentrations of the compounds (200 – 1.56 µM) and BST-2 was subsequently introduced. The analysis was done using the GST detection kit (PerkinElmer) which consists of

Streptavidin-coated donor beads and GST-tagged acceptor beads. The IC_{50} values of the compounds were calculated relative to the uninhibited interaction of HIV-1 Vpu with BST-2 using the dose-response curves shown in Figure 4.7. These values were calculated as the concentration of compound at which the AlphaScreen signal was reduced by half, and the obtained results for the two compounds are shown in Table 4.1. This table shows that Compound 1 had a lower IC_{50} value of 11.6 ± 1.1 µM, while Compound 8 had an IC_{50} value of 17.6 ± 0.9 µM. A significant difference ($p < 0.05$), as determined by student t-test, was observed between the IC_{50} values of these two compounds, meaning that the activity of Compound 1 in inhibiting the interaction of HIV-1 Vpu with BST-2 was significantly better than that of Compound 8.

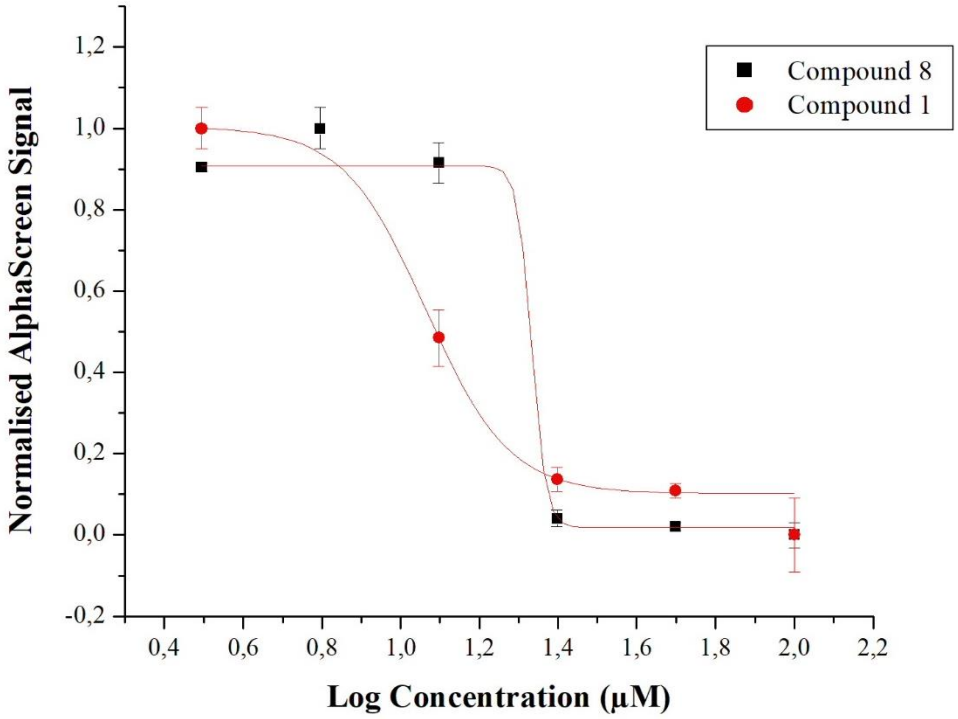

Figure 4.7: Dose response curves used to generate the IC_{50} values of Compound 1 and 8 using the AlphaScreen assay. Compound concentrations ranging between 3.13 and 100 µM were used, and the IC_{50} values were determined to be 11.6 ± 1.1 and 17.6 ± 0.9 µM for Compound 1 and 8, respectively. The error bars represent standard errors from three independent experiments.

Table 4.1: IC_{50} (µM) values of the two hit compounds that showed high activity in inhibiting the HIV-1 Vpu/BST-2 interaction

Compound	IC_{50} (µM)
Compound 1	11.6 ±1.1
Compound 8	17.6 ±0.9

4.6 Evaluation of the Biological and Biophysical properties of the identified compounds

4.6.1 In silico prediction of the drug-like properties of the compounds

In silico screening is advantageous in the drug discovery field as it allows for the evaluation of drug-likeness in compounds through the use of screening tools such as Lipinski's rule-of-five (Lipinski *et al*., 1997). In this study, the rule-of-five (Lipinski *et al*., 1997) was used as a screening tool to predict the drug-likeness of the compounds that showed potential activity in disrupting the interaction of HIV-1 Vpu with BST-2, and to identify any compound showing a possibility of poor oral-bioavailability. According to this rule, a compound is considered ideal if the molecular weight does not exceed 500 mg/mL, contains no more than 10 hydrogen bond acceptors, no more than 5 hydrogen bond donors and has an octanol-water partition coefficient (LogP) value of less than 5 (Lipinski *et al*., 1997). For a compound to be considered as a potential lead, it should violate no more than one of the four rules stipulated by the rule-of-five. The hit compounds were tested along with two control compounds, 6-aza-2-thiouridine and Lapachol, which were previously reported to restore cell surface levels of BST-2 in a HIV-1 Vpu dependent manner (Zhang *et al*., 2016; Mi *et al*., 2015). As shown in Table 4.2, all the compounds tested in this study passed the rule-of-five without any violations.

Table 4.2: Analysis of the drug-likeness of the test compounds using Lipinski's rule-of-five.

Compound name	2D Chemical Structure	Molecular weight {g/mol} (ideal<500)	H-bond Donors (ideal<5)	H-bond Acceptors (ideal<10)	LogP (ideal<5)	Violations
Compound 1	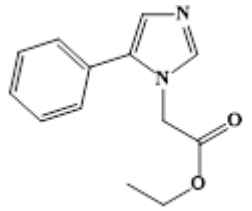	230.26	2	0	2.995	0
Compound 8	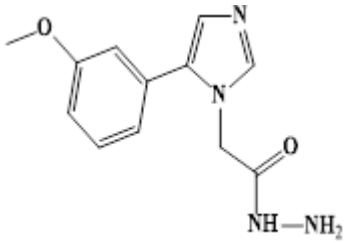	246.27	3	2	0.094	0
6-aza-2-thiouridine	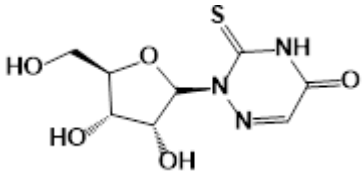	262.25	4	7	-1.500	0
Lapachol	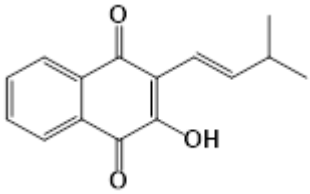	242.27	1	3	2.800	0

4.6.2 Assessment of the Aqueous Solubility of the Compounds

The aqueous solubility of the test compounds was determined *in vitro* using the 96-well MultiScreen Solubility Filter plate system from Millipore. For this experiment, a standard curve was first obtained for each compound using the following concentrations: 500, 200, 50, 12.5 and 3.13 µM, according to the manufacturer's specifications. Representative overlaid spectra and standard curve for Chloramphenicol are shown in Figure 4.8 A and B, respectively. For the analysis, the compounds, at 100 and 200 µM, were dissolved in PBS (pH 7.4), incubated at room temperature, filtered to remove precipitates and the final concentration of each compound was measured using UV-Vis spectroscopy. Using the standard curves obtained for each compound (data not shown), aqueous solubility was determined. The results obtained from this study (illustrated in Table 4.3) show that Chloramphenicol, Compound 1, Compound 8 and 6-aza-2-thiouridine showed over 100% dissolution at both 100 and 200 µM (i.e. solubility ≥ 100 and 200 µM for all four compounds, respectively), while Lapachol showed ~87% dissolution at 100 µM and ~68% dissolution at 200 µM. (i.e. solubility of ~87 and 136 µM, respectively).

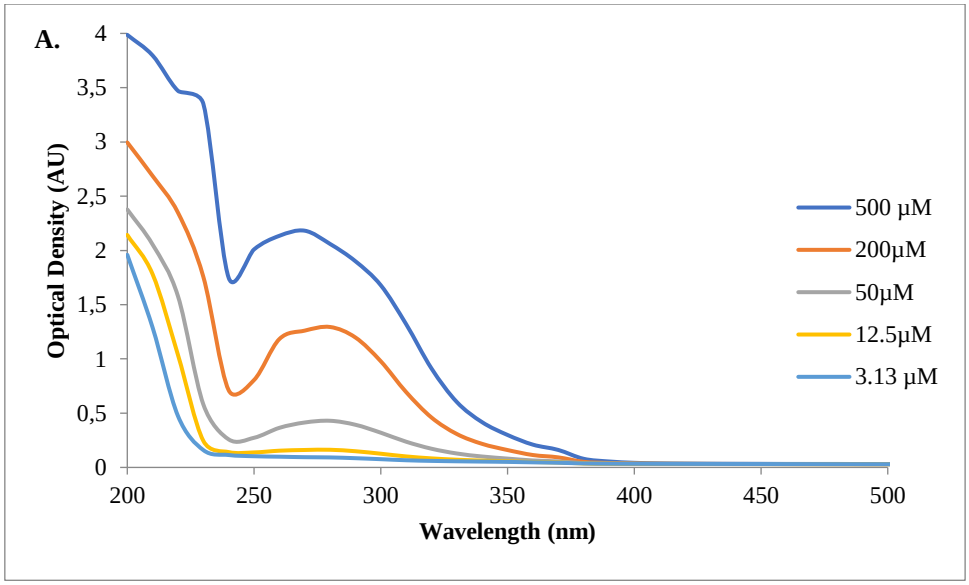

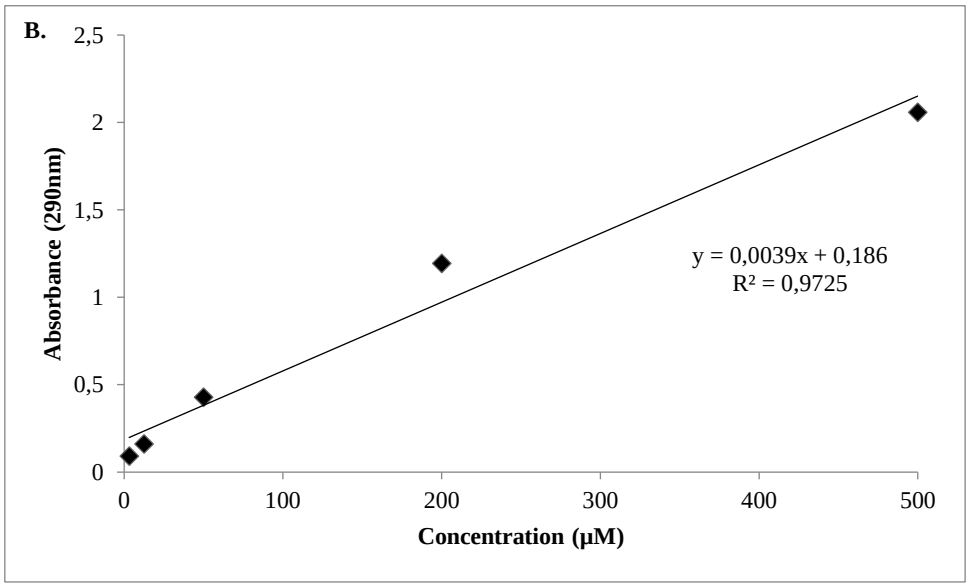

Figure 4.8: Representative aqueous solubility graphs. A. The overlaid standard spectra of Chloramphenicol at pH 7.4 with concentrations ranging from 3.13 µM to 500 µM. **B.** Representative standard curve for the aqueous solubility of Chloramphenicol at pH 7.4 and a wavelength of 290 nm.

Table 4.3: Summary of the aqueous solubility data obtained for the two hit compounds in comparison 6-aza-2-thiouridine, Lapachol and Chloramphenicol

Compound	**Maximum Wavelength (nm)**	**%Dissolution**		**Solubility (µM)**	
		100 µM	200 µM	100 µM	200 µM
Compound 1	250	100	100	≥ 100	≥ 200
Compound 8	250	100	100	≥ 100	≥ 200
6-aza-2-thiouridine	260	100	100	≥ 100	≥ 200
Lapachol	260	87	68	87	136
Chloramphenicol	290	100	100	≥ 100	≥ 200

4.6.3 Determination of the Cytotoxicity effects of the compounds

The cytotoxicity effects of the compounds that were investigated in this study against mammalian cells were determined using the MT-4 cell line. Auranofin, a gold-based compound that has been shown to exhibit toxicity against mammalian cells, was used as a control in this study. For this assay, MT-4 cells were incubated with two-fold serial dilutions of the test compounds, ranging from 200 to 1.56 µM. Following 72 hours of incubation, the viability of the cells was quantified using the MTS assay, where the absorbance of the reduced formazan product was read at 490nm. The concentrations of compounds which caused 50% cytotoxicity (CC_{50}) in MT-4 cells, with reference to untreated control cells which represented 100% cell viability, were subsequently determined. As shown in Table 4.4, Compound 1, Compound 8 and Lapachol showed minimal toxicity against the human cells, with their CC_{50} values ranging between ~153 and 185 µM. Also evident from Table 4.4 is that 6-aza-2-thiouridine had a very low CC_{50} value of 14.6 ± 0.5 µM, denoting toxicity of

this compound against the cells. The control compound, Auranofin, showed a CC_{50} value of 6.5 µM, which was consistent with the CC_{50} value of 4.5 µM that was previously reported by Harbut *et al*. (2015) for the same compound against human HepG-2 human liver cells.

4.6.4 Determination of the anti-HIV-1 activity of the compounds

The activity of the test compounds against the replication of HIV-1 was evaluated using the MT-4 cell line in an *in vitro* phenotypic assay. The cells were infected with the HIV-1 LAV virus, incubated with two-fold serial dilutions of the compounds (100 – 1.56 µM) for 72 hours, and subsequently tested for expression of the p24 protein using an ELISA-based test. The compounds were tested alongside Raltegravir, a known inhibitor of HIV-1 replication, as a positive control. The viral inhibition percentages of the compounds at each concentration were calculated relative to '*no drug'* control wells which contained HIV-1 infected cells without any compound treatment. The obtained values were used to determine the concentration of compound required to reduce the expression of p24, which is equivalent to viral replication, by 50% (EC_{50}), and these are shown in Table 4.5. According to this Table, Compound 1 had an EC_{50} value of 6.3 ± 0.7 µM, followed by Lapachol at 17.3 ± 0.6 µM, 6-aza-2-thiouridine at 24.1 ± 0.8 µM and Compound 8 at 157.5 ± 1.2 µM. Raltegravir yielded an EC_{50} of 7.9 ± 0.9 nM, which correlates with a previously reported EC_{50} value of ≤ 8 nM for this compound (Heredia *et al.*, 2017).

Table 4.4: CC_{50} values (µM) indicating the effect of the test compounds on the viability of MT-4 cells. Mean values ± standard error of three independent experiments are shown.

Compound Name	**CC_{50} (µM)**
Compound 1	184.5 ± 0.8
Compound 8	159.5 ± 0.9
6-aza-2-thiouridine	14.6 ± 0.5
Lapachol	152.8 ±0.6
Auranofin	6.5 ± 0.7

Table 4.5: EC_{50} values (µM) indicating the potency of the test compounds in inhibiting the replication of the HIV-1 LAV strain in MT-4 cells. Mean values ± standard error of three independent experiments are shown.

Compound	**EC_{50} (µM)**
Compound 1	6.3 ± 0.7
Compound 8	157.5 ± 1.2
6-aza-2-thiouridine	24.1 ± 0.8
Lapachol	17.3 ± 0.6
Raltegravir	7.9×10^{-3} ± 0.9

4.6.5 Determination of the Therapeutic Index values of the test compounds

The EC_{50} and CC_{50} values obtained for the compounds were further used to determine the therapeutic index (TI) values of these compounds. The therapeutic index is defined as a comparison of the dose of compound that causes the desired therapeutic effect to the amount that elicits toxicity (i.e. CC_{50}/EC_{50}; Gan *et al.*, 2006). This ratio is considered as a safety margin; the wider the margin, the safer the therapeutic agent and the lower the need for monitoring drug concentrations upon administration. According to Muller & Milton (2012), a drug is generally considered to have a good safety profile if the TI value is greater than 10. The TI values obtained for Compound 1, Compound 8, 6-aza-2-thiouridine and Lapachol are shown in Table 4.6 below.

Table 4.6: Therapeutic Index values indicating the safety profiles of the two newly identified HIV-1 Vpu/BST-2 inhibitors alongside the two control compounds.

Compound Name	**TI value**
Compound 1	29.2
Compound 8	1.0
6-aza-2-thiouridine	0.6
Lapachol	8.8

4.7 Discussion

The screening of the in-house synthesised compounds as possible inhibitors for the binding of HIV-1 Vpu to BST-2 was conducted using an ELISA test. The assay was developed using the recombinant HIV-1 Vpu and a commercial BST-2 ELISA kit. Of the 24 compounds that were tested, eight showed inhibition percentages ≥ 50%, and a novel AlphaScreen assay was subsequently developed as a secondary screening tool for the validation of these potential hit compounds. For most of these compounds (seven out of eight), the results obtained from the AlphaScreen assay were comparable to those obtained from the ELISA test, with Compound 23 being the only outstanding exception. In the ELISA test, Compound 23 had an inhibition percentage of ~72%, while the same compound had an inhibition value of ~61% when tested *via* the AlphaScreen assay. Following statistical analysis, the change in activity exhibited by this compound between the two screening assays was found to be significant, with a p-value of 0.0019. The AlphaScreen assay was further used to quantify the affinity of HIV-1 Vpu for BST-2. This was done by determining the dissociation constant (K_D) of binding of the two proteins. The K_D is defined as the concentration at which protein A is bound to half of all the available sites on protein B in equilibrium (Kastritis & Bonvin, 2013). Therefore, the smaller the K_D of binding between two interacting proteins, the higher the affinity of the two proteins (Perkins *et al.*, 2010). The K_D of binding between HIV-1 Vpu and BST-2 was found to be ~4.7 nM and according to Kastritis *et al.* (2011), the binding affinity of a protein-protein complex is considered high if the K_D value is less than 0.1 nM, moderate if K_D is between 0.1 nM and 1000 nM, and low if K_D greater than 1000 nM. Based on this classification, the binding affinity of HIV-1 Vpu with BST-2 is thus in the moderate affinity category.

Compound 1 and Compound 8 showed inhibition percentages of ~82% and 70% (respectively) against the interaction of HIV-1 Vpu with BST-2 at the single dose of 100 µM in the ELISA test. Inhibition percentages of ~83% and 68% were observed for the same compounds from the AlphaScreen assay. Because of the invariably high inhibition values exhibited by these compounds from both screening assays, the two compounds were selected for further characterisation studies. Dose-response studies conducted on these compounds showed that Compound 1 and Compound 8 had IC_{50} values of ~11.6 µM and ~17.6 µM, respectively. For a compound to successfully inhibit the interaction of HIV-1 Vpu with BST-2, it should be able to compete with BST-2 for binding to HIV-1 Vpu. This means that the binding affinity of the ligand for HIV-1 Vpu would have to be higher than that of BST-2 for

HIV-1 Vpu. This, however, was not the case for the two potential inhibitors identified in this study. These results show that Compound 1 binds HIV-1 Vpu with an affinity that is almost 2500-fold lower compared to BST-2, while the binding affinity of Compound 8 is about 3700-fold lower than that of BST-2. This suggests that the binding of these compounds to HIV-1 Vpu is not tight enough to inhibit the binding of HIV-1 Vpu to BST-2. Displacement ITC titrations in which the HIV-1 Vpu/BST-2 protein complex would be titrated with the respective ligands, and the ability of the ligands to competitively displace BST-2 would be monitored could be a valuable addition to this study. The lack of sufficient amounts of recombinant BST-2, however, was a limitation. Several attempts were made to develop a working protocol for the overexpression and purification of this protein (highlights of the methodology and results from the purification trials shown in Appendix C), however, none of the methods used resulted in high quantity and purity recombinant BST-2. The commercial recombinant BST-2 used in the development of the AlphaScreen assay was also not enough for use in ITC experiments.

The development of an effective drug compound is a long and expensive process. It takes an average of 10 to 15 years for a compound to go through the different stages of the drug discovery and development pipeline shown in Figure 4.9, with an estimated cost of approximately 2 billion US dollars per compound. As shown in Figure 4.9, the stages involved in the drug discovery and development process include: target identification and validation, high throughput screening of compounds and hit identification, lead identification and optimisation, pre-clinical trials, phase I, phase II and phase III clinical trials, as well as FDA reviews and approval. Having a compound fail in later stages of development can thus be very costly. In the past, withdrawal of drug candidates from clinical trials was mainly due to adverse effects such as toxicity and poor pharmacokinetic properties (Prentis *et al.,* 1998; Lombardo *et al*., 2003). A comparison of attrition rates between the early 1990s and early 2000s, however, shows that an improvement has occurred in preventing failures that are due to undesirable pharmacokinetic profiles. Kola & Landis (2004) reported that late drug failures dropped from 40% to 10% between 1998 and 2000. This decrease in drug failure coincides with the development and growth in the usage of virtual screening techniques that can be used to predict the absorption, distribution, metabolism, excretion and toxicity (ADME-T) properties of newly identified compounds early in the drug development process, to recognise poor candidates as early as possible (Li, 2001; Kerns & Di, 2003); thereby avoiding loss in expenditure by pharmaceutical companies downstream the discovery process when it

becomes apparent that the compounds are not drug-like. The drug-likeness of the two compounds that showed high inhibition percentages against the HIV-1 Vpu/BST-2 interaction were predicted alongside the two control compounds (6-aza-2-thiouridine and Lapachol) using Lipinski's rule-of-five. All four of these compounds passed the rule-of-five without any violations, suggesting that these compounds are drug-like and are likely to remain active if administered orally (Lipinski *et al*., 1997).

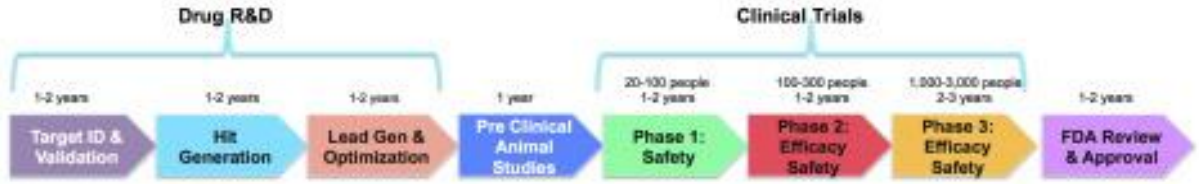

Figure 4.9: Representation of the stages involved in the drug discovery and development process.

Furthermore, aqueous solubility data provides a guide for the range of concentrations that can be used for *in vitro* assays. Poor solubility of a compound in an *in vitro* assay may lead to misleading results where, for example, a compound precipitates out of solution, resulting in reduced concentrations available to bind to the drug target and poor reproducibility. Compound 1, Compound 8 and 6-aza-2-thiouridine showed 100% dissolution at 100 and 200 µM, while Lapachol showed 87% and 68% dissolution at 100 and 200 µM, respectively. According to the classification guidelines for orally absorbed compounds that were established by Rogge & Taft (2010), the results obtained for all these compounds show acceptable solubility profiles.

The effect of the test compounds on the viability of human cells was evaluated using the MT-4 cell line and cell viability profiles were monitored using the MTS assay. Cytotoxicity testing forms an important part of the lead optimisation process and should be done in the early stages of compound screening to allow for modifications to be made on the compound's structure to improve the toxicity profile. The concentrations of compounds that resulted in loss of 50% viability in the human cells were in the high Micromolar range (between ~153 and ~185 µM) for Compound 1, Compound 8 and Lapachol, suggesting that these compounds exhibited minimal cytotoxicity against the cells. 6-aza-2-thiouridine, on the other hand, displayed toxicity properties against the MT-4 cells, with a low CC_{50} value of ~14.6 µM. In 1974, Li and co-workers reported that 6-aza-2-thiouridine exhibited cytotoxic effects

towards leukemia positive cells. The sensitivity of the MT-4 cells used in this study towards this compound could be attributed to this, as MT-4 cells were isolated from a leukemia positive patient, and carry the human T-cell leukemia virus Type I. There are no reports of this compound exhibiting cytotoxicity against any healthy/normal human cell line in literature.

Simultaneous to the cytotoxicity evaluation of the test compounds, the ability of these compounds to inhibit the replication of HIV-1 in MT-4 human cells were tested. As shown in Table 4.5, Compound 1 had the lowest *in vitro* EC_{50} value of ~6.3 µM, followed by Lapachol with an EC_{50} value of ~17.3 µM, 6-aza-2-thiouridine with ~24.1 µM and Compound 8 with ~157.5 µM. Apparent from the CC_{50} and EC_{50} values obtained for 6-aza-2-thiouridine is that the concentration required for this compound to inhibit the replication of HIV-1 is greater than the concentration that elicits toxicity (i.e. EC_{50} is greater than the CC_{50}). This therefore suggests that even the supposed activity that was exhibited by this compound was a result of toxicity, as opposed to antiviral activity. The difference observed between the CC_{50} (~14.6 µM) and the EC_{50} (~24.1 µM) values obtained for 6-aza-2-thiouridine was likely due to variabilities in the two assays. The poor safety of this compound is also evident from the TI value of ~0.6 observed in Table 4.6. For compound 8, the obtained CC_{50} and EC_{50} values were very close to each other. This indicates the plausibility that what appeared to be antiviral activity induced by this compound at 157.5 ± 1.2 µM was due to toxicity (CC_{50} ~ 159.5 µM). Furthermore, the very narrow margin displayed by the TI value of this compounds (TI of ~ 1) suggests that small changes in dosage of Compound 8 or interactions with other drugs could potentially cause adverse effects in patients if this compound would be administered as it currently is, structurally. Furthermore, the CC_{50}, EC_{50} and TI values obtained above show that only Compound 1 and Lapachol showed activity in inhibiting the replication of HIV-1 *in vitro* at concentrations notably lower than their minimum cytotoxic concentrations. Compound 1 showed approximately 3-times better activity in inhibiting the replication of HIV-1 in the infected cells compared to Lapachol. The TI values obtained for these two compounds were ~29.2 and ~8.8 for Compound 1 and Lapachol, respectively. These values show that Compound 1 had a very good safety margin, while that of Lapachol is considered to be moderate. Furthermore, the data obtained for the two hit compounds reveal that Compound 1 showed activity in both the direct and the cell-based assays, while Compound 8 was mainly active in the direct assays only. Although these compounds were designed to bind the same site of HIV-1 Vpu, it is possible that the binding positions on the protein differ

slightly. The observations suggest that the binding site for Compound 1 was likely exposed in both the aqueous environment and membrane-embedded environment, while the site for Compound 8 was likely exposed in the absence of a membrane but embedded in presence of the membrane. These findings further suggest that Compound 8 would exhibit minimal activity *in vivo*, as the cell-based assays mimic the physiological environment better than the direct plate-based assays.

The activity of Compound 1 was found to be fairly comparable to that of BIT225, a first-in-class HIV-1 Vpu inhibitor that is currently in phase II clinical trials. According to Khoury *et al.* (2009), BIT225 had an EC_{50} value of 2.25 ± 0.23 µM, a CC_{50} value of 284 ± 22 µM and a TI value of 126 in MDM cells. This shows that the EC_{50} value obtained for Compound 1 in this study is only ~2.8-fold less than the EC_{50} value reported for BIT225. The comparability of these values shows that Compound 1 makes a promising lead compound for the development of novel anti-HIV-1 drugs targeted against HIV-1 Vpu. Additionally, BIT225 recently showed potential activity in decreasing viral load in HIV-1 infected patients. The patients were treatment naïve, and BIT225 was used in conjunction with a cART regimen, Atripla. Atripla is comprised of Efavirenz (NNRTI), Tenofovir Disoproxil Fumarate (NRTI) and Emtricitabine (NRTI) and is widely used as a first-line cART regimen. The results of the clinical activity of BIT225 came after the United States Department of Health and Human Service downgraded Atripla from a '*recommended'* to an '*alternative'* first-line regimen, owing to the low genetic barrier of NNRTIs to resistance, which ultimately leads to low clinical efficiency of these compounds (US Department of Health and Human Services, 2015; Sluis-Cremer, 2018). Adding an inhibitor that acts on a different target to this regimen may improve its antiviral activity and resistance profile. HIV-1 Vpu inhibitors, including the active compound identified in this study, Compound 1, could potentially be used as alternatives to NNRTIs in this regimen.

4.8 References

Amidon, G.L., Lennernäs, H., Shah, V.P. and Crison, J.R., 1995. A theoretical basis for a biopharmaceutic drug classification: the correlation of in vitro drug product dissolution and in vivo bioavailability. *Pharmaceutical research*, *12*(3), pp.413-420.

Di, L. and Kerns, E.H., 2008. *Drug-like properties: concepts, structure design and methods from ADME to toxicity optimization*. Academic press.

Di, L. and Kerns, E.H., 2015. *Drug-like properties: concepts, structure design and methods from ADME to toxicity optimization*. Academic press.

Floris, M., Masciocchi, J., Fanton, M. and Moro, S., 2011. Swimming into peptidomimetic chemical space using pepMMsMIMIC. *Nucleic acids research*, *39*(suppl_2), pp.W261-W269.

Gan, L.S., Lee, F.W., Nagaraja, N., Li, P., Labutti, J., Yin, W., Xia, C., Yang, H., Uttamsingh, V., Lu, C. and Pusalkar, S., 2006. Case History—Use of ADME Studies for Optimization of Drug Candidates. In *Optimizing the "Drug-Like" Properties of Leads in Drug Discovery* (pp. 81-97). Springer, New York, NY.

Harbut, M.B., Vilchèze, C., Luo, X., Hensler, M.E., Guo, H., Yang, B., Chatterjee, A.K., Nizet, V., Jacobs, W.R., Schultz, P.G. and Wang, F., 2015. Auranofin exerts broad-spectrum bactericidal activities by targeting thiol-redox homeostasis. *Proceedings of the National Academy of Sciences*, p.201504022.

Heredia, A., Hassounah, S., Medina-Moreno, S., Zapata, J.C., Le, N.M., Han, Y., Foulke Jr, J.S., Davis, C., Bryant, J., Redfield, R.R. and Wainberg, M.A., 2017. Monotherapy with either dolutegravir or raltegravir fails to durably suppress HIV viraemia in humanized mice. *Journal of Antimicrobial Chemotherapy*, *72*(9), pp.2570-2573.

Kastritis, P.L., Moal, I.H., Hwang, H., Weng, Z., Bates, P.A., Bonvin, A.M. and Janin, J., 2011. A structure-based benchmark for protein–protein binding affinity. *Protein Science*, *20*(3), pp.482-491.

Kastritis, P.L. and Bonvin, A.M., 2013. On the binding affinity of macromolecular interactions: daring to ask why proteins interact. *Journal of The Royal Society Interface*, *10*(79), p.20120835.

Kola, I. and Landis, J., 2004. Can the pharmaceutical industry reduce attrition rates?. *Nature reviews Drug discovery*, *3*(8), p.711.

Li, A.P., 2001. Screening for human ADME/Tox drug properties in drug discovery. *Drug discovery today*, *6*(7), pp.357-366.

Lipinski, C.A., Lombardo, F., Dominy, B.W, Feeney, P.J. 1997. Experimental and computational approaches to estimate solubility and permeability in drug discovery and development settings. *Advanced Drug Delivery Reviews*, **23**, 3-25.

Lombardo, F., Gifford, E. and Shalaeva, M.Y., 2003. In silico ADME prediction: data, models, facts and myths. *Mini reviews in medicinal chemistry*, *3*(8), pp.861-875.

Mi, Z., Ding, J., Zhang, Q., Zhao, J., Ma, L., Yu, H., Liu, Z., Shan, G., Li, X., Zhou, J. and Wei, T., 2015. A small molecule compound IMB-LA inhibits HIV-1 infection by preventing viral Vpu from antagonizing the host restriction factor BST-2. *Scientific reports*, *5*, p.18499.

Muller, P.Y. and Milton, M.N., 2012. The determination and interpretation of the therapeutic index in drug development. *Nature reviews Drug discovery*, *11*(10), p.751.

Park, S.H., De Angelis, A.A., Nevzorov, A.A., Wu, C.H. and Opella, S.J., 2006. Three-dimensional structure of the transmembrane domain of Vpu from HIV-1 in aligned phospholipid bicelles. *Biophysical journal*, *91*(8), pp.3032-3042.

Pérez, J., Díaz, C., Salado, I.G., Pérez, D.I., Peláez, F., Genilloud, O. and Vicente, F., 2013. Evaluation of the effect of compound aqueous solubility in cytochrome P450 inhibition assays. *Advances in bioscience and biotechnology.-Irvine, CA, 2010, currens*, *4*(5), pp.628-639.

Perkins, J.R., Diboun, I., Dessailly, B.H., Lees, J.G. and Orengo, C., 2010. Transient protein-protein interactions: structural, functional, and network properties. *Structure*, *18*(10), pp.1233-1243.

Prentis, R.A., Lis, Y. and Walker, S.R., 1988. Pharmaceutical innovation by the seven UK-owned pharmaceutical companies (1964-1985). *British journal of clinical pharmacology*, *25*(3), pp.387-396.

Rogge, M.C. and Taft, D.R. (2010) Preclinical drug development. 2nd Edition, *D.A.T.P. Sciences*, **187**, In- forma Healthcare USA, Inc., New York.

Rogge, M. and Taft, D.R. eds., 2016. *Preclinical drug development*. CRC Press.

Sluis-Cremer, N., 2018. Future of nonnucleoside reverse transcriptase inhibitors. *Proceedings of the National Academy of Sciences*, *115*(4), pp.637-638.

United States Department of Health and Human Services. [cited 22 April 2015]; Guidelines for the Use of Antiretroviral Agents in HIV-1-Infected Adults and Adolescents, viewed 26 May 2019. Available from: http://aidsinfo.nih.gov/guidelines/html/1/adult-and-adolescent-arv-guidelines/0.

Zhang, Q., Mi, Z., Huang, Y., Ma, L., Ding, J., Wang, J., Zhang, Y., Zhou, J., Guo, F., Li, X. and Cen, S., 2016. 2-thio-6-azauridine inhibits Vpu mediated BST-2 degradation. *Retrovirology*, *13*(1), p.13.

Chapter 5: Analysis of the binding of the Ligands to HIV-1 Vpu

5.1 Introduction

Quantification and characterisation of binding interactions between biological targets and potential drug candidates are crucial during drug discovery and development. The primary objective is to develop compounds that bind the target of interest with high binding affinity and selectivity, relative to other biological molecules (Gleeson *et al*., 2011). In theory, this should significantly reduce the possibility of the drug molecule interacting with other potential binding partners within a cell, as interactions of compounds with off-target molecules *in vivo* may lead to undesirable side-effects (Huggins *et al*., 2012). Although the correlation between binding affinity and specificity is not clearly defined, the general perception is that higher binding affinity of the ligand for the target should result in higher efficacy and better specificity *in vivo* (Eaton *et al*., 1995).

Over the past decades, understanding the thermodynamics of binding between ligands and target proteins has become an integral part of drug development (Garbett & Chaires, 2012). Thermodynamic data provides insights into the physical forces underlying a binding interaction and are usually used to complement structural data obtained through X-ray crystallography and/or NMR studies (Ferenczy & Keserű, 2010; Su & Xu, 2018). However, in cases where there is no structural data available on the binding of the ligand and the target, thermodynamic data can be used to understand the nature of the binding interactions (Ferenczy & Keserű, 2010). The most reliable tool for determining thermodynamic parameters of a binding interaction without any labelling is with the use of isothermal titration calorimetry (ITC; Ladbury & Chowdhry, 1996). ITC provides more than just the dissociation constant of the interaction (K_D); a single titration experiment gives information about the binding affinity constant (K_a), change in enthalpy (ΔH), change in entropy (ΔS), change in Gibbs free energy (ΔG) and the stoichiometry of the association (N). By measuring the binding enthalpy over a range of temperatures, the change in heat capacity (ΔC_p) of a biomolecular interaction can also be obtained.

The aim of this chapter was to evaluate the binding affinity of the hit compounds identified in this study towards HIV-1 Vpu. The ability of the compounds to directly bind to HIV-1 Vpu was first analysed using a thermal shift assay and a fluorescent-based binding assay. This was followed by characterisation of the thermodynamic parameters of the HIV-1 Vpu-ligand interactions using ITC.

5.2 Effects of ligand binding on the thermal stability of HIV-1 Vpu

Thermal induced unfolding analysis of HIV-1 Vpu was conducted to assess the relative stability of the protein using circular dichroism (CD) spectroscopy. This was achieved by monitoring the extent of α-helical denaturation (at 222 nm) in response to changes in temperature (range 20 °C to 100 °C). Ellipticity at 222 nm is directly proportional to the α-helical content of a protein and was thus chosen as an indicator since HIV-1 Vpu is predominantly α-helical in nature. Thermal unfolding studies can be used to determine the melting temperature (T_m), enthalpy (ΔH) and heat capacity increment (ΔC_p) of a specific protein, and these parameters may in-turn be used to calculate the Gibbs free-energy (ΔG) change of the unfolding (Luke *et al*., 2007; Privalov 1979; Pace *et al*., 1989). However, because the thermal denaturation of HIV-1 Vpu was irreversible (data not shown), the ΔH, ΔC_p and ΔG values could not be obtained for this protein. The T_m value, defined as the temperature at which 50% of the protein is unfolded, was thus used to estimate HIV-1 Vpu's relative stability. Figure 5.1 shows that HIV-1 Vpu unfolded with a single transition, which occurred between 64 °C and 84 °C, and the T_m value of HIV-1 Vpu was found to be 75.2 °C.

The effect of Compound 1, Compound 8, 6-aza-2-thiouridine and Lapachol on the thermal stability of HIV-1 Vpu was also assessed. This was achieved by measuring the change in the T_m value (ΔT_m) of HIV-1 Vpu upon binding of the ligands. A 1:1 molar ratio of HIV-1 Vpu to the compounds was used, and the analysis was conducted under the same conditions as the ligand-free HIV-1 Vpu. Figure 5.1 and Table 5.1 show that upon binding of Compound 1 and Lapachol, the T_m value of HIV-1 Vpu decreased from 75.2 °C to 72.7 °C and 73.9 °C, with ΔT_m values of –2.5 °C and –1.3 °C, respectively. Also evident from Figure 5.1 and Table 5.1 is that the T_m value increased to 75.7 °C and 77.1 °C when Compound 8 and 6-aza-2-thiouridine were bound, giving rise to ΔT_m values of 0.5 °C and 1.9 °C, respectively.

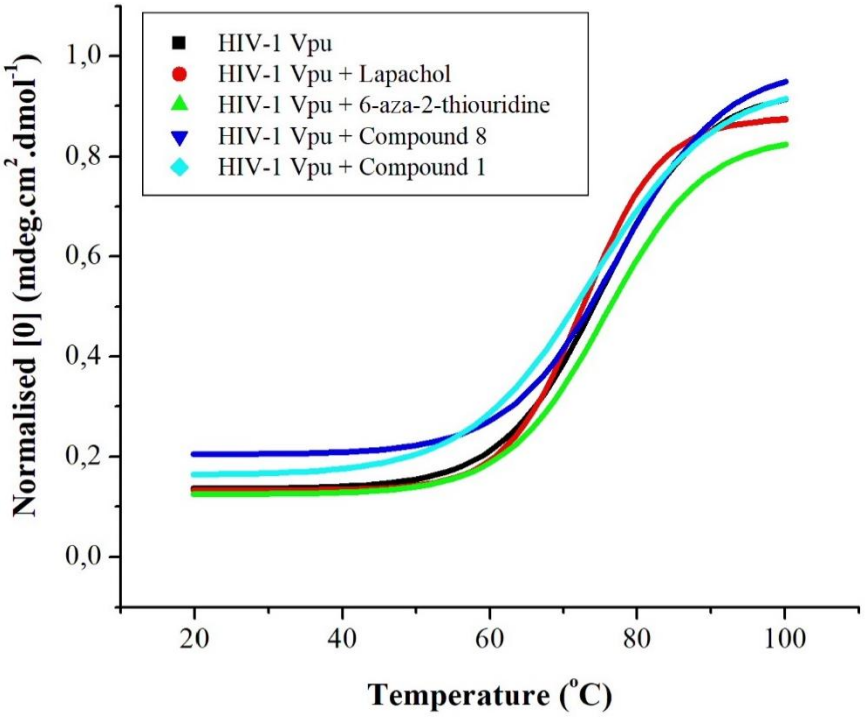

Figure 5.1: Thermal shift assay for the binding of the ligands to HIV-1 Vpu. The denaturation of HIV-1 Vpu was monitored in the absence (black) and presence of Compound 1 (cyan), Compound 8 (blue), 6-aza-2-thiouridine (green) and Lapachol (red). The progression of the unfolding was monitored by CD spectroscopy at 222 nm. The readings were done using 5 µM HIV-1 Vpu and 5µM of the compounds in 20 mM Tris (pH 7.4), 50 mM NaCl in the 20 – 100 °C temperature range using a 1 °C.min^{-1} gradient.

Table 5.1: Melting temperature of HIV-1 Vpu in the presence and absence of the identified hit compounds. The *Tm* values were determined using CD spectroscopy at 1:1 molar ratios of HIV-1 Vpu to the compounds. The values are mean *Tm* ± SE of three independent experiments.

Sample	***Tm* Value (°C)**	***ΔTm* (°C)**
HIV-1 Vpu	75.2 ± 0.61	-
HIV-1 Vpu + Compound 1	72.7 ± 0.45	-2.5
HIV-1 Vpu + Compound 8	75.7 ± 0.55	0.5
HIV-1 Vpu + 6-aza-2-thiouridine	77.1 ± 0.60	1.9
HIV-1 Vpu + Lapachol	73.9 ± 0.42	-1.3

5.3 Ligand binding analysis using intrinsic Fluorescence

The binding affinity of Compound 1, Compound 8, 6-aza-2-thiouridine and Lapachol towards HIV-1 Vpu were analysed using a fluorescence-based assay. This was conducted by measuring the quenching or enhancement of the intrinsic tryptophan fluorescence of HIV-1 Vpu upon titration with the ligands. The tryptophan residues were selectively excited at 295 nm and emission spectra were recorded from 280 to 500 nm. The results from this analysis, as illustrated in Figure 5.2 below, show that the titration of 6-aza-2-thiouridine and Lapachol induced quenching of HIV-1 Vpu's fluorescence signal, while Compound 1 and Compound 8 caused enhancement of the signal. Also evident from Figure 5.2 is that while 6-aza-2-thiouridine and Lapachol caused saturation (from around 200 and 400 µM for each compound, respectively), the two in-house compounds did not show any saturation. The observed fluorescence increased continually with the titration of Compound 1, and a maximum peak was observed with Compound 8, afterwhich the observed fluorescence decreased again. Titration of Compound 1 and Compound 8 into buffer (without protein) showed similar responses to the ones shown in Figure 5.2, suggesting that this fluorescence signal was likely due to the compounds, and not necessarily their binding to HIV-1 Vpu (Figure D.1, A and B, Appendix D). The titration of 6-aza-2-thiouridine and Lapachol into buffer (without protein) on the other hand showed much less fluorescence signals compared to the presence of HIV-1 Vpu (Figure D.1, C and D, Appendix D), suggesting potential binding of these compounds to HIV-1 Vpu. The data obtained for 6-aza-2-thiouridine and Lapachol were therefore used to estimate the dissociation constants (K_D) of both compounds from HIV-1 Vpu as the concentration of compound that resulted in 50% saturation. K_D values of 62 ± 1.29 and 180 ± 0.83 µM were obtained for 6-aza-2-thiouridine and Lapachol, respectively.

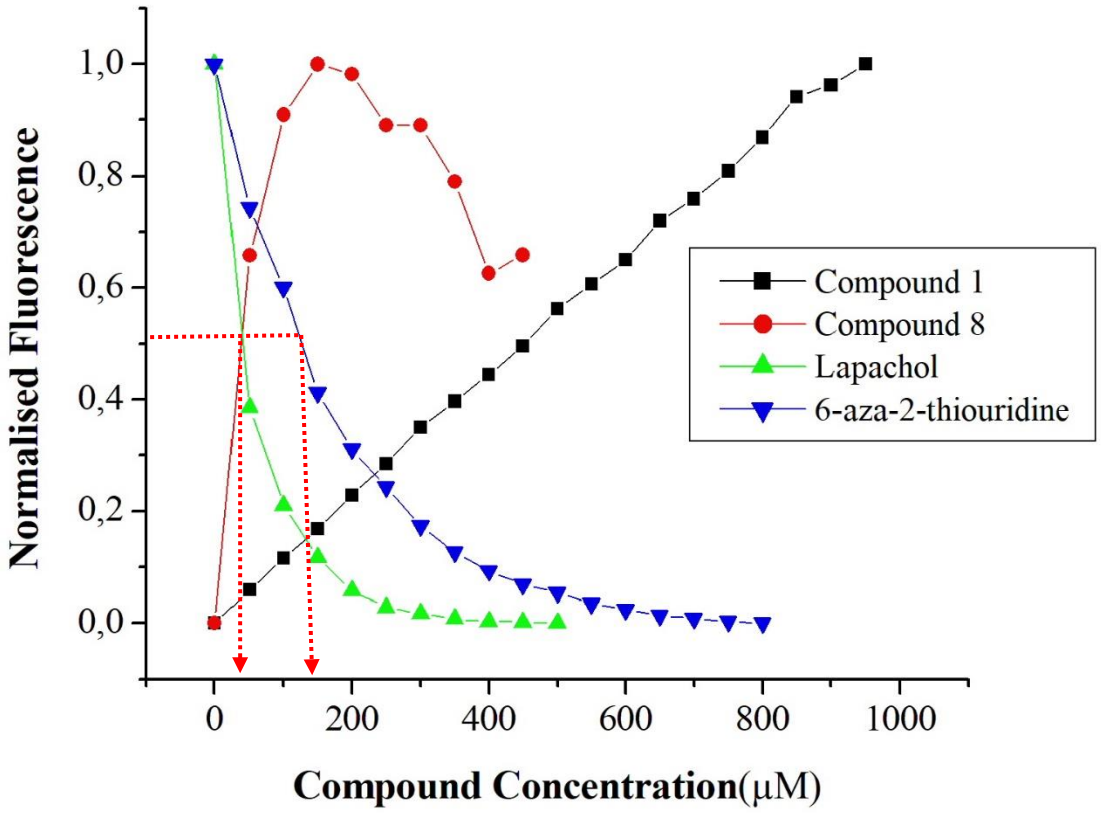

Figure 5.2: Intrinsic Tryptophan fluorescence spectra of HIV-1 Vpu with the test compounds. The protein was titrated with Compound 1 (black), Compound 8 (red), Lapachol (green) and 6-aza-2-thiouridine (blue). The readings were done using 5 μM HIV-1 Vpu in 20 mM Tris (pH 7.4), 100 mM NaCl and 50 μM increments of the compounds were added at each time point. The K_D values for 6-aza-2-thiouridine and Lapachol were 62 ± 1.29 μM and 180 ± 0.83 μM, respectively, as shown by the red dotted arrows on the graph.

5.4 Thermodynamic analysis of the binding of the identified inhibitors to HIV-1 Vpu

Isothermal titration calorimetry (ITC) was used to obtain a complete energy profile of the binding of the test compounds to HIV-1 Vpu. The experiments were performed using the Standard Volume Nano ITC (TA Instruments) at 20 °C, with 10 µM HIV-1 Vpu, and compound concentrations ranging between 0.2 – 1 mM. Control reactions in which the ligands were titrated into the reaction buffer were conducted and represented the heats of dilution. The heats of dilution obtained for each compound were corrected for from the heats of the protein-ligand dilutions. This was done to ensure that any heat signals observed during the ligand into protein titrations were solely due to the binding of the compounds to HIV-1 Vpu. Figures 5.3 – 5.6 show representative results for the calorimetric titrations of Compound 1, Compound 8, 6-aza-2-thiouridine and Lapachol into HIV-1 Vpu, respectively. The peaks in the top panels of Figure 5.3 – 5.6 represent the titration of the ligands into the protein, while the bottom panel represents the binding isotherms obtained by plotting the integrated heat obtained after each injection against the ratio of the concentration of the ligand and protein added, corrected for heats of dilution. The negative heats of binding observed on all four of the isotherms are an indication of exothermic binding events between HIV-1 Vpu and the compounds. The minimal changes in the heat of binding following each injection (apparent from Figure 5.3 to 5.6), however, suggest that the binding of the test compounds to HIV-1 Vpu was weak. The analysis of Lapachol by ITC proved to be very challenging as the compound repeatedly precipitated out of solution during the experiments. Figure 5.6 shows that no binding was observed between HIV-1 Vpu and Lapachol at concentrations up to 200 µM of this compound, and the compound could not be maintained in solution at concentrations higher than 200 µM, as such, the thermodynamic variables could not be obtained for this compound.

Table 5.2 shows a summary of the thermodynamic parameters obtained for the binding of Compound 1, Compound 8 and 6-aza-2-thiouridine to HIV-1 Vpu. Briefly, the compounds bind to HIV-1 Vpu with binding affinities (K_a) ranging from 4.80 x 10^4 to 2.23 x 10^5 M^{-1}, and unfavourable entropic terms (ΔS) between 24.03 J/mol.K and 86.50 J/mol.K. The binding of these compounds yielded Gibbs free energy of binding (ΔG) values of –26.54 kJ/mol, –26.26 kJ/mol and –30.40 kJ/mol and was characterised by favourable enthalpic terms (ΔH) of –3.98 kJ/mol, –0.99 kJ/mol and –23.36 kJ/mol for Compound 1, Compound 8 and 6-aza-2-

thiouridine, respectively. Furthermore, the binding constant (K_D) for Compound 1 was found to be 18.5 µM, 20.82 µM for Compound 8 and 4.49 µM for 6-aza-2-thiouridine. In terms of stoichiometry (*N*), the values obtained for all three compounds were comparable (i.e. 5.23, 5.67 and 5.88).

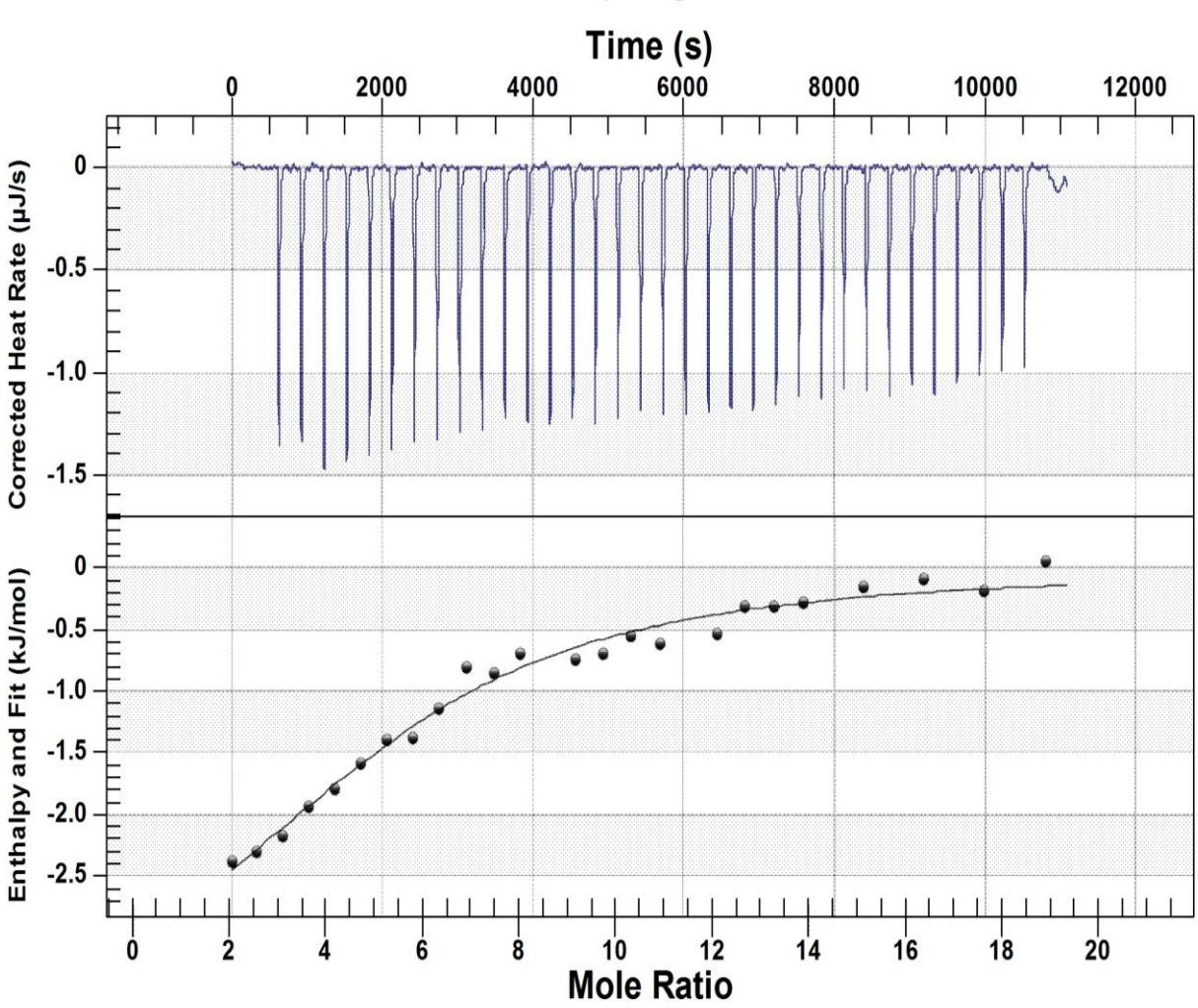

Figure 5.3: A representative calorimetric profile of the titration of HIV-1 Vpu with Compound 1. The titrations were performed using 700 µM Compound 1 into 10 µM HIV-1 Vpu at 20 ºC. Panel A. shows raw exothermic heats generated upon each injection of Compound 1 into HIV-1 Vpu. Panel B. shows the integrated heats corresponding to the data in panel A plotted against molar ratio of Compound 1 to HIV-1 Vpu.

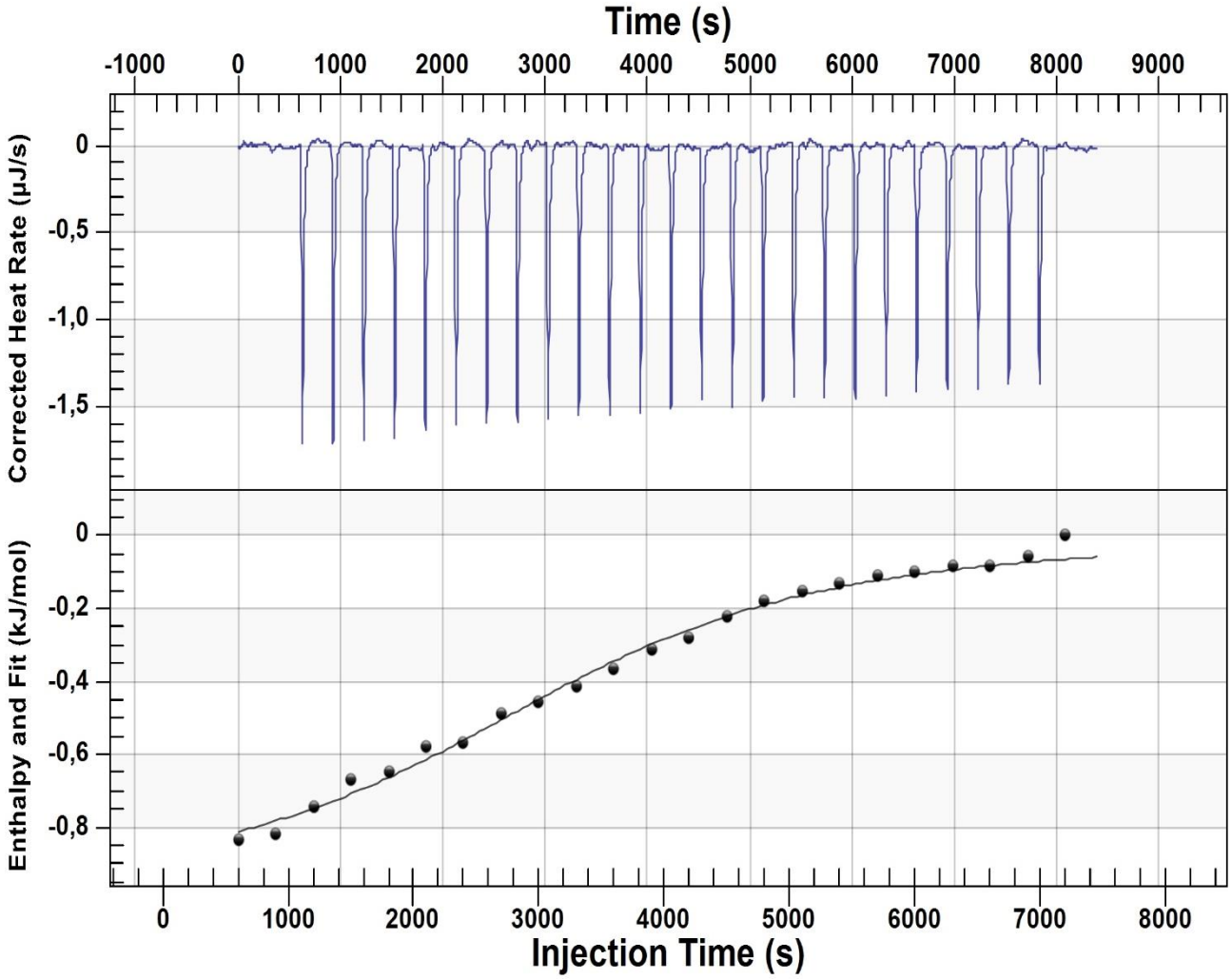

Figure 5.4: A representative calorimetric profile of the titration of HIV-1 Vpu with Compound 8. The titrations were performed using 1 mM Compound 8 into 10 µM HIV-1 Vpu at 20 ºC. Panel A. shows raw exothermic heats generated upon each injection of Compound 8 into HIV-1 Vpu. Panel B. shows the integrated heats corresponding to the data in panel A plotted against the molar ratio of Compound 8 to HIV-1 Vpu.

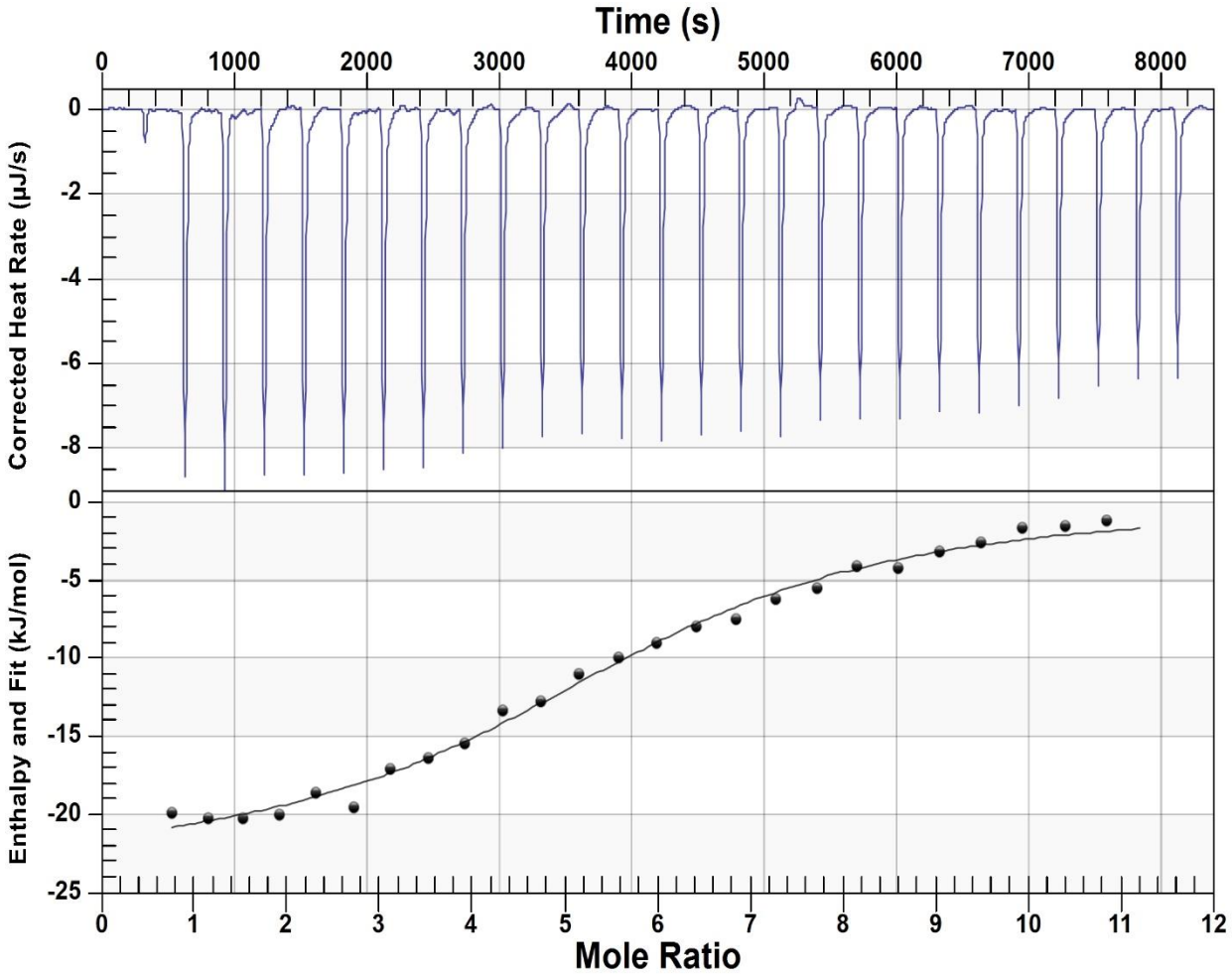

Figure 5.5: A representative calorimetric profile of the titration of HIV-1 Vpu with 6-aza-2-thiouridine. The titrations were performed using 400 µM 6-aza-2-thiouridine into 10 µM HIV-1 Vpu at 20 ºC. Panel A. shows raw exothermic heats generated upon each injection of 6-aza-2-thiouridine into HIV-1 Vpu. Panel B. shows the integrated heats corresponding to the data in panel A plotted against the molar ratio of 6-aza-2-thiouridine to HIV-1 Vpu.

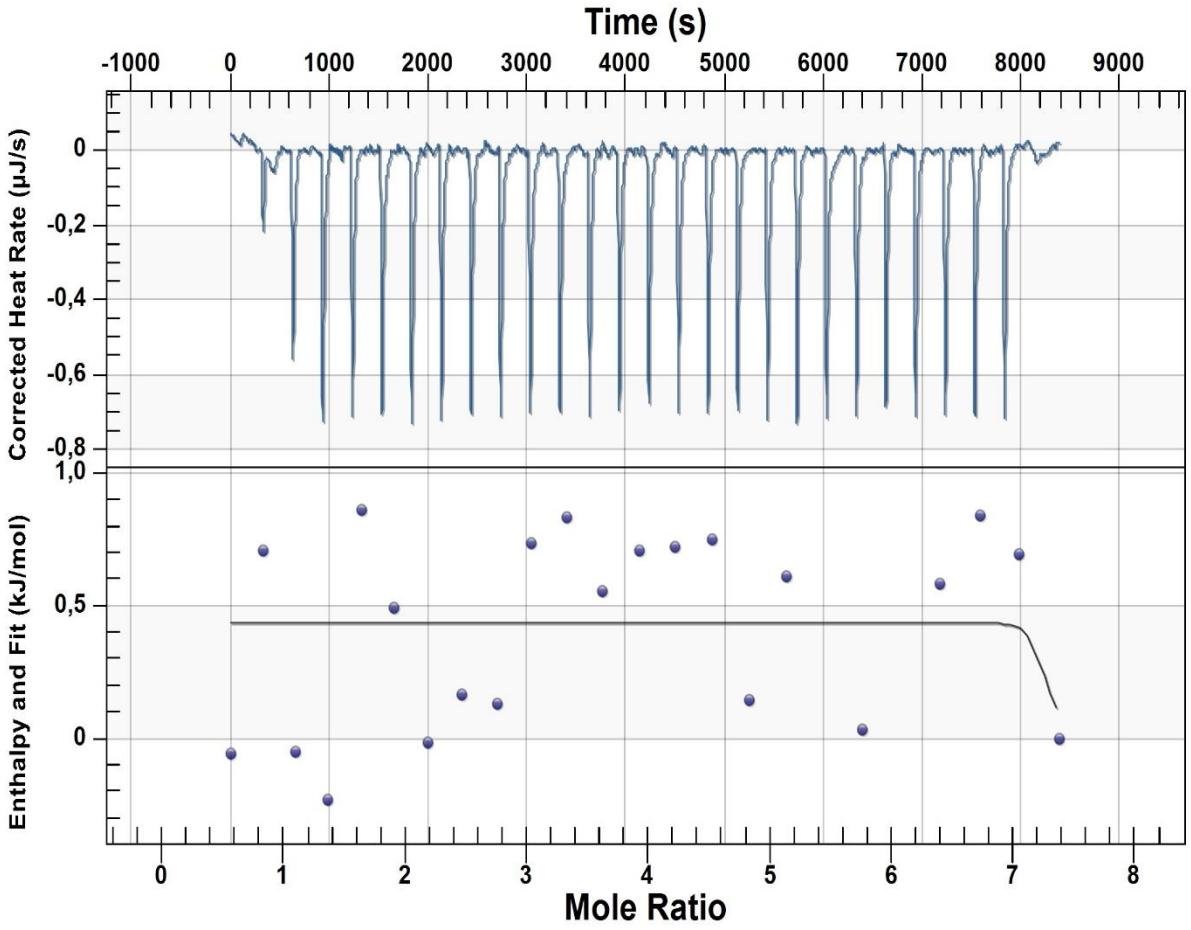

Figure 5.6: A representative calorimetric profile of the titration of HIV-1 Vpu with Lapachol. The titrations were performed using 200 µM Lapachol into 10 µM HIV-1 Vpu at 20 ºC. Panel A. shows raw exothermic heats generated upon each injection of Lapachol into HIV-1 Vpu. Panel B. shows the integrated heats corresponding to the data in panel A plotted against the molar ratio of Lapachol to HIV-1 Vpu.

Table 5.2: Thermodynamic parameters obtained for the interaction of HIV-1 Vpu with Compound 1, Compound 8 and 6-aza-2-thiouridine using ITC at 20 ºC.

Compound	***N***	***K*D (μM)**	***ΔH* (kJ/mol)**	***ΔS* (kJ/mol/K)**	***ΔG* (kJ/mol)**
Compound 1	5.23	18.50	-3.98	0.077	-26.54
Compound 8	5.88	20.82	-0.99	0.086	-26.26
6-aza-2-thiouridine	5.67	4.49	-23.36	0.024	-30.40

5.5 Discussion

Several methods are used for measuring the binding affinity of potential drug candidates towards molecular targets in the pharmaceutical industry. One of the main methods with broad applicability is the monitoring of the conformational stability of the target protein in the absence and presence of ligands. The conformational stability of proteins is usually altered upon binding with ligands, and this results in a shift in the observed T_m value of the protein of interest. Therefore, subjecting the target protein to thermal denaturation in the absence and presence of drug candidates can be used as a measure to identify potential candidates as those that cause a shift in the T_m relative to the unbound protein (Cimmperman *et al.*, 2008). According to Matulis *et al*. (2005), the magnitude of the shift in the T_m value of a protein is proportional to both the concentration and the binding affinity of the bound ligand. Most ligands stabilise proteins upon binding, causing an increase in the T_m value of the protein. However, this is not always the case, as some ligands can destabilise proteins, causing a decrease in the melting temperature of the target protein.

Figure 5.1 and Table 5.1 show that the four test compounds only caused marginal shifts in the T_m value of HIV-1 Vpu when equimolar concentrations of the protein to compounds were used. With ΔT_m values of -2.5, 0.5, 1.9 and -1.3 for Compound 1, Compound 8, 6-aza-2-thiouridine and Lapachol, respectively. Statistical tests were performed to test the significance the thermal shifts induced by the four compounds on HIV-1 Vpu. The obtained results showed that the T_m values obtained for Compound 8, 6-aza-2-thiouridine and Lapachol were statistically insignificant, as their p-values exceeded 0.05 ($p > 0.05$). Compound 1 was the only compound that induced a statistically significant thermal shift upon binding to HIV-1 Vpu ($p < 0.05$). These findings denoted weak affinity of these compounds for HIV-1 Vpu. Consistent with the IC_{50} values obtained for the two hit compounds, where Compound 1 showed better activity compared to Compound 8, these results show that Compound 1 had better affinity for HIV-1 Vpu.

Fluorescence spectroscopy has also become a crucial tool in biochemical and pharmaceutical research because of its robustness, high sensitivity and non-invasiveness (Ladokhin *et al.*, 2000). Amongst the three fluorescent amino acid constituents of proteins, Tryptophan is the most sensitive to changes in its local environment and can thus be used as a valuable probe to monitor local tertiary structural changes that occur in the protein. HIV-1 Vpu consists of two tryptophan residues at positions 22 and 76, as shown in Figure 1.4 B. Trp22 is located in the

transmembrane domain of HIV-1 Vpu and is one of the residues that are involved in the interaction with BST-2. As mentioned earlier, Compound 1 and Compound 8 were also designed to bind to Ala14, Ala18 and Trp22 of HIV-1 Vpu, to block the ability of HIV-1 Vpu to bind to BST-2. This therefore suggests that Trp22 is in the proximity of the bound ligands and should be sensitive to any structural changes that occur as a result of the ligands binding to HIV-1 Vpu.

As stated above, the titration of Compound 1 and Compound 8 in the presence and absence of HIV-1 Vpu yielded similar responses, suggesting that the observed fluorescence signals were likely due to the compounds. These observations could be due to the resemblance of the structures of these two compounds (shown in Table 4.2) to that of Tryptophan. The backbone structures of Compound 1 and Compound 8 consist of a benzene ring, a pyrrole ring and a carboxylic acid functional group. Although the benzene and pyrrole rings are not fused together in the case of these compounds, as is the case with Tryptophan, the presence of these functional groups could potentially result in the compounds interfering at the excitation wavelength. The obtained K_D vales of 62 and 180 µM for 6-aza-2-thiouridine and Lapachol, respectively, suggest that the binding affinity of these compounds to HIV-1 Vpu was rather weak. Looking at the two values, however, 6-aza-2-thiouridine showed ~3-times better binding compared to Lapachol. These findings were the first to show the ability of these two compounds to bind to HIV-1 Vpu.

The affinity of the test compounds for HIV-1 Vpu was further characterised through ITC. ITC is one of the most sensitive and accurate methods available for characterisation of macromolecule-ligand interactions (Perozzo *et al.*, 2004; Liang, 2008). In a typical ITC experiment, the ligand solution in the syringe is titrated into the macromolecule solution in the sample cell, and upon each injection of the ligand, a heat difference is observed. The ITC technique directly measures the heat absorbed or generated during the binding of ligands to macromolecules and it gives a complete energy profile of the biomolecular interaction. This technique provides more than just the binding affinity constant (K_D) of an interaction, it also gives details about the forces underlying an interaction (i.e. enthalpic and/or entropic contributions). One drawback of this method is that it is a low throughput technique and requires relatively large amounts of protein, and as such, it is not suited to be used as a primary screening method.

Figures 5.3 – 5.6 show that the binding between all four of the compounds tested in this study and HIV-1 Vpu was weak. This is evident from the low changes in heat following the titrations of the ligands into the protein shown by the binding isotherms, as well as the high concentrations of compounds required to saturate the binding site of HIV-1 Vpu. However, despite the weakness of the interactions of the ligands with HIV-1 Vpu, the thermodynamic parameters for most of the binding interactions could still be determined and are summarised in Table 5.2. Evident from Table 5.2 is that the binding of these compounds to HIV-1 Vpu at 20 ºC was characterised by favourable (negative) enthalpic changes and very weak entropic terms. This means that the dominant force underlying the binding of these compounds to HIV-1 Vpu was the negative enthalpy changes and this is also supported by the exothermic nature of these reactions. According to Perozzo *et al*. (2004) and Freire (2004), enthalpic contributions primarily reflect the strength of the hydrogen bonds and van der Waals interactions between the ligand and the target protein in relation to those of the protein and the surrounding solvent. Entropically driven binding interactions on the other hand are associated with non-specific hydrophobic interactions between the ligand and the target protein (Freire, 2004). This therefore suggests that the ligands tested in this study formed strong and specific hydrogen bonds with HIV-1 Vpu. 6-aza-2-thiouridine showed stronger binding to HIV-1 Vpu with a ΔH value of -23.36 kJ/mol, followed by Compound 1 at ΔH -3.98 kJ/mol and Compound 8 with a ΔH of -0.99 kJ/mol.

The results obtained in this study show that the binding affinity of the compounds towards HIV-1 Vpu was rather weak, with K_D values all in the micromolar range. From these results, 6-aza-2-thiouridine showed greater binding affinity for HIV-1 Vpu compared to the rest of the other compounds at 20 ºC. The binding affinity of 6-aza-2-thiouridine for HIV-1 Vpu (4.49 µM) was found to be ~four-fold greater than that of Compound 1 and Compound 8 (18.5 µM and 20.82 µM, respectively). The strength of the interaction of 6-aza-2-thiouridine for HIV-1 Vpu is also evident from the more negative Gibbs free energy change (ΔG) value of this compound. The Gibbs free energy change is said to be one of the most important parameters in the thermodynamic description of a binding reaction as it determines the stability of the biological complex. The tighter the binding affinity, the smaller the K_D, and the more negative the ΔG becomes (Frasca, 2016). Table 5.2 shows that 6-aza-2-thiouridine had a ΔG value of -30.4 kJ/mol, followed by Compound 1 (-26.54 kJ/mol) and lastly, Compound 8 (-26.26 kJ/mol), further suggesting that the 6-aza-2-thiouridine/HIV-1 Vpu complex was tighter than the other two ligands. As a result of poor solubility, the

thermodynamic parameters of binding for Lapachol could not be determined. The poor solubility of this compound was also evident from Table 4.3, which showed that as the concentration of this compound was increased from 100 to 200 µM, the solubility decreased from 87% to 67% dissolution.

Since HIV-1 Vpu is not an enzyme and does not have a well-defined active site, designing compounds against this protein was rather challenging. Drug molecules are usually targeted against the active site of the target protein, competitively inhibiting the catalytic activity of the enzyme. In the case of HIV-1 Vpu, however, the compounds were designed to bind to the amino acid residues that are involved in the interaction with BST-2 (i.e. A10, A14, A18 and W22), thereby blocking the ability of HIV-1 Vpu to bind to BST-2. This therefore means that each ligand was designed to bind to multiple positions on the HIV-1 Vpu, and this could be the reason for the high binding stoichiometry values observed for the test compounds. Furthermore, Nguyen *et al.* (2018) reported that if the concentrations of the reactants used in the titration experiments are not well optimised, that could result in errors in the observed *N* values. It is possible that the *N* values observed in this study could be erroneous, as the concentrations of HIV-1 Vpu and the test compounds used in this study still require further optimisation for saturation to be reached.

5.6 References

Cimmperman, P., Baranauskienė, L., Jachimovičiūtė, S., Jachno, J., Torresan, J., Michailovienė, V., Matulienė, J., Sereikaitė, J., Bumelis, V. and Matulis, D., 2008. A quantitative model of thermal stabilization and destabilization of proteins by ligands. *Biophysical journal*, *95*(7), pp.3222-3231.

Eaton, B.E., Gold, L. and Zichi, D.A., 1995. Let's get specific: the relationship between specificity and affinity. *Chemistry & biology*, *2*(10), pp.633-638.

Ferenczy, G.G. and Keserű, G.M., 2010. Thermodynamics guided lead discovery and optimization. *Drug discovery today*, *15*(21-22), pp.919-932.

Frasca, V., 2016. Biophysical characterization of antibodies with isothermal titration calorimetry. *Journal of Applied Bionalysis*, *2*(3), p.90.

Freire, E., 2004. Thermodynamic in drug design. High affinity and selectivity. *Proceedings of the chemical theatre of biological systems*, p.1e13.

Garbett, N.C. and Chaires, J.B., 2012. Thermodynamic studies for drug design and screening. *Expert opinion on drug discovery*, *7*(4), pp.299-314.

Gleeson, M.P., Hersey, A., Montanari, D. and Overington, J., 2011. Probing the links between in vitro potency, ADMET and physicochemical parameters. *Nature reviews Drug discovery*, *10*(3), p.197.

Huggins, D.J., Sherman, W. and Tidor, B., 2012. Rational approaches to improving selectivity in drug design. *Journal of medicinal chemistry*, *55*(4), pp.1424-1444.

Ladbury, J.E. and Chowdhry, B.Z., 1996. Sensing the heat: the application of isothermal titration calorimetry to thermodynamic studies of biomolecular interactions. *Chemistry & biology*, *3*(10), pp.791-801.

Ladokhin, A.S., Jayasinghe, S. and White, S.H., 2000. How to measure and analyze tryptophan fluorescence in membranes properly, and why bother? *Analytical biochemistry*, *285*(2), pp.235-245.

Liang, Y., 2008. Applications of isothermal titration calorimetry in protein science. *Acta biochimica et biophysica Sinica*, *40*(7), pp.565-576.

Matulis, D., Kranz, J.K., Salemme, F.R. and Todd, M.J., 2005. Thermodynamic stability of carbonic anhydrase: measurements of binding affinity and stoichiometry using ThermoFluor. *Biochemistry*, *44*(13), pp.5258-5266.

Nguyen, T.H., Rustenburg, A.S., Krimmer, S.G., Zhang, H., Clark, J.D., Novick, P.A., Branson, K., Pande, V.S., Chodera, J.D. and Minh, D.D., 2018. Bayesian analysis of isothermal titration calorimetry for binding thermodynamics. *bioRxiv*, p.327676.

Perozzo, R., Folkers, G. and Scapozza, L., 2004. Thermodynamics of protein–ligand interactions: history, presence, and future aspects. *Journal of Receptors and Signal Transduction*, *24*(1-2), pp.1-52.

Scott, D.E., Spry, C. and Abell, C., 2016. Differential scanning fluorimetry as part of a biophysical screening cascade. *Fragment-based drug discovery lessons and outlook, Erlanson, DA and Jahnke W., Eds*.

Su, H. and Xu, Y., 2018. Application of ITC-Based Characterization of Thermodynamic and Kinetic Association of Ligands With Proteins in Drug Design. *Frontiers in pharmacology*, *9*.

Chapter 6: Summary of Findings and General Conclusions

6.1 Successful Expression and Purification of HIV-1 Vpu

Given the important role played by HIV-1 Vpu in the replication cycle of HIV-1, this makes the structural biology of this protein of interest in the HIV research field. The first step towards understanding the biological functions played by HIV-1 Vpu in the HIV-1 lifecycle would be to characterise its structural features and determine its three-dimensional structure. Understanding these characteristics is a prerequisite for therapeutic developments in order to build up a detailed picture of how HIV-1 Vpu functions at a molecular level. However, the membrane bound nature of HIV-1 Vpu has been a limitation in many structural characterisation efforts made for this protein. Structural characterisation studies of proteins require sufficient quantities (usually milligrams) of highly purified proteins, and membrane bound proteins are inherently difficult to overexpress and purify in sufficient quantities, owing to their hydrophobic nature. One of the aims of this study was to develop a working method for the overexpression and purification of this protein.

Chapter 3 of this thesis describes a novel method of overexpressing, solubilising and purifying a full-length recombinant HIV-1 Vpu that was developed in this study. Given the yields and the purity of the recombinant HIV-1 Vpu obtained, the method described here solves a fundamental problem that has been a challenge in studies involving HIV-1 Vpu, in that sufficient quantities of highly purified, properly folded and functional full-length HIV-1 Vpu was successfully obtained. Scaling up of this overexpression and purification method could potentially allow for production of HIV-1 Vpu in quantities suitable for three-dimensional structural characterisations of this protein using X-ray crystallography to advance the efforts of pursuing HIV-1 Vpu as a target for HIV-1 therapy.

Overall, the data obtained from the secondary, tertiary and quaternary structural characterisation studies conducted on the recombinant HIV-1 Vpu produced in this study correlate with what has been previously reported about the native characteristics of this protein. A comparison of the urea unfolded HIV-1 Vpu with the folded protein showed the folded to be more compact, with the emission properties of its tryptophan residues suggesting that they are partially accessible to solvent. These findings suggest that this protein was likely

to have an intact structure that is comparable to that of a native HIV-1 Vpu. The ability of this protein to bind to its binding partner, BST-2, further proved this protein to be functional, or to at least assume a conformation that is able to bind BST-2.

6.2 Evaluation of the identified hit compounds

The discovery of the human restriction factor, BST-2, did not only reveal a novel component of the innate immune system, but it also provided a promising strategy for development of new anti-HIV-1 therapeutics with a novel mode of action. The ability of HIV-1 Vpu to directly interact with BST-2 through their respective transmembrane domains has been proven to be critical in the HIV-1 Vpu mediated downregulation of BST-2. This therefore suggests that disrupting the interaction between HIV-1 Vpu and BST-2 should hypothetically expose HIV-1 to the restriction activity of BST-2.

As detailed in Chapter 4 of this thesis, biological assays were developed for the screening of novel compounds against the HIV-1 Vpu/BST-2 interaction. Two hit compounds, Compound 1 and Compound 8, were identified from the screening tests and were evaluated through a process called lead optimisation. The evaluation of the compounds involved theoretically predicting their pharmacokinetic properties, using several biochemical and biological assays to determine their effective doses, assessing their effect on host cells and viral replication, as well as to investigate their affinity for HIV-1 Vpu. The compounds were tested along with 6-aza-2-thiouridine and Lapachol, which previously showed activity in restoring cell surface expression levels of BST-2 in the presence of HIV-1 Vpu in cell-based assays. To the best of our knowledge, Compound 1 and Compound 8 are novel and have never been investigated for the inhibition of the interaction of HIV-1 Vpu with BST-2 or their binding to HIV-1 Vpu. The findings obtained from the characterisation studies conducted on each compound in Chapter 3 and 4 of this thesis are summarised in Table 6.1 below.

Table 6.1: Summary of the Lipinski Score, IC_{50}, CC_{50}, EC_{50}, Therapeutic Indexes, ΔTm, K_D and ΔG values obtained from the characterisation studies conducted on the test compounds

Compound	Chemical Structure	Lipinski Score	IC_{50} (µM)	CC_{50} (µM)	EC_{50} (µM)	TI value	ΔT_m (°C)	K_D (µM)	ΔG (kJ/mol/K)
Compound 1	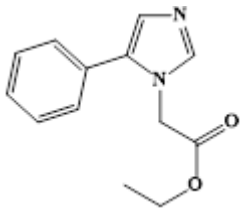	4	11.6	184.5	6.3	29.3	-2.5	18.5	-26.5
Compound 8	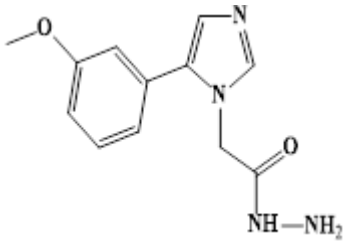	4	17.6	159.5	157.5	1.01	0.5	20.8	-26.3
6-aza-2-thiouridine	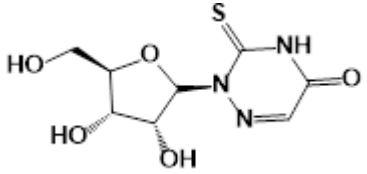	4	N.D.	14.6	24.1	0.6	1.9	4.5	-30.4

Lapachol	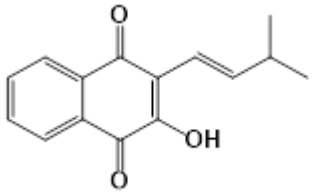	4	N.D.	152.8	17.3	8.8	-1.3	N.D.	N.D.

* N.D denotes Not Determined

6.2.1 Analysis of the drug-likeness of the compounds

As shown in Table 6.1, the four compounds (two hit compounds and the two control compounds) were fully compliant to all the requirements stated by Lipinski's rule-of-five and scored a perfect four out of four, predicting good absorption and permeability profiles. These compounds, however, lacked substantial solubility in water (i.e. aqueous media) alone, and required initial solubilisation in DMSO. Savjani *et al.* (2012) reported that more than 40% of all new drug candidates developed in the pharmaceutical industry are estimated to be insoluble in water, and this tends to be a major challenge as drug compounds need to be dissolved in the aqueous fluids of the gastrointestinal tract for them to be successfully absorbed orally. The solubility of the compounds could be improved in the later stages of the drug discovery and development process using techniques such as developing salts of these compounds or making use of surfactants or micellars to enhance solubility (Savjani *et al.*, 2012).

6.2.2 Effects of the compounds on the HIV-1 Vpu/BST-2 interaction

A closer look at the IC_{50} values obtained for the two hit compounds shows that Compound 1 was relatively more potent in inhibiting the HIV-1 Vpu/BST-2 interaction compared to Compound 8. It is not unusual for initial hits from the first-generation of compounds in drug discovery to show moderate inhibition (usually between 0.1 and 1 mM; Chabner & Longo, 2011). However, to become effective drugs, the activity of the compounds needs to be improved to the nanomolar range or lower. These first-generation compounds are used as starting points for synthesis of structurally related compounds in order to increase the biological activity and improve the affinity of the compounds for the target protein (Chabner & Longo, 2011).

6.2.3 Effects of the compounds on host cells and viral replication

The cytotoxicity data showed that Compound 1, Compound 8 and Lapachol exhibited minimal toxicity traits towards the MT-4 mammalian cells, while 6-aza-2-thiouridine proved to be highly cytotoxicity against these cells. In terms of viral replication, Compound 1 and Lapachol were able to inhibit viral replication at non-toxic doses, while Compound 8 showed minimal to no activity in inhibiting the replication of HIV-1. Because 6-aza-2-thiouridine was toxic to the MT-4 cells, it is likely that the supposed antiviral activity displayed by this compound was attributed to its cytotoxicity against the cells.

The HIV-1 LAV viral isolate and the HIV-1 Vpu used in this study belong to the subtype B strain of the pandemic HIV-1 Group M. Subtype B is the most studied of the HIV-1 strains, and as a result, most of the data that is available on HIV-1 Vpu, and HIV-1 in general, was attained using this strain. By contrast, less clinical research has been done on HIV-1 subtype C, despite this strain being the most prevalent and accounting for nearly 50% of all HIV-1 infections worldwide. The choice of using the subtype B strain in this study was to be able to accurately compare the activity of any identified hit compounds to known potential HIV-1 Vpu inhibitors, such as BIT225 and the two control compounds, 6-aza-2-thiouridine and Lapachol, whose activities were also tested against HIV-1 subtype B. Once the activity of the compounds has been established, testing of the compounds against the HV-1 subtype C strain, which is the most prevalent in Southern Africa, would then be conducted.

6.2.4 Affinity of the compounds for HIV-1 Vpu

The ability of the ligands to directly bind to HIV-1 Vpu was first tested by monitoring the change in the melting temperature of HIV-1 Vpu upon binding of the ligands using CD spectroscopy. Compound 1 is the only compound that a caused significant shift in the melting temperature of HIV-1 Vpu. An intrinsic tryptophan fluorescence-based assay was subsequently established, however, the binding affinity of the hit compounds for HIV-1 Vpu could not be accurately determined, owing to the fluorescent properties of these compounds. Between the two control compounds, 6-aza-2-thiouridine showed ~3-times greater affinity for HIV-1 Vpu compared to Lapachol on the fluorescence-based assay. The binding energetics of the test compounds to HIV-1 Vpu were further investigated using ITC and the obtained K_D values were all in the micromolar range. These results further confirmed the moderate binding affinity of these compounds towards HIV-1 Vpu. From the K_D and ΔG values, 6-aza-2-thiouridine showed greater binding affinity towards HIV-1 Vpu, followed by Compound 1 and Compound 8. The affinity of Compound 1 for HIV-1 Vpu was ~1.1-fold greater compared to that Compound 8.

Overall, the data obtained in this study shows that Compound 1, with the chemical name ethyl 2-[(5-phenyl)-1*H*-imidazol-1-yl]acetate, showed greater activity in inhibiting the binding of HIV-1 Vpu to BST-2, was more potent in hindering the replication of HIV-1 *in vitro* and also showed better affinity for HIV-1 Vpu compared to Compound 8 (5-(3-methoxyphenyl)-1*H*-imidazol-1-yl]acetohydrazide). This means that between the two hit compounds that were identified in this study, Compound 1 qualifies as a better lead

compound. The chemical structure of this compound can provide basis for potential HIV-1 Vpu inhibitors with improved biological activity and selectivity to be developed for the fight against HIV-1. However, it is not clear at this point if this compound could possibly show activity in disrupting the interaction of HIV-1 Vpu with BST-2 in the direct ITC assay, as the displacement ITC studies could not be performed. Additionally, the results obtained in this study proved the ability of 6-aza-2-thiouridine and Lapachol to bind to HIV-1 Vpu, with 6-aza-2-thiouridine showing greater affinity compared to Lapachol. It is also important to note that to the best of our knowledge, this study was the first to make use of AlphaScreen and ITC techniques for screening and determination of binding energetics of ligands to HIV-1 Vpu.

6.3 Concluding Remarks

In conclusion, novel biological assays were established as a screening tool for the identification of novel small molecule inhibitors for the binding interaction of HIV-1 Vpu with BST-2. These assays can be advantageous in screening libraries of compounds against the HIV-1 Vpu/BST-2 interaction in the future, as they are amenable to high throughput screening. Two novel hit compounds, Compound 1 and Compound 8, were identified as showing promising activity in inhibiting the binding interaction between HIV-1 Vpu and BST-2 from a group of 24 compounds. Further characterisation of the compounds, which included *in vitro* toxicity and antiviral activity screening, showed that Compound 1 exhibited moderate potency against the replication of HIV-1 *in vitro*, while the same could not be shown for Compound 8. Preliminary analysis of binding interactions between the hit compounds and HIV-1 Vpu showed that Compound 1 had better affinity for HIV-1 Vpu compared to Compound 8. Taken together, this work presents a novel candidate (Compound 1) that could be optimised and researched further as a potential inhibitor of HIV-1 replication with a novel mode of action.

6.4 Recommendations for Future Work

Findings from the present study can be advanced through the following recommendations:

1. Optimising the purification protocol for the recombinant BST-2 and further characterising the interaction of HIV-1 Vpu with BST-2 using ITC. The thermodynamics data provided by ITC can help understand the physical forces underlying the interaction of the two proteins and that could further advance the efforts of pursuing this interaction as a drug target.

2. Optimisation of the ITC experiments to obtain better binding isotherms and potentially reach saturation with the test compounds. Evaluating the thermodynamic binding parameters of the compounds to HIV-1 Vpu at the physiological temperature (37 ºC) would also be valuable for this study.

3. Evaluation of the cytotoxicity and antiviral activity of the compounds in peripheral blood mononuclear cells (PBMCs). PBMCs can be isolated from whole blood using density gradient centrifugation and Ficoll-Paque, a hydrophilic polysaccharide that separates layers of blood. For cytotoxicity studies, the cells can be treated with varying concentrations of the compounds and incubated as outlined for the MT-4 cells in section 2.2.8.3. Similarly, for the antiviral activity evaluations, the cells can be infected and treated as outlined in section 2.2.9.

4. Testing the activity of the compounds in inhibiting the replication of the HIV-1 subtype C, which is the prevalent strain in southern Africa, and comparing the findings against the subtype B data reported in this thesis.

5. Modifications of the structures of the identified hit compounds (as well as the control compounds) by introducing various functional groups at specific positions to generate a second generation of HIV-1 Vpu/BST-2 inhibitors with improved activity.

6.5 References

Chabner, B.A. and Longo, D.L., 2011. *Cancer chemotherapy and biotherapy: principles and practice*. Lippincott Williams & Wilkins.

Herbert, B., 1999. Advances in protein solubilisation for two-dimensional electrophoresis. *ELECTROPHORESIS: An International Journal*, *20*(4-5), pp.660-663.

Li, L.H., Neil, G.L., Moxley, T.E. and Olin, E.J., 1974. Antitumor activity and mode of action of 2-thio-6-azauridine (NSC-146268) on L1210 leukemia. *Cancer chemotherapy reports*, *58*(3), p.345.

Lipinski, C.A., Lombardo, F., Dominy, B.W. and Feeney, P.J., 1997. Experimental and computational approaches to estimate solubility and permeability in drug discovery and development settings. *Advanced drug delivery reviews*, *23*(1-3), pp.3-25.

Savjani, K.T., Gajjar, A.K. and Savjani, J.K., 2012. Drug solubility: importance and enhancement techniques. *ISRN pharmaceutics*, *2012*.

Appendix A:

A.1.1 Plasmid map of pcDNA-Vphu

Figure A.1: Map of the *pcDNA-Vphu* plasmid vector that was used for the overexpression of HIV-1 Vpu.

Appendix B:

B.1.1 BLAST results obtained for the pcDNA-Vphu sequence:

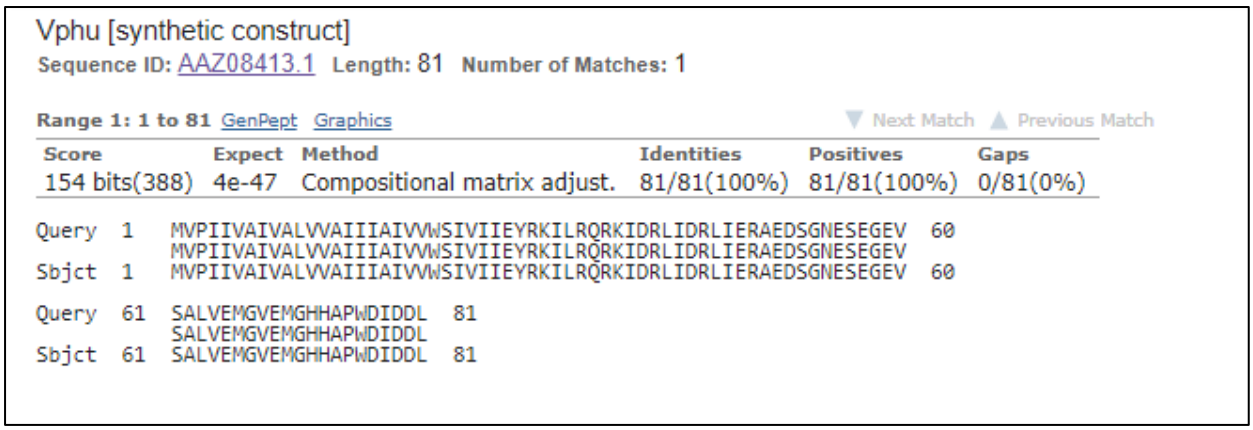

Vphu [synthetic construct]

Sequence ID: AAZ08413.1 **Length:** 81 **Number of Matches:** 1

Range 1: 1 to 81 GenPept Graphics ▼ Next Match ▲ Previous Match

Score	Expect	Method	Identities	Positives	Gaps
154 bits(388)	4e-47	Compositional matrix adjust.	81/81(100%)	81/81(100%)	0/81(0%)

```
Query  1   MVPIIVAIVALVVAIIIAIVVWSIVIIEYRKILRQRKIDRLIDRLIERAEDSGNESEGEV  60
           MVPIIVAIVALVVAIIIAIVVWSIVIIEYRKILRQRKIDRLIDRLIERAEDSGNESEGEV
Sbjct  1   MVPIIVAIVALVVAIIIAIVVWSIVIIEYRKILRQRKIDRLIDRLIERAEDSGNESEGEV  60

Query  61  SALVEMGVEMGHHAPWDIDDL  81
           SALVEMGVEMGHHAPWDIDDL
Sbjct  61  SALVEMGVEMGHHAPWDIDDL  81
```

Figure B.1: Sequence alignment results of the pcDNA-Vphu sequence obtained from Inqaba Biotech using protein BLAST. The sequence showed 100% identity to the Vphu synthetic construct.

Appendix C:

C.1.1 Expression and Purification Trials of BST-2

C.1.1.1 Codon optimisation of BST-2 and cloning into a pET15b vector

The BST-2 coding cDNA fragment was synthesised and subsequently cloned into the pET15b vector, in frame with the C-terminal *polyhistidine* tag (GenScript USA Incorporated). The amino acids in the BST-2 gene were codon-optimised for increased protein production and solubility in bacterial cells. The cloning of the gene into the pET15b vector was done using the *NdeI* and *XhoI* restriction enzymes.

C.1.1.2 Characterisation of the recombinant pET15b-BST-2 clones

Recombinant pET15b-BST-2 plasmid DNA sample was sent to Inqaba Biotechnical Industries (Pty) Ltd to verify the orientation of the insert, and to ensure that the insert was in frame with the *polyhistidine tag* sequence.

C.1.1.3 Expression of BST-2 in *E. Coli*

BST-2 was over-expressed in *E. coli* BL21 (DE3) cells. Briefly, the *E. Coli* BL21 (DE3) cells were transformed with the recombinant plasmid carrying the BST-2 gene as outlined above for HIV-1 Vpu. Bacterial colonies harbouring the pET15-BST-2 plasmid DNA were inoculated into 50 mL LB medium containing ampicillin (100 μg/mL) at 37 °C. The culture was grown for approximately 16 hours overnight and subsequently diluted 100-fold into fresh LB medium. The culture was allowed to grow under continuous shaking for 3 hours at 37 °C until OD_{600nm} reached mid-log phase. Protein production was induced using IPTG to a final concentration of 1 mM, and the culture was allowed to grow for an additional 4 hours.

C.1.1.4 BST-2 extraction

After 4 hours of induction at 37 °C, the cells were harvested by centrifugation at 3220 x g for 30 minutes at 4 °C. The supernatant was discarded, and the pellet was stored at -80 °C. The 13.4 g pellet from 1L bacterial culture was resuspended in 20 mL ice-cold lysis buffer (20 mM Tris-Cl pH 8.0, 250 mM NaCl, 1 mg/mL lysozyme, 5 mM EDTA, 1 mM DTT, 1 mM PMSF) and the cells were incubated at 4 °C for an hour with gentle shaking to ensure

thorough lysis. The cells were sonicated on ice using the Labsonic M ultrasonic processor, and DNase I, to a final concentration of 5 µg/mL, was added to the cell lysate. The lysate was incubated at 4 °C with shaking for an additional 30 minutes and subsequently centrifuged at 16 000 x g at 4 °C for 30 minutes, and the supernatant and pellet were analysed for the presence of BST-2. The codon-optimised BST-2 was found to be soluble and present primarily in the supernatant.

C.1.1.5 Purification of the recombinant BST-2

BST-2 was purified using a Nickel affinity chromatography as detailed below.

C.1.1.5.1 Nickel Affinity Chromatography

The overexpressed His-tagged recombinant BST-2 from the *E. Coli* BL21 (DE3) cells was loaded onto a HiTrap IMAC HP column (GE Healthcare). The column was equilibrated with five column volumes of equilibration buffer (20 mM Tris-Cl pH 7.4 and 250 mM NaCl). The supernatant containing BST-2 was loaded onto the Nickel affinity column at a flow rate of 1 mL/min, and the column was washed with 10 column volumes of the equilibration buffer. The protein was eluted at a gradient with the equilibration buffer as the starting buffer and a set final target of 100% elution buffer (20 mM Tris-Cl pH 7.4, 250 mM NaCl, and 100 mM Imidazole). The elution fractions were collected at a flow rate of 3 mL/min and 3mL per fraction. The fractions containing BST-2 were pooled and concentrated using an Amicon ultra-filtration device with a 10 kDa cut off (Millipore Merck).

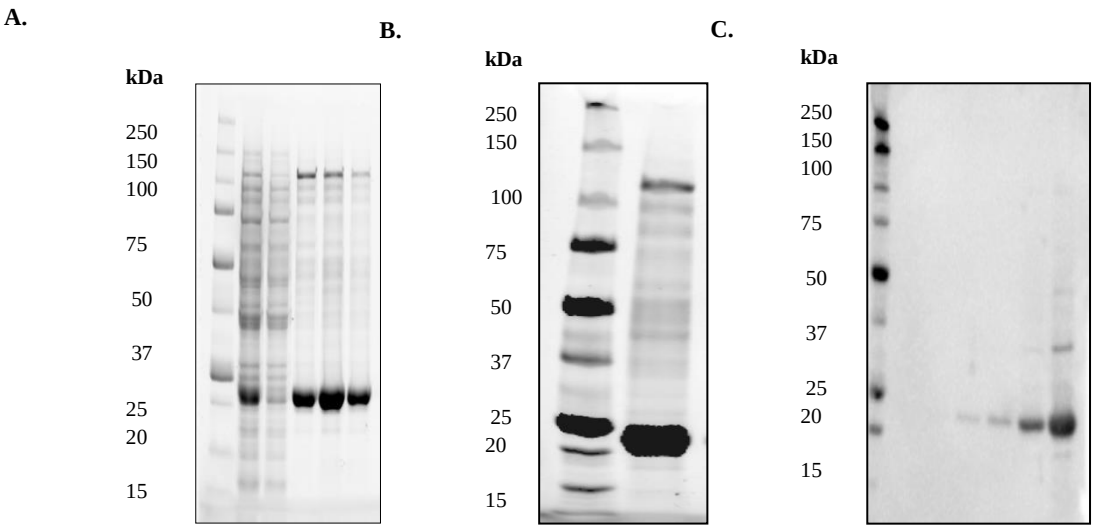

Figure C.1: SDS-PAGE and Western blot analysis of the recombinant BST-2. A. SDS-PAGE of BST-2 fractions from Nickel affinity purification. **B.** SDS-PAGE of concentrated BST-2 fractions. **C.** Western blot analysis of BST-2 serial dilutions using anti-BST-2 antibodies.

Appendix D:

D.1.1 Fluorescence Spectra of the Titration of the Test Compounds into reaction Buffer

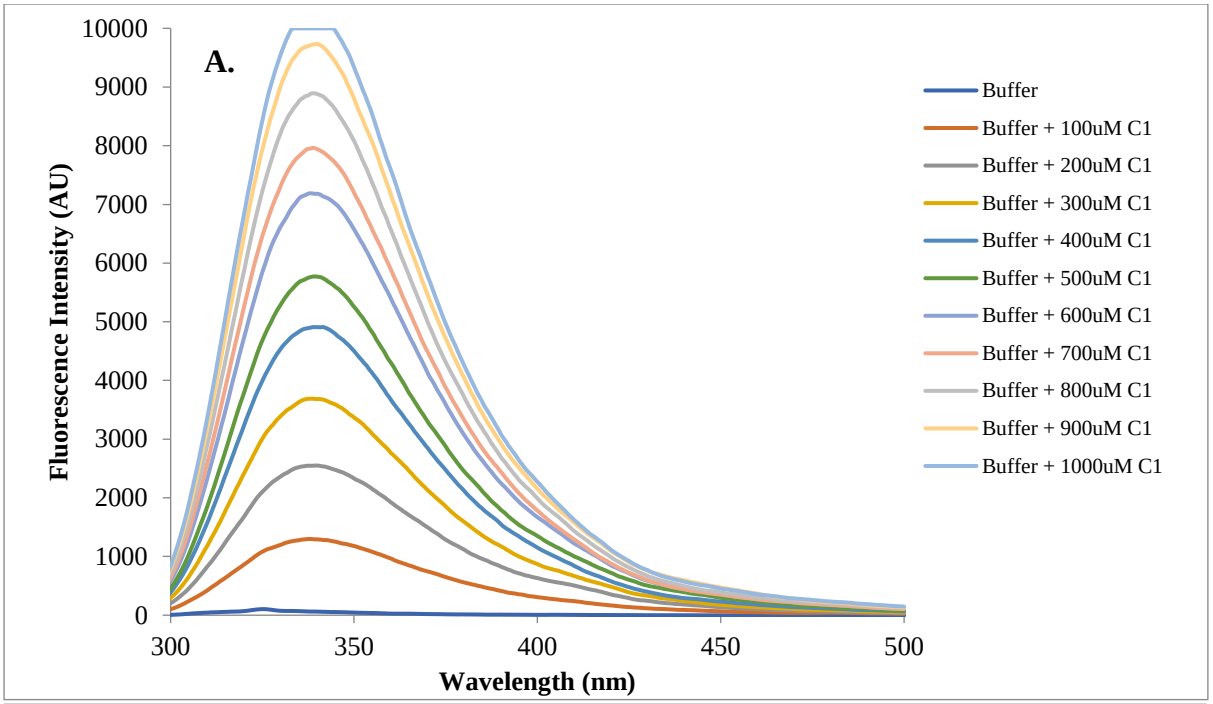

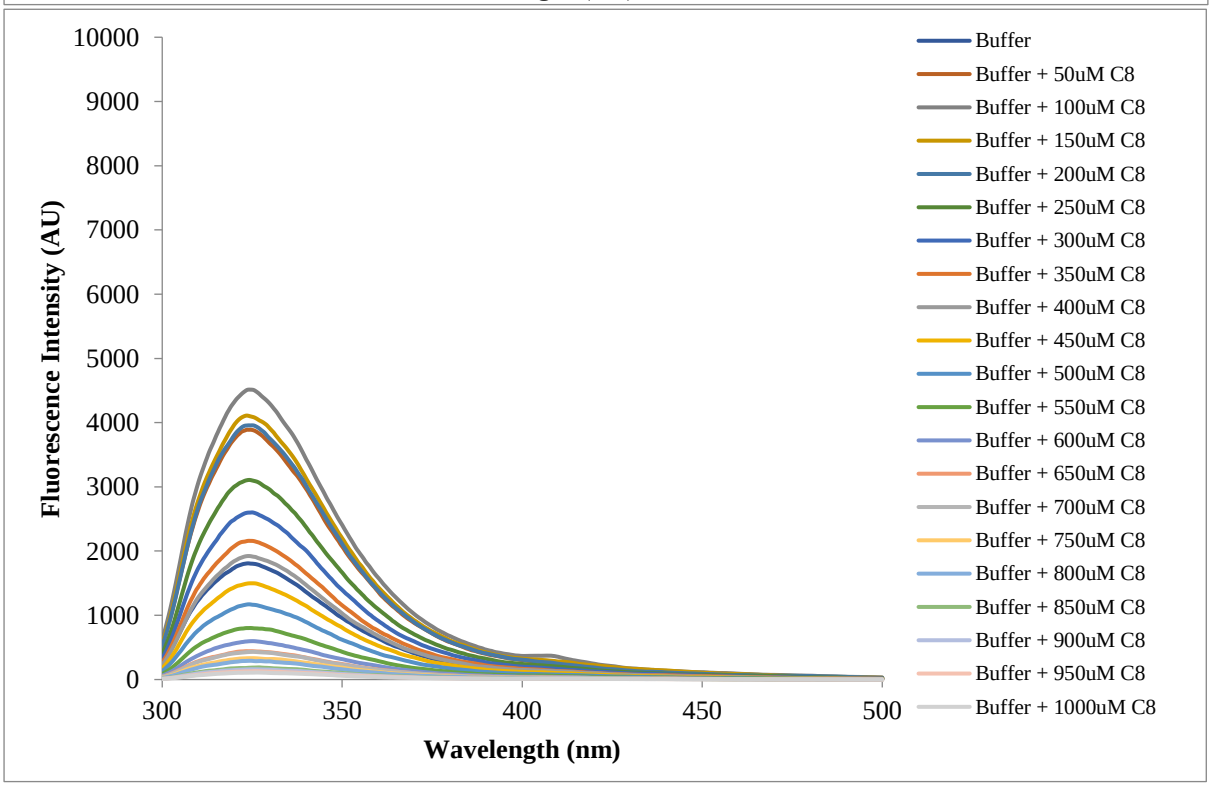

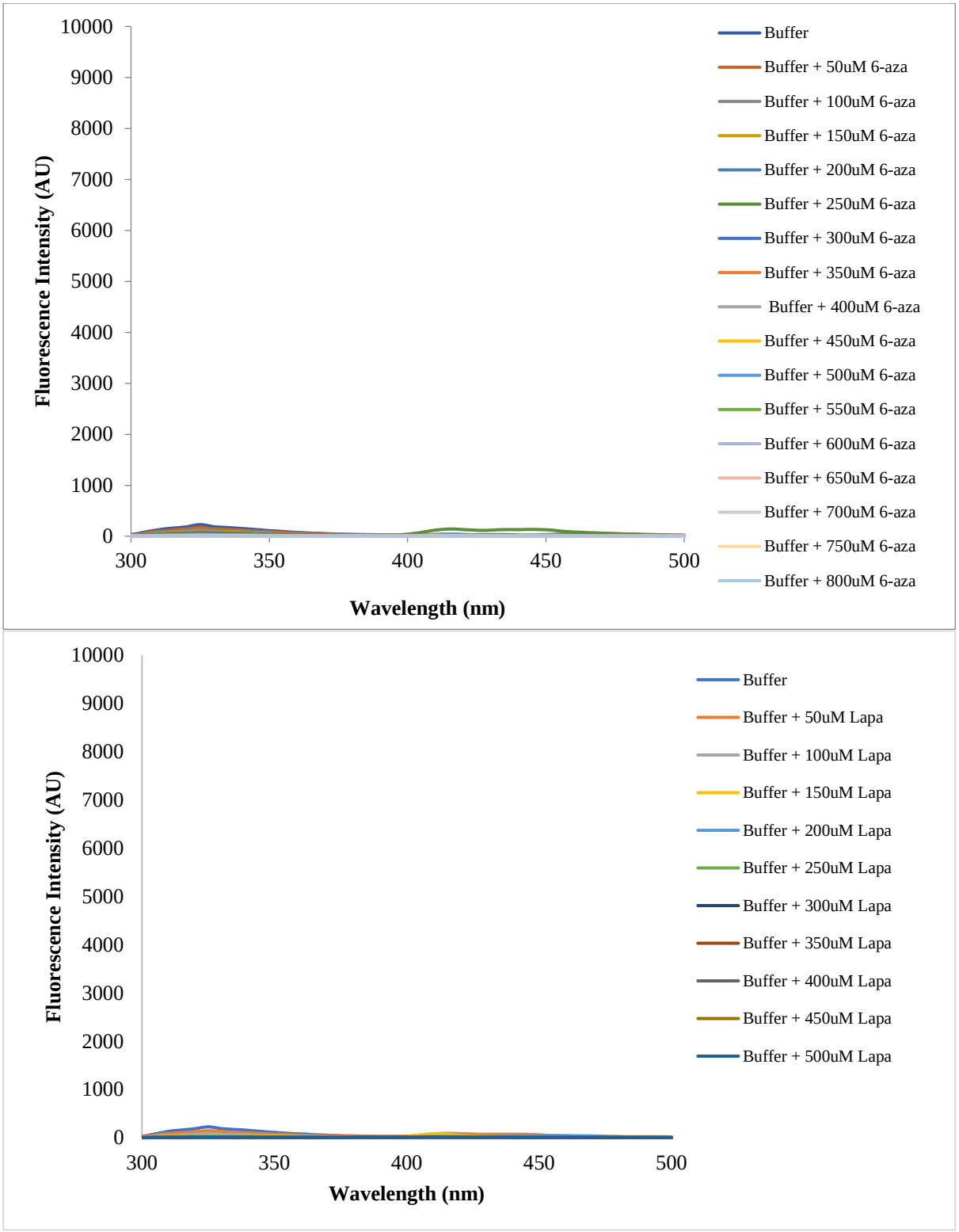

Figure D.1: Intrinsic tryptophan fluorescence spectra of the titrations of the test compounds into reaction buffer. A. Titration of Compound 1 (100 – 1000 µM) into buffer. **B.** Titration of Compound 8 (50 – 1000 µM) into Buffer. **C.** Titration of 6-aza-2-thiouridine (50 – 800 µM) into buffer. **D.** Titration of Lapachol into buffer.

D.1.2 Fluorescence Spectra of the Titration of the Test Compounds into HIV-1 Vpu

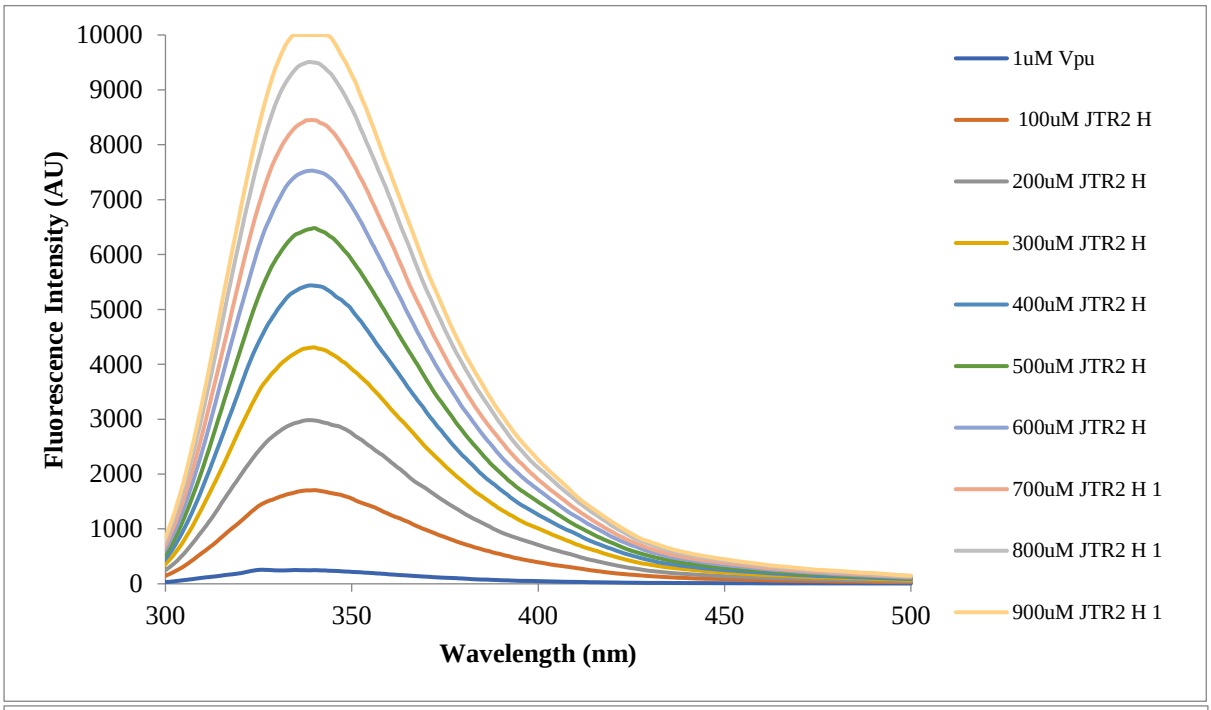

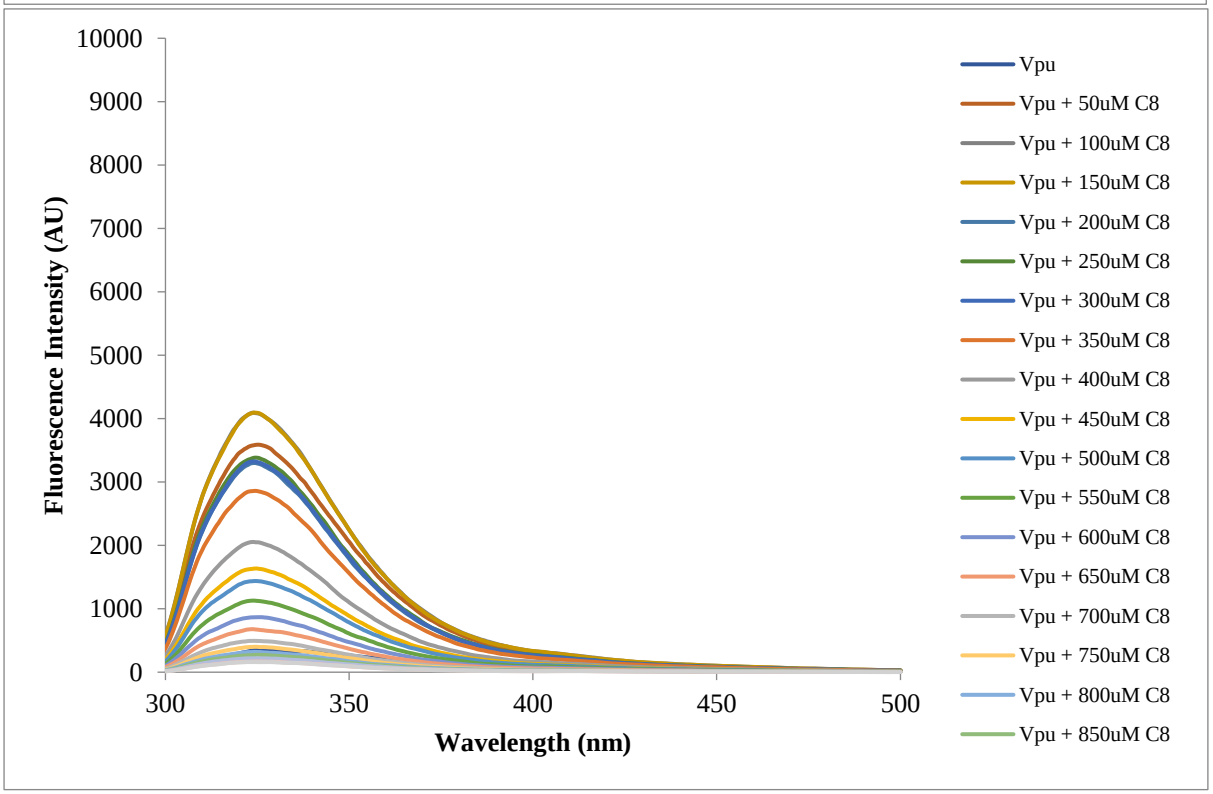

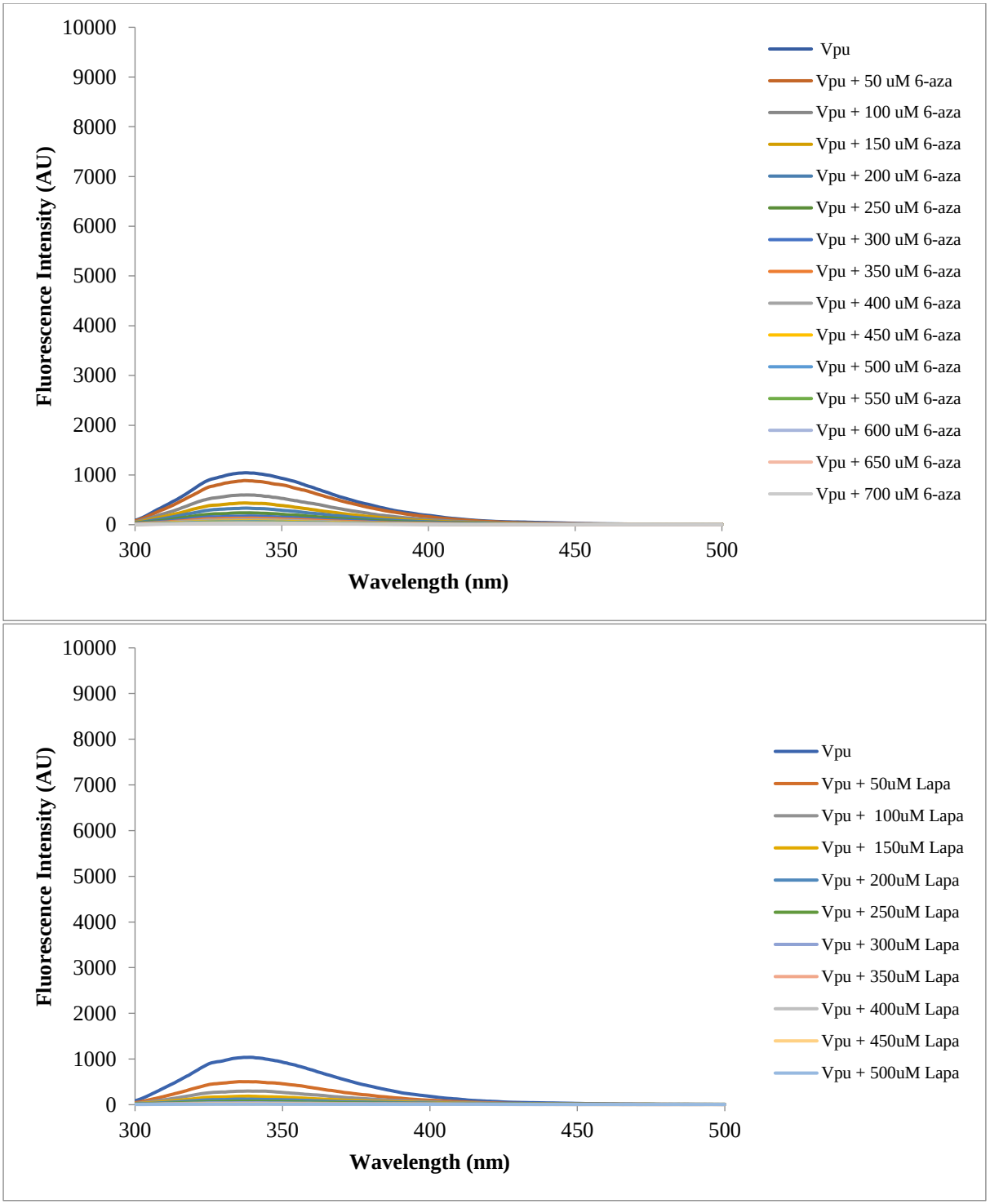

Figure D.2: Intrinsic tryptophan fluorescence spectra of the titrations of the test compounds into 5 µM HIV-1 Vpu. **A.** Titration of Compound 1 (50 – 950 µM) into HIV-1 Vpu. **B.** Titration of Compound 8 (50 – 1000 µM) into HIV-1 Vpu. **C.** Titration of 6-aza-2-thiouridine (50 – 700 µM) into HIV-1 Vpu. **D.** Titration of Lapachol (50 – 500 µM) into HIV-1 Vpu.